THE UNIVERSITY OF CALGARY

Searching for Marduk: Tomlinson-Harashima Pre-Coding and the Indoor Radio Channel

by

Brian Alexander Ebel

A THESIS

SUBMITTED TO THE FACULTY OF GRADUATE STUDIES

IN PARTIAL FULFILMENT OF THE REQUIREMENTS FOR THE

DEGREE OF MASTER OF SCIENCE

DEPARTMENT OF

ELECTRICAL AND COMPUTER ENGINEERING

CALGARY, ALBERTA

DECEMBER, 1994

THE UNIVERSITY OF CALGARY

FACULTY OF GRADUATE STUDIES

The undersigned certify that they have read, and recommend to the Faculty of Graduate Studies for acceptance, a thesis entitled "Searching for Marduk: Tomlinson-Harashima Pre-Coding and the Indoor Radio Channel" submitted by Brian Alexander Ebel in partial fulfilment of the requirements for the degree of Master of Science.

Supervisor, Dr. A. Sesay
Department of Electrical and Computer Engineering

Dr. M. Fattouche
Department of Electrical and Computer Engineering

Dr. B. Nowrouzian
Department of Electrical and Computer Engineering

Mr. G. Squires
Vice President, Research and Technology, TRLabs

December 14, 1994

Date

ABSTRACT

A wireless local area network (LAN), operating at 20 megabits per second or more over the indoor radio channel, requires techniques to combat intersymbol interference (ISI) and achieve low error rates. For this application, computer simulations show the effectiveness of equalization methods at reducing bit error rates below 10^{-5}, when used with switched antenna diversity and (15,7) BCH channel coding.

Tomlinson-Harashima (TH) pre-coding, a transmitter-based equalization method, pre-distorts the transmit signal constellation, using channel ISI and modulo reduction for constellation recovery at the receiver. The base station of a wireless LAN employs the TH pre-coding technique to equalize transmitted signals. Intersymbol interference is removed from received data symbols with a conventional decision feedback equalizer (DFE). Concentrating all equalization functions at a base station implements an asymmetric communication system which maximizes terminal portability and minimizes terminal cost.

ACKNOWLEDGEMENTS

I am deeply indebted to my supervisor, Dr. Abu Sesay, for his patience and support during the preparation of this work.

TRLabs has provided financial assistance and a well-equipped, comfortable environment for graduate research. I am grateful to TRLabs and its sponsors for this munificence and, in particular, to George Squires and Leila Southwood for their role in fostering this environment.

Mark Gibbard has been a source of advice, encouragement and assistance. Both Mark and Shavantha Kularatna have patiently endured my excesses during a laborious proofreading process.

In carrying out my research project, Grant McGibney and Gerald Morrison have assisted me with the vagaries of computing. I am also appreciative of the indoor channel measurement database, created by Gerald Morrison and David Tholl, from which channel models used in this work have been taken.

Thanks are also due to all TRLabs students and staff for their friendly acceptance of surliness, hoarding of CPU time, book thieving, halitosis and other characteristics associated with thesis preparation.

To my parents

TABLE OF CONTENTS

Approval Page ... ii
Abstract ... iii
Acknowledgements ... iv
Dedication ... v
Table of Contents ... vi
List of Tables ... ix
List of Figures ... x
List of Symbols and Abbreviations ... xii
Epigraph ... xix

CHAPTER 1: PURPOSE AND SCOPE OF STUDY ... 1
1.1 Introduction ... 1
1.2 Context ... 1
1.3 Motivation ... 4
1.4 Organization ... 6
1.5 Goals ... 7
1.6 Conclusion ... 8

CHAPTER 2: TOMLINSON-HARASHIMA PRE-CODING: THEORETICAL BACKGROUND, APPLICATION AND EXTENSIONS ... 9
2.1 Introduction ... 9
2.2 Purpose of Equalization ... 9
2.3 Conventional Equalization ... 13
2.3.1 Linear and Non-Linear Equalizer Structures ... 13
2.3.2 Performance Criteria ... 16
2.3.3 Adaptive Equalization ... 18
2.4 Motivation for Pre-Coding ... 19
2.5 TH Pre-Coding Basics ... 20
2.6 A Feed-Forward Filter for Eliminating Precursors ... 24
2.7 TH Pre-Coding Performance ... 30
2.7.1 Error Performance ... 30
2.7.2 Power Performance ... 35
2.7.3 Shaping ... 39
2.7.4 Spectrum ... 42
2.7.5 Hardware Requirements ... 43
2.8 Relationship of TH Pre-Coding and Partial Response Signalling ... 44
2.9 TH Pre-Coding and Trellis Coding ... 46
2.10 Other Forms of Pre-Coding ... 48
2.10.1 Trellis Pre-Coding ... 48
2.10.2 Flexible Pre-Coding ... 51
2.11 Structure of Pre-Coder Selected for Study ... 54
2.12 Conclusion ... 56

CHAPTER 3: ERROR RATE REDUCTION WITH DIVERSITY AND CODING 58
3.1 Introduction 58
3.2 Diversity 59
3.2.1 Purpose 59
3.2.2 Classifications 60
3.2.3 Antenna Separation 61
3.2.4 Testing Signal Quality 61
3.2.5 Combining Methods 62
3.2.6 Performance 63
3.2.7 TH Pre-Coding and Diversity 64
3.3 Coding Methods 65
3.3.1 Purpose and Performance Measures 65
3.3.2 Coding Strategies 71
3.3.3 Encoding and Decoding 74
3.3.4 Block Codes 79
3.3.5 Convolutional Codes 82
3.3.6 Coded Modulation 83
3.3.7 Code Selected for Simulation 84
3.4 Conclusion 87

CHAPTER 4: SIMULATION OF TOMLINSON-HARASHIMA PRE-CODING 89
4.1 Introduction 89
4.2 Simulation Approach 90
4.2.1 Monte Carlo Analysis 90
4.2.2 Confidence Limits 91
4.2.3 Verification 94
4.3 Simulation Design Details 95
4.3.1 Simulation Platform 95
4.3.2 Simulation Overview 96
4.3.3 Gibbard Pre-coder 98
4.3.4 Decision Feedback Equalizer 99
4.3.5 Channel Modelling 103
4.3.6 Carrier Phase Recovery 110
4.3.7 Symbol Timing Recovery 111
4.3.8 Automatic Gain Control 117
4.3.9 Noise 119
4.3.10 Diversity 120
4.3.11 Coding 121
4.4 Conclusion 121

CHAPTER 5: SIMULATION RESULTS 124
5.1 Introduction 124
5.2 BER Performance 124

5.2.1 Performance of Basic System (Without Diversity and Coding) 124
5.2.2 Basic Gibbard Pre-Coding and DFE Performance Comparison 128
5.3 Switched Antenna Diversity Performance 135
5.4 Channel Coding 138
5.4.1 Error Correction 138
5.4.2 Error Detection and Ideal ARQ 141
5.5 Combined Diversity and Coding 143
5.6 Transmit Power 145
5.6.1 Effect of TH Pre-Coder Stage 145
5.6.2 Effect of Feed-Forward Filter Stage 148
5.7 Hardware Requirements 152
5.8 Conclusion 154

CHAPTER 6: SUMMARY 156
6.1 Introduction 156
6.2 Error Performance 157
6.3 Transmit Power Performance 159
6.4 Recommendations for Future Work 160
6.5 Conclusion 162

BIBLIOGRAPHY 163

LIST OF TABLES

4.1 DFE Sizes 102
4.2 Bandwidths of Channel Models 105
4.3 RMS Delay Spread 108
4.4 AGC Amplification Factors 119

5.1 Estimated Hardware Complexity For Gibbard Pre-Coding 153
5.2 Estimated Hardware Complexity For DFE Coefficient Adaptation 154

LIST OF FIGURES

2.1 Magnitude of Discrete Time Channel Impulse Response 10
2.2 16 QAM Signals 13
2.3 Linear Feedback Equalizer 14
2.4 Decision Feedback Equalizer 15
2.5 Simple Postcursor Pre-cancellation 21
2.6 Equivalent Simple Postcursor Pre-cancellation 22
2.7 TH Pre-Coding Block Diagram 23
2.8 Baseband Representation of Communication System and Transfer Functions 25
2.9 Comparison of Conventional TH and Gibbard Pre-Coding 28
2.10 4 QAM Signal Constellation Showing Voronoi Cells and Periodic Extension 31
2.11 Data Flipping Caused By Modulo 2M Reduction 32
2.12 16 QAM With Kissing Numbers 33
2.13 Modulo 2M Reduction Operator Output Constellations 36
2.14 Hexagonal TH Boundary Regions 41
2.15 Nyquist and Partial Response Pulse Shaping 44
2.16 Trellis Pre-Coding Transmitter 48
2.17 Trellis Pre-Coding Receiver 49
2.18 Flexible Pre-Coding Transmitter 52
2.19 Flexible Pre-Coding Receiver 53
2.20 Simulation Model 55

3.1 Switched Diversity at Base Station Only 64
3.2 Two Dimensional Repetition Code 68
3.3 Three Dimensional Repetition Code 69
3.4 Sequential Decoding Error 79
3.5 Gray Coded Constellations 84

4.1 Main Functional Blocks of the Asymmetric Communication System Simulation Model 97
4.2 Functional Diagram of Gibbard Pre-Coder With Dimension (3,3) 99
4.3 DFE Signal-to-Distortion Performance Surface 101
4.4 Distribution of Significant Multipath Components in Channel Impulse Response 107
4.5 Magnitude of Channel Response Spectrum Before and After Symbol Rate Sampling 112
4.6 Advanced Timing Example 115
4.7 Performance Index Distribution 116
4.8 Role of the AGC 118

5.1 BER of Basic Gibbard Pre-Coder 125
5.2 Transmitted Frames Containing Errors for Basic Gibbard Pre-Coder 126

5.3 Gibbard Pre-Coder Link - Magnitude of Error Standard Deviation at Output of Receiver Mod 2M Reduction Operator, 10 Msymbol/s, 22.6 dB SNR Per Bit 127
5.4 BER Comparison of Basic DFE and Gibbard Pre-Coder 128
5.5 BER Performance of Ideal DFE (No Error Feedback) 129
5.6 Transmitted Frames Containing Errors for Basic DFE and Gibbard Pre-Coder 130
5.7 Transmitted Frames Containing Errors for Basic DFE and Gibbard Pre-Coder, 10 Msymbol/s Data Rate 132
5.8 Gibbard Pre-Coder and DFE Error Magnitude Probability Distribution, 10 Msymbol/s Data Rate 133
5.9 BER Versus Transmit Power - Comparison of Basic DFE and Gibbard Pre-Coder Link 134
5.10 BER of Gibbard Pre-Coder With Switched Dual Antenna Diversity 136
5.11 Transmitted Frames Containing Errors For Gibbard Pre-Coding With Switched Dual Antenna Diversity 137
5.12 Gibbard Pre-Coder Link - Magnitude of Error Standard Deviation at 10 Msymbol/s, 22.6 dB SNR Per Bit For Switched Dual Antenna Diversity 138
5.13 BER of Gibbard Pre-Coder With (15,7) BCH Channel Code 139
5.14 Transmitted Frames Containing Errors for Gibbard Pre-Coding with (15,7) BCH Channel Code 140
5.15 Automatic Repeat Request (ARQ) Bit Error Rate at 10 Msymbol/s 142
5.16 BER of Gibbard Pre-Coder With Switched Dual Antenna Diversity and (15,7) BCH Channel Code 143
5.17 Combined Performance of Dual Switched Antenna Diversity and (15,7) BCH Channel Code at 10 Msymbol/s 144
5.18 Average Output Power of TH Pre-Coder Stage 145
5.19 Average Output Power of TH Pre-Coder Stage For (15,7) BCH Coded Input Data, 10 Msymbol/s Data Rate 146
5.20 Average Output Power of Gibbard Pre-Coder Feed-Forward Filter 148
5.21 Gibbard Pre-Coder Feed-Forward Filter Output Power, 10 Msymbol/s 150
5.22 Gibbard Pre-Coder Peak-To-Average Transmit Power Ratio 151

LIST OF SYMBOLS AND ABBREVIATIONS

Symbols

A	geometric mean of a transfer function
a	basis vector scaling factor
B	bandwidth
b	basis vector scaling factor
C	channel capacity
$c(k)$	quantized post-cursor cancellation vector
C_S	a trellis shaping code
$c_S(z)$	a sequence of trellis shaping codes
$Ȼ_C$	a trellis code
D	peak distortion due to intersymbol interference or Hamming distance between codewords
D^H	Hamming distance
D^H_{min}	minimum Hamming distance
$d(k)$	dither signal
E_b	energy per bit
e	base of the natural exponential function (2.71828...)
exp	natural exponential function e^x
$F(z)$	discrete time receiver matched filter transfer function
$G_{AGC}(i)$	gain of an AGC for channel i
G_{RC}	gain of a square root raised cosine filter
$GF(\cdot)$	Galois field
$G(z)$	discrete time minimum phase factor of system transfer function
$g(\cdot)$	code generator polynomial

$H(n)$	discrete frequency domain channel transfer function
$H(z)$	discrete time channel transfer function
$h(\cdot)$	discrete time channel impulse response
I	in-phase component
i	channel index
J_{min}	minimum mean square error
j	a discrete time index or the square root of -1
$K(z)$	discrete time whitening filter transfer function
K_N	noise scaling factor
k	a discrete time index or number of information bits in a codeword
k_1, k_2, k_3	data vector lengths
$\ln(\cdot)$	natural logarithm
$\log_2(\cdot)$	logarithm to base 2
M	number of one-dimensional levels in a square QAM constellation
mod	modulo reduction
N	filter order, diversity order or sequence length
N_0	single sided noise power spectral density
$n(k)$	an integer scaling factor
n	a discrete frequency index or length of a codeword
$P_{AVERAGE}$	average power
$P_b(e)$	probability of bit error
P_i	intersymbol interference power
P_n	noise power
P_o	probability of outage
P_{PEAK}	peak power
P_S	received symbol power

p^k	order of a Galois field
Q	quadrature component
$Q(\cdot)$	Gaussian tail distribution probability function
$S(z)$	discrete time overall transfer function
R	the set of real numbers
R^2	the Cartesian product RxR
r	code rate
S_1,S_3	error syndromes
T	symbol period
U^T	a syndrome forming matrix
$(U^{-1})^T$	left inverse of a syndrome forming matrix
V,V_k	lattice vector(s)
V_0	a lattice subset
V32.bis	1991 CCITT modem standard with a maximum data rate of 14 400 bits per second
w	a signal at a modulo reduction operator input
$w(\cdot)$	discrete time channel input
w_k^{ff}	feedback filter coefficient k
w_k^{ff}	feed-forward filter coefficient k
x	a one-dimensional coordinate of a symbol or a dummy variable for algebraic code polynomials
$X(\cdot)$	received signal spectrum
$x(\cdot)$	discrete time ideal data
x_x,x_y	in-phase and quadrature components of x
XOR	exclusive or
$y(\cdot)$	discrete time channel output

y_x, y_y	in-phase and quadrature components of y
Z	set of integers
z	complex discrete-time z-transform variable
z^{-1}	unit time delay
1D	one dimensional space
2D	two dimensional space
α	raised cosine filter roll off
η	efficiency
$\theta(\cdot)$	sum of postcursor intersymbol interference
μ	mean
ξ	peak-to-average power ratio
π	pi (3.141592654...)
ρ_D	signal-to-distortion performance measure
Σ	summation
σ	standard deviation
τ_{RMS}	root mean square delay spread
ω	frequency in radians per second
/	per
%	percentage
$\pm$	plus or minus
*	conjugate
$\lvert\cdot\rvert$	magnitude
$\lfloor\cdot\rfloor$	smallest integer less than or equal to
$\in$	element of
^	estimate of

Abbreviations

A/D	analog to digital
AGC	automatic gain control
ARQ	automatic request for retransmission
ASIC	application specific integrated circuit
AT & T	American Telephone and Telegraph Company
AWGN	average white Gaussian noise
BCH	Bose-Chaudhuri-Hocquengham
BER	bit error rate
bps	bits per second
CAD	computer aided design
CCITT	Comité Consultatif International de Téléphonie et Télégraphie
cm	centimetre
CPU	central processing unit
DFE	decision feedback equalizer
DSP	digital signal processing
dB	decibel
FB	feedback
FEC	forward error correction
FIR	finite impulse response
FF	feed forward
FFT	Fast Fourier Transform
GHz	gigahertz or billions of cycles per second
HDSL	high-speed digital subscriber lines
HIPERLAN	High Performance European Radio LAN
IC	integrated circuit

IEEE	Institute of Electrical and Electronics Engineers
IFFT	Inverse Fast Fourier Transform
IIR	infinite impulse response
ISI	intersymbol interference
ISM	industrial, scientific and medical uses
Kbit	kilobit or one thousand bits
LAN	local area network
LMS	least mean square
MAC	multiply and accumulate calculation
Mbps	megabits per second
MHz	megahertz or millions of cycles per second
MD	multi-dimensional
MLSE	maximum-likelihood sequence estimation
MPE	minimum probability of error
MMSE	minimum mean square error
Msamples	millions of samples
Msymbol	millions of symbols
MSE	mean square error
MT	modulo transmitter or matched transmission
NCR	National Cash Register
ns	nanosecond, a billionth of a second (10^{-9})
PAM	pulse amplitude modulation
PSD	power spectral density
QAM	quadrature amplitude modulation
RC	raised cosine
RLS	recursive least squares

RS	Reed-Solomon
RSSE	reduced state sequence estimation
RX	receive
s	second
SNR	signal to noise ratio
SPW™	Signal Processing WorkSystem
SQRT	square root
TCM	trellis coded modulation
TDL	tapped delay line
TDMA	time division multiple access
TH	Tomlinson-Harashima
TX	transmit
W	watt
ZF	zero-forcing

They set up in their midst one constellation,

And then they addressed Marduk their son,

'May your decree, O lord, impress the gods!

Command to destroy and to recreate, and let it be so!

Speak and let the constellation vanish!

Speak to it again and let the constellation reappear.'

He spoke, and at his word the constellation vanished.

He spoke to it again and the constellation was recreated.

When the gods his fathers saw how effective his utterance was,

They rejoiced, they proclaimed: 'Marduk is King!'

- The Mesopotamian Epic of Creation,
Tablet IV
(Translation by Stephanie Dalley)

Chapter 1

Purpose and Scope of Study

1.1 Introduction

This is the beginning. Here the didactic sluice gates begin to overflow with descriptions of a method for modifying transmit signal constellations, known as Tomlinson-Harashima (TH) pre-coding. Pedantic floodwaters, unless held firmly in check, constantly jeopardize analysis and research results, threatening to grind them both to a churning, disordered slurry. In a probably futile but necessary effort to ward off chaos, the following sections attempt to impose order on subsequent chapters by describing the context, motivation, organization and goals of this study.

1.2 Context

This study examines the application of TH pre-coding to wireless local area networks (LANs), adding some minor extensions to the seminal work of Gibbard [Gibbard1]. Local area networks connect data gathering and processing equipment, permitting communication between devices spread over a geographic area not exceeding a few kilometres in diameter [Keiser, 2][Spragins, 1]. Traditionally, LANs are realized with wired cable connections between equipment. The most popular LAN protocol is the IEEE 802.3 Ethernet standard, supporting a raw bit rate of 10 megabits per second (Mbps), with a 100 Mbps standard under development[1] [Spragins, 12][Wilson, 26][Chen2, 53]. Although high speed is an advantage, wired connections have a number of drawbacks,

---

[1] Under development by IEEE 802.12 and 802.14 committees [Muller, 22].

including a lack of mobility for data terminals at a time when portable computers are increasingly common [Khayata, 460]. Additional drawbacks include the difficulty in laying cable in such environments as factory floors and older buildings, the monetary and time cost of cable installation and rearrangement and the expertise required for LAN configuration and maintenance [Sacks, 24] [Freeburg, 58-9][Flanagan, 30].

In an era of cellular and portable telephones, the application of wireless communication technology to LANs is not surprising. Wireless LANs enhance computer portability and simplify network installation, configuration and rearrangement. The cost of rearranging a cabled network may impose a significant, recurrent cost; according to one estimate, a third of all office computers are moved at least once a year [Freeburg, 58][Sacks, 24]. Wireless LANs avoid the cost and disruption associated with rearranging a cabled network layout, a task which may be accomplished without specialized knowledge if wireless technology is used [Flanagan, 30]. In general, wireless LANs, are initially more expensive than cabled LANs, but the cost of rearranging a cabled network can eliminate the latter's price advantage [Wilson, 26][Flanagan, 30].

In addition to a higher initial cost, wireless LANs suffer from slower and less predictable throughput relative to their cabled counterparts [Flanagan, 30] [Wilson, 26]. In part, this is due to regulatory constraints on channel bandwidth but lower throughput performance is primarily a consequence of the wireless channel, which is inherently less reliable than cable and causes more frequent outages and delays.

For some users, higher short term cost and throughput limitations are outweighed by the advantages of wireless LANs, and these products have won a share of the total LAN market [Muller, 18]. The development of IEEE 802.11 and HIPERLAN wireless LAN standards is expected to further increase market acceptance [Wilson, 26][Bucholz, 31][Links][Kruys][Khayata][Hayes]. According to some forecasts, wireless LANs will fill niche markets and act as a complement to cabled LANs, adding flexibility to a wired backbone [Steele, 6][Freeburg, 59-60]. Others foresee wireless LANs moving beyond these markets to more general applications [Sacks, 25]["Wireless"]. Regardless of which prediction is correct, the market for wireless LANs is expected to grow, motivating research on wireless data transmission techniques [Muller, 18].

Three types of wireless LAN technology are currently available, employing radio, infra-red and laser transmission, respectively, with radio systems holding the largest market share [Wilson, 27][Tolly, 62]. Radio systems are further classified into spread-spectrum and narrowband transmission technologies. Many of the higher data rate spread spectrum wireless LANs operate at 2 Mbps, including NCR's *WaveLAN®*, Persoft's *Intersect Remote Bridge* and Solectek's *AirLAN* [Tuch, 25][Tolly, 62][Rash, 294]. These and lower data rate spread spectrum systems, such as Cylink's *Airlink*, generally operate in the 902-928 MHz ISM frequency range, where limited bandwidth prevents expansion to higher data rates [Bantz, 49][Tolly, 62]. Narrowband products include Olivetti's *Net3* and Motorola's *ALTAIR™* system [Wilson, 28]. The latter operates in the 18-19 GHz range where more plentiful spectrum permits a raw data rate exceeding 5 Mbps [Duch, 39][Eglowstein][Tolly, 62]. An additional method of transmitting data at radio frequencies uses an interface to the cellular telephone network, but this method is unsuited for intra-office data communications given the low data rate and the high cost and overhead of cellular network connections [Flanagan, 26-28]["Compaq"].

Although there are a variety of wireless LAN applications and technologies, this study will focus on the specific area of intra-office radio communication. Several considerations favour the use of the radio channel. Compared with radio, infra-red transmissions are more vulnerable to shadowing and have a limited range, while infra-red radiation is a potentially greater health hazard than radio waves, particularly to the human eye [Hashemi4, 562] [Fernandes, 72-72]. This study will also be concerned with high data rate transmission. For comparable performance with the 10 Mbps Ethernet standard and its 100 Mbps planned extension, the radio link will carry raw data at a rate of 20, 40 and 80 Mbps, exceeding the capacity of most currently available wireless LAN products [Muller, 235]. A large database of indoor channel measurements in the 900-1300 MHz range was available for this study. The communication system under consideration will therefore operate across a channel centred at 1100 MHz, close to the frequency range occupied by many spread spectrum wireless LANs. Due to regulatory restrictions, an actual system operating at the proposed data rates would need to be located in a higher frequency range, where greater bandwidth is available. Despite the prevalence of spread spectrum wireless LANs, this study will examine another promising modulation technique, namely TH pre-coding.

1.3 Motivation

Two basic LAN topologies are *distributed peer-to-peer* and *centralized base station*. Terminals communicate directly with each other in the former while, in the latter, communications are routed through a base station [Bantz, 50]. By centralized scheduling of network access, the base station topology allows efficient use of the wireless channel [Rypinski, 158]. Additionally, a base station connected to the mains power supply may consume greater power and be more complex than portable terminals [Kahn, 12]. Given the limited charge of portable computer batteries and power requirements for transmission and processing of wireless signals, a shift of complexity from portable terminals to a base station is advantageous for wireless LAN users. Total manufacturing cost might also be reduced through simplification of more numerous portable terminals at the expense of less plentiful base stations.

Significant amounts of signal processing are generally required to overcome, or *equalize*, signal distortion introduced by the wireless channel. In fact, the power needed by the receiver's digital signal processor (DSP) may exceed the power originally needed to transmit the signal [Chen2, 53]. Power consumption and complexity of the DSP become even greater at high data rates. This study is concerned with shifting these significant signal processing requirements from the portable to the base station. Equalization will be performed on signals received *and transmitted* from the base station, alleviating processing requirements at the portable. The concentration of equalization operations at the base station will be termed *asymmetric communication*, reflecting the differential processing burden imposed on base station and portable.

Signals *received* by the base station may be processed with conventional decision feedback equalization. For signals *originating* at the base station, this study will examine TH pre-coding, used to pre-equalize transmitted signals in anticipation of channel distortion. The employed TH technique is a novel structure developed by Gibbard which increases the asymmetry of the communication system by concentrating more signal processing operations at the base station than conventional TH methods [Gibbard1]. The original work of Gibbard will be extended by enlarging the signal constellation from 4 to 16 QAM to achieve a high bit rate. Techniques for lowering the probability of received bit errors will also be analyzed. A pair of base station antennas, implementing *antenna diversity*, is one of the means for reducing the number of errors in received data. This study will also examine the effectiveness of *channel coding* for lowering the bit error rate (BER).

1.4 Organization

Five additional chapters follow this one. An overview of their contents is here given, seriatim.

- Chapter 2. This gives a theoretical explanation of conventional TH pre-coding and the variant developed by Gibbard, styled *Gibbard pre-coding.* To contextualize the description of pre-coding methods, this chapter also covers conventional equalization and partial response signalling, a type of pre-coding. Further evidence of the utility and potential of TH pre-coding is provided by a discussion of TH extensions, such as trellis and 'flexible' pre-coding, although these methods are not included in subsequent simulations and analysis.

- Chapter 3. Methods for improving bit error rate performance are covered in this chapter. The first part discusses diversity, focussing on the dual antenna diversity approach used in this study. Channel coding is discussed in the latter part, including an overview of coding theory, possible coding methods and the (15,7) BCH code ultimately used in computer simulations.

- Chapter 4. An asymmetric communication system model, for assessing the performance of Gibbard pre-coding, is described. This chapter is devoted to the simulation platform, methodology and design decisions involved in representing communication system hardware and the indoor wireless channel.
- Chapter 5. Results from computer simulation of the asymmetric communication system are presented and discussed.
- Chapter 6. To complete the process of intellectual saturation, this chapter gives a recapitulation of the study and its conclusions.

1.5 Goals

The purpose of this study is to assess the efficacy and suitability of Gibbard pre-coding, a variation of conventional TH pre-coding, for use in a high data rate LAN operating over the indoor radio channel. The organizational paradigm for this wireless LAN is asymmetric communication, requiring a shift in processing complexity from portable to base station wherever practicable. Gibbard pre-coding accomplishes equalization at the transmitter rather than receiver and is thus consistent with the asymmetric paradigm.

In a general communication system employing equalization, there is an irreducible bit error rate, below which the BER will not descend when transmit power is increased. Diversity and coding will be tested to determine if these methods may achieve bit error rate reductions in excess of those possible using equalization alone. Three criteria will be used to assess performance of Gibbard pre-coding, by itself and in combination with diversity and coding methods. The bit error rate is the first and most fundamental criterion. The second criterion, the proportion of time division multiple access (TDMA) frames containing errors, is necessary to show the extent to which received data is contaminated. For a given number of error events, a temporal error concentration, rather than a uniform distribution, is desirable to maximize error-free throughput. Transmit power is the third criterion. Because the Gibbard pre-coder alters the transmitted signal, attention must be directed to the distribution of average and peak power levels at the transmitter output. A small spread in these values is desired for higher efficiency of the transmit power amplifier.

1.6 Conclusion

Anticipated growth in the wireless LAN market motivates this study of TH pre-coding, a transmitter-based equalization method. Early chapters provide theoretical background for the study. Subsequently, computer model implementations and simulation results are presented, the latter providing the basis for conclusions about the utility of Gibbard pre-coding in wireless LAN applications.

Chapter 2

Tomlinson-Harashima Pre-Coding: Theoretical Background, Application and Extensions

2.1 Introduction

Tomlinson-Harashima (TH) pre-coding is a signal processing technique that allows correction of anticipated channel distortion *at the transmitter.* This feature supports the objective of asymmetric communication, specifically the concentration of signal processing and related overhead on one side of a two-way link.

This chapter situates TH pre-coding in the larger framework of equalization theory. Within this context, the principles of TH pre-coding are developed and its performance advantages and disadvantages examined.

Various generalizations and extensions to TH pre-coding have appeared, primarily since 1989. An overview of these methods provides further appreciation for the simple structure of TH pre-coding as well as awareness of its limitations.

2.2 Purpose of Equalization

Data signals sent from a transmitter to a receiver must pass through a channel which, to some degree, will corrupt the signal and reduce the probability of accurate data reconstruction at the receiver. Causes of corruption may include thermal noise, interference from other users of the spectrum, Doppler spread (dispersion of the signal over a range of frequencies), and multipath spread (dispersion of the signal over a time period) [Kennedy, 40]. The latter is often a significant problem in wireless channels. Due to reflection, refraction and scattering, a signal emitted by the transmitter travels to the receiver over multiple paths. Different versions of the signal arrive at the receiver at various times with different amplitude and phase.

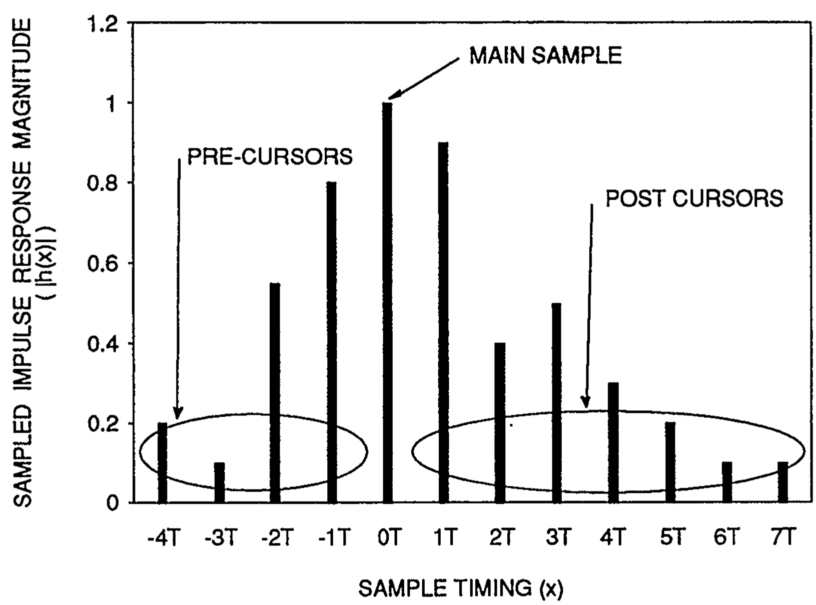

FIGURE 2.1 MAGNITUDE OF DISCRETE TIME CHANNEL IMPULSE RESPONSE

If multipath spread is small compared to the data symbol period, signals travelling over various paths arrive at the receiver at nearly the same time. These signals may have comparable amplitudes but differences in phase, possibly causing destructive interference across the entire signal bandwidth, a condition called *flat fading* [Woerner, 44]. In this circumstance, an equalizer cannot recover the signal. Multipath spread may also be significant compared to the data symbol period, with fades generally confined to only a part of the signal spectrum, resulting in *frequency selective fading* [Chuang, 879]. This is the consequence of significant *delay spread* which causes received data symbols to be smeared out in time [Hashemi1, 943]. Because of this smearing, signals transmitted in neighbouring time periods tend towards overlap and mutual distortion, a phenomenon called intersymbol interference (ISI).

The channel may be modelled as a filter which shapes the spectrum of the transmitted signal. The ideal channel has a flat magnitude frequency response, while the real channel has a magnitude response that varies with frequency and includes fades, of various width and depth, caused by the time dispersion of the signal. In the time domain, the *impulse response* may be used to characterize a channel. An example of impulse response magnitudes for a discrete time channel model appears in Figure 2.1. The complex numbers $\{h(k)\}$ represent the vector sum of the signals arriving at the sampling instant k and are identified by their position relative to a *main sample* h(0). The main sample is often, but not necessarily, taken as the sample with greatest energy. Samples prior to the main sample are called precursors while samples following the main are called postcursors, each giving the channel a memory. Using this model, the received signal sequence may be calculated as the linear time domain convolution of the impulse response and a discrete time transmitted data sequence $\{x(k)\}$ [Morrison1, 4]. The convolution operation can be represented by:

$$y(k) = \sum_{j=-\infty}^{\infty} x(k-j)h(j) \tag{2.1}$$

Intersymbol interference may cause signal distortion, but it is not always an undesirable effect. Partial response systems, described in Section 2.8, use controlled interference in order to achieve bandwidth efficient transmission. Multipath introduces diversity into a wireless channel that can be exploited to assist an equalizer in reconstructing a signal [Monsen, 62-63][Pahlavan, 166].

An ISI channel, because it has memory, can be regarded as a finite state machine which is capable of yielding a coding gain and an error-rate performance that can exceed the ISI-free channel, albeit at considerable increase in signal processing complexity [Simmons].

Although this study will be restricted to a linear ISI model, it should also be recognized that non-linear effects are also possible. For transmission over telephone lines, non-linear ISI may be due to the channel itself [Falconer, 2589]. For wireless indoor channels, non-linear effects are caused by limitations of signal processing circuitry, such as a non-linear amplifier response [Kammeyer, 271][Hamsher, 1-24].

The ideal transmitted signal sequence $\{x(k)\}$, for the purposes of this study, will be drawn from a set of QAM symbols. These symbols belong to a two-dimensional signal space. Amplitudes of an in-phase and quadrature carrier are used to represent one dimension each of this 2D space [Feher, 210]. The symbol set is called a *signal constellation*. It is helpful for later analysis of coding and pre-coding schemes to regard the constellation as the subset of a *lattice*. A lattice is a set of m-dimensional points, closed under ordinary addition and integer multiplication. Each point in the lattice may be located by a sum of integer multiples of lattice *basis vectors* [Biglieri, 209-210].

Large signal constellations are spectrally efficient; for a fixed symbol rate, a larger constellation allows more bits to be transmitted in a given time interval. This improvement is achieved at the expense of increased transmit power and reduced margin against noise. An example of rectangular 16 QAM constellation is shown in Figure 2.2, together with a scatter diagram of the received signals, obtained when 16 QAM is passed at 5 Msymbol/s through an impulse response taken from a Calgary office building.

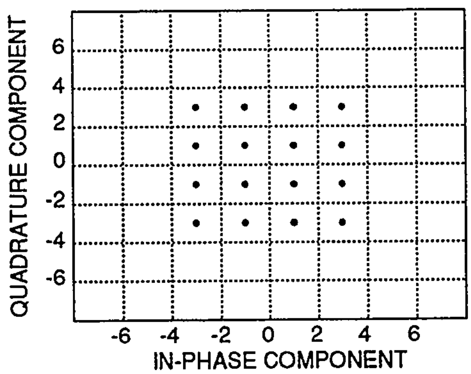

(A) IDEAL 16-QAM CONSTELLATION

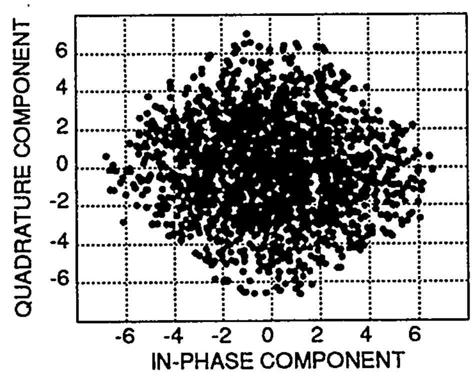

(B) ISI DISTORTED 16-QAM CONSTELLATION

FIGURE 2.2 16 QAM SIGNALS

Distortion of the signal constellation by ISI makes recovery of the transmitted data prone to error. Countermeasures can be taken, at both the transmitter and receiver, to overcome the effect of ISI and reduce detection errors. These measures are effected by an *equalizer*, a term which originated with attempts to flatten the amplitude frequency response of the channel and linearize the phase, and now applied generally to any ISI-combatting signal processing technique [Qureshi, 1349][Lucky1, 548].

2.3 Conventional Equalization[1]

2.3.1 Linear and Non-Linear Equalizer Structures

A transversal filter is the simplest and most common form of equalizer [Qureshi, 1352][Gitlin1, 275]. As well, it is a canonic structure and has been shown to be an optimal linear device for symbol-by-symbol detection [Gersho,

---

[1]Conventional equalizers are generally implemented at the receiver, a fact reflected in the following discussion. With the exception of sequence estimation, many of the techniques from this section are also applicable at the transmitter.

56-57] [Gitlin2, 491]. The sum of weighted signal samples, stored in a tapped delay line, is used by this FIR structure to form an output, implementing linear convolution of the filter coefficients and equalizer input [Sklar, 105].

Separating the linear equalizer into feed-forward and feedback filter sections yields computational savings [Cowan, 227-28]. In this arrangement, the feed-forward filter inverts precursors. The feedback filter acts as a *canceller*, removing postcursors from the feed-forward output.

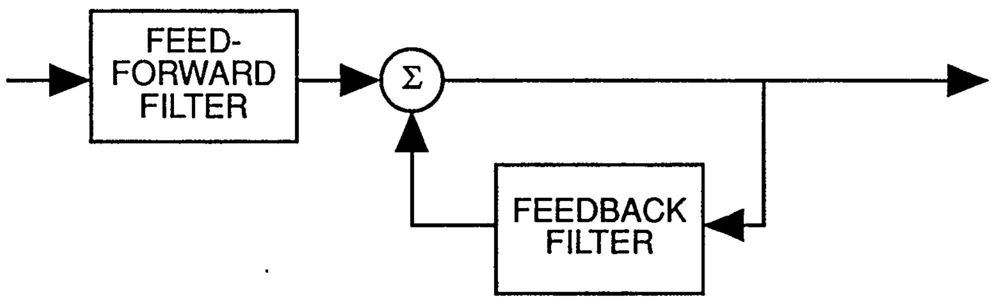

FIGURE 2.3. LINEAR FEEDBACK EQUALIZER

In a linear equalizer, each filter coefficient multiplies a noisy sample, potentially increasing noise power, a drawback from which linear equalizers suffer. This problem can become severe if the linear filter encounters a spectral null. Depending on the performance criterion, the equalizer may attempt to compensate by enhancing signal frequencies in the null's vicinity, thereby amplifying noise [Proakis2, 335]. Adding a decision slicer at the output of a linear equalizer can compensate for this problem. The filters and slicer are collectively called a decision feedback equalizer (DFE). Decisions from the slicer enter the feedback filter, which uses them to cancel postcursors. Because these decisions are noise-free, postcursor cancellation is more accurate with a DFE than a linear equalizer whilst the problem of noise enhancement by the feedback filter is avoided. These improvements, in turn, permit greater freedom in setting feed-forward filter taps [Qureshi, 1357]. This flexibility allows selection of feed-forward taps that will better avoid noise enhancement and compensate for aliasing distortion from poor selection of signal sampling phase [Feher, 655][Salz, 1471]. The latter phenomenon will be further dealt with in Section 4.3.7 on timing recovery.

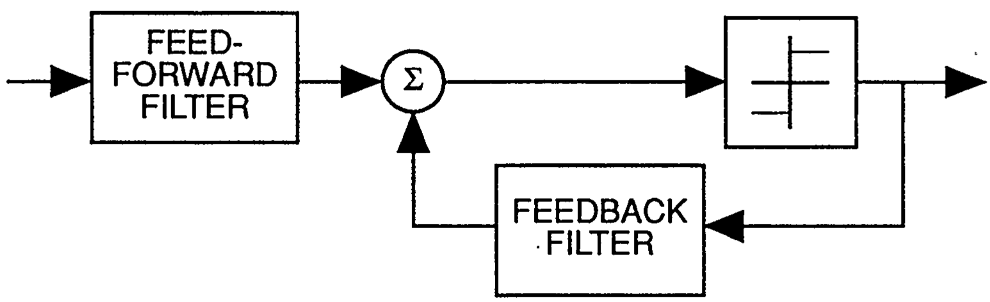

FIGURE 2.4 DECISION FEEDBACK EQUALIZER

A drawback of the DFE is its susceptibility to burst errors. These occur when an incorrect decision is made, generating additional errors as the spurious decision passes through the feedback filter in a process called *error propagation.* Duration of burst error sequences, although finite, is difficult to predict [Gitlin2, 508]. Because of its complex behaviour, error propagation is often ignored in analytic evaluations of error probability. If error propagation is neglected or the probability of an initial error is low due to mild channel conditions, the performance of a DFE is superior to linear equalization [Monsen, 62][Balaban1, 345].

Further performance improvements are possible through probabilistic detection of received signal sequences. Maximum-likelihood sequence estimation (MLSE), as the name suggests, is based on examining a sequence of received signal samples and determining the most probable transmitted data based on the *entire sequence* collectively rather than with symbol-by-symbol decisions [Forney2, 368]. Maximum-likelihood sequence estimation is the optimum detection algorithm for estimating received data, exceeding the performance of a DFE [Proakis2, 337][Fukawa, 548].

Sequence estimation exploits dependence between symbols, created at the transmitter by passing original data through a finite state machine, such as a convolutional encoder. Because of mutual dependence between symbols, only a subset of all possible sequences can actually be generated at the transmitter. Given the received sequence and, with knowledge of the channel, MLSE can be used to recover the transmitted data by selecting the nearest possible sequence to the one received.

Simplified but suboptimal MLSE can be implemented using the Viterbi algorithm. An efficient means of sequence estimation, the algorithm's performance does not come without a price. Relative to the linear equalizer or DFE, it is computationally intensive. Despite its superior performance, the simplicity of linear or decision feedback equalization often make these more attractive [Balaban2, 887].

2.3.2 Performance Criteria

Discussion of equalizer performance has so far been carried out without having defined an appropriate performance measure. For a data transmission system, an obvious performance criterion is *minimum probability of error* (MPE). This criterion will lead to the lowest bit error rate but is extremely difficult to apply in practice, requiring the solution of coupled non-linear equations [Belfiore, 1143] [Gitlin2, 489]. As a result simpler intermediate criteria are generally used.

The zero-forcing criterion (ZF) minimizes the peak ISI distortion, defined as:

$$D = \frac{1}{h(0)} \left(\sum_{k=-\infty}^{-1} |h(k)| + \sum_{k=1}^{+\infty} |h(k)| \right) \qquad (2.2)$$

where h(0) is the main sample of the channel impulse response and the first and second terms in brackets represent precursor and postcursor ISI, respectively. By forcing ISI to zero, the eye opening of a received signal becomes maximally open [Lucky1, 549]. An advantage of this criterion is its simplicity. This was an attractive feature when the criterion was first published in 1965 and signal processing capabilities were relatively crude. In future, the ZF will still be useful in applications where high speed (gigabits per second) is required [Gitlin2, 518]. A disadvantage of ZF is exhibited when ISI becomes severe (D>1), corresponding to closure of the eye pattern. In this event, the minimum value of D does not occur when ISI is zero and the effectiveness of zero-forcing is lost [Lucky1, 554]. The criterion also does not account for noise. Straightforward minimization of ISI with ZF can lead to noise enhancement [Forney4, 29].

An alternative performance criterion is minimum mean square error (MMSE), where error is defined as the Euclidean distance, in signal space, between the unsliced equalizer output and the ideal transmitted symbol. By minimizing the error at the equalizer output, this criterion accounts for both noise and ISI; the two are jointly minimized. MMSE is not identical to MPE, but the two have been shown to be equivalent in many situations [Monsen, 58].

2.3.3 Adaptive Equalization

The impulse response of the indoor wireless channel is dependent upon an often time-varying environment, making advance construction of a suitable equalizer almost impossible [Hashemi2, 968][Sexton, 115]. For optimal detection, *adaptive* equalizers must be used to dynamically update equalizer coefficients to suit the channel[1]. A training sequence known at the receiver is prefixed to data transmissions, allowing the equalizer to measure error and compensate for ISI using performance criteria described in the previous section to adjust tap weights.

If ISI is mild, a ZF adaptive algorithm can equalize the channel response with the lowest computational overhead. For each iteration, one addition operation per tap weight is required to descend the convex peak distortion function D [Lucky1, 557]. Convergence is slow, requiring on the order of 100 iterations [Gitlin2, 591]

Only a small increase in complexity allows the least mean square (LMS) algorithm to converge about one order of magnitude faster than ZF. This algorithm descends the MSE cost function based on an *estimate* of the statistics of the incoming data. One multiplication and addition operation is required each iteration for each tap weight. A low computational overhead has earned the LMS algorithm widespread usage [Qureshi, 1350]. However, the algorithm exhibits *excess* mean square error, the difference between the error from using adaptive

---

[1] Although some early literature draws a distinction between *automatic* equalization, relying on a training sequence, and *adaptive* equalization, relying on continual tracking of channel characteristics , this study will use the latter term for both cases [Lucky2, 256].

filter coefficients given by this algorithm and the error from using the optimum Wiener filter. This stems from the use of a noisy estimate of the error function gradient. Reductions in this excess MSE are achieved at the cost of slower coefficient convergence time [Haykin, 333-34].

Significant improvement in convergence time is possible with the recursive least squares (RLS) algorithm. Unlike the LMS, which descends an MSE function based on *estimated* statistics of the incoming data, RLS descends an MSE function using the *actual* values of received data [Cowan, 33][Haykin, 477-78]. If the channel is stationary and the training period infinite, an RLS trained equalizer will converge to the MSE of the Wiener filter. For any length training period where the channel is stationary and SNR is high, the RLS will exhibit an order of magnitude improvement in convergence time over LMS. However, the RLS is less effective tracking a non-stationary channel, even with an optimized forgetting factor which weights recently received data more heavily than older data [Haykin, 501]. There is a large increase in required computation to realize the performance improvements of the RLS algorithm. Required multiplications are on the order of N^2, where N is the equalizer length [Gitlin2, 591]. For large equalizer lengths, the complexity of the RLS algorithm can prohibit its use [Cowan, 34-35].

2.4 Motivation for Pre-Coding

Unless the channel characteristics are known in advance, distortion introduced by the channel is most easily identified, *a posteriori,* at the receiver. For this reason, it is the receiver where efforts to equalize the channel have usually been applied, an approach that can have drawbacks. Signal processing circuitry and the power it requires can oppose the goal of receiver portability.

Additionally, receiver equalization may enhance noise at the equalizer input, reducing the accuracy of symbol detection. Finally, the requirement that accurate decisions be fed back to a DFE can be troublesome. If an initial error is made, error propagation may occur. Another difficulty is the combination of a DFE and the Viterbi algorithm or other sequence estimator. Accurate decisions at the output of the sequence estimator are generally not available to feed to the DFE in time to be used by the feedback filter, a consequence of the processing delay of sequence estimation [Kasturia, 1086]. For these reasons, efforts have been made to move equalization operations from the receiver to the transmitter by implementing pre-coding [Kasturia][Pottie][Aman][Eyuboglu2][Eyuboglu1] [Laroia].

A distinction will be drawn between the operations of *pre-coding* and of *predistortion*, although they overlap and their difference is primarily one of emphasis. The emphasis of pre-coding is with combatting anticipated signal distortion due to transmission through a channel. These techniques are closely related to conventional methods of equalization. The focus of predistortion is on compensating for anticipated signal degradation from system hardware, particularly the transmitter amplifier [Karam]. Predistortion will not be dealt with in this study.

2.5 TH Pre-Coding Basics

A transmitter-based equalization technique was developed independently by Tomlinson and Harashima and Miyakawa in the early 1970s [Tomlinson] [Harashima]. Their design is known by a variety of names: the Tomlinson filter, the modulo-transmitter (MT) technique, the matched transmission (MT) technique generalized partial response and Tomlinson-Harashima (TH) pre-coding [Pitstick, 2006][Mazo, 348][Harashima, 774]. To reduce confusion, the term *TH pre-coding* will be used in this study.

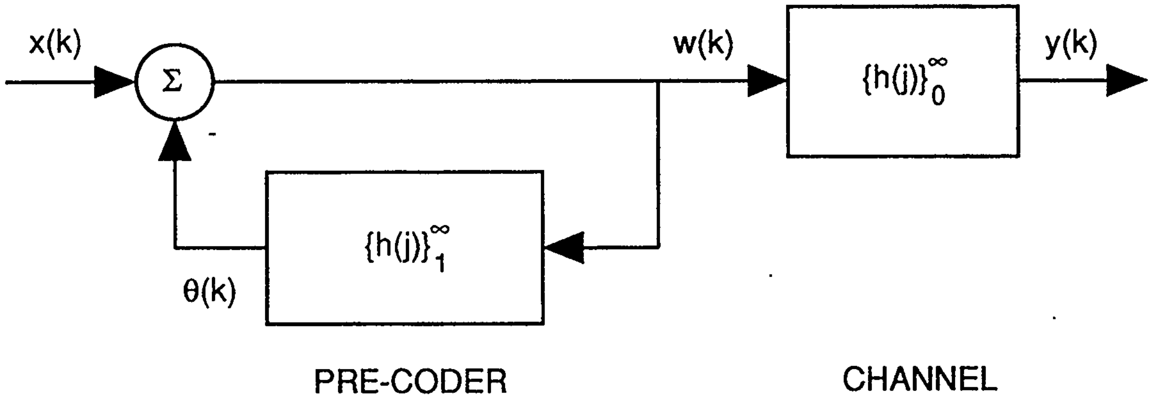

FIGURE 2.5 SIMPLE POSTCURSOR PRE-CANCELLATION

The basis of TH pre-coding is transmitter cancellation of postcursors introduced by channel ISI. For simplicity, assume the discrete time channel impulse response, h(k) is monic (h(0)=1) and causal (h(k)=0 for k<0). The channel output, y(k) can be given in terms of h(k) and the channel input w(k) as

$$y(k) = \sum_{j=0}^{\infty} w(k-j)h(j) = w(0) + \sum_{j=1}^{\infty} w(k-j)h(j) \tag{2.3}$$

Postcursor ISI is given by the term

$$\theta(k) = \sum_{j=1}^{\infty} w(k-j)h(j) \tag{2.4}$$

Knowledge of previously transmitted symbols is available at the transmitter. If the channel impulse response is also known, θ(k) can be calculated and pre-subtracted at the transmitter. The addition of postcursor ISI in the channel will, therefore, be nullified [Tomlinson][Harashima]. This method was originally developed for the 1D (PAM) case but also works for the 2D (QAM) case by straightforward extension.

Operation of this simple pre-coder can be represented as shown in Figure 2.5. Collapsing the feedback loop gives an equivalent system diagram shown in Figure 2.6

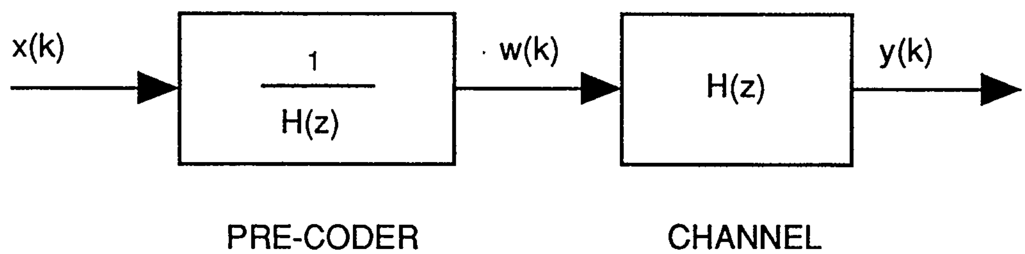

FIGURE 2.6 EQUIVALENT SIMPLE POSTCURSOR PRE-CANCELLATION

From Figure 2.6, it can be seen that the simple pre-coder inverts the causal channel. The simple pre-coder will be unstable if the channel is not invertible and the pre-coder output w(k) may increase without bound. Tomlinson and Harashima proposed an innovation to guarantee stability, the use of modulo 2M reduction.

The pre-coder output w(k) may be regarded as the sum of two terms:

$$w(k) = d(k) + n(k)V \tag{2.5}$$

where d(k) is a dither sequence, n(k) an integer and V a vector sum of integer multiples of lattice basis vectors. This equation represents the separation of the transmitted sequence into a continuous and a discrete part. Appropriate selection of n(k)V can guarantee that d(k) will be bounded within a given interval.

By accounting for the n(k)V at the receiver, only the bounded d(k) needs to be transmitted.

Tomlinson-Harashima pre-coding uses a modulo 2M reduction operator to eliminate n(k)V at the transmitter and account for it at the receiver, where M is the number of symbols along one dimension of a square QAM constellation. The operator acts upon each signal co-ordinate x according to the following rules:

if x>M	Subtract 2M the minimum number of times needed so that x<=M
if x<=-M	Add 2M the minimum number of times needed so that x>-M [Tomlinson, 138].

The placement of the modulo 2M reduction operator is shown in Figure 2.7. For QAM, this operator ensures that the transmitted symbol w(k) will be confined in signal space to the bounded square half-open plane given by the Cartesian product $(-M,M]^2$. A signal confined to this region will always have finite energy, even if the channel is not strictly invertible.

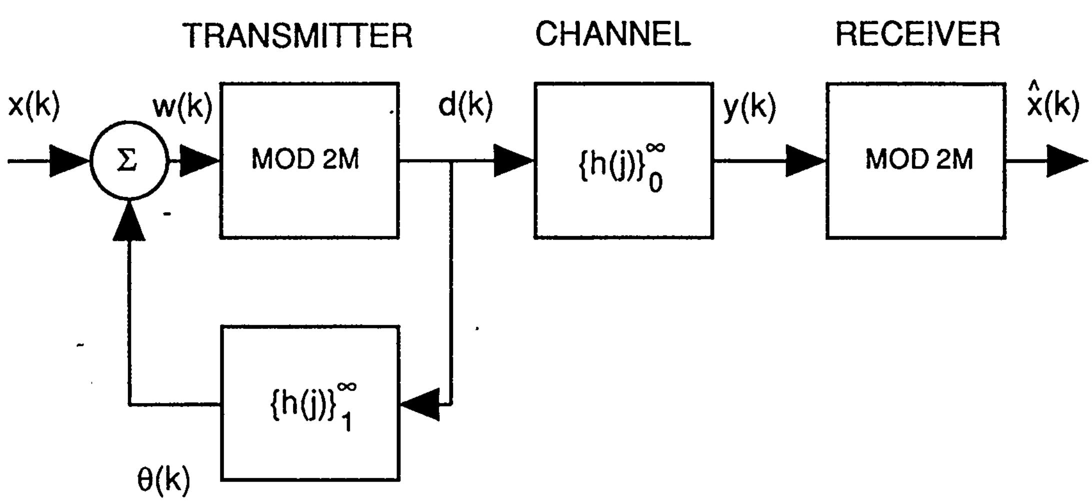

FIGURE 2.7 TH PRE-CODING BLOCK DIAGRAM

At the receiver, a matching modulo 2M reduction operator will "undo" the effect of the transmitter reduction operator. This may be shown, for the one dimensional case, where V is of length 2M, by the following set of equations:

$$
\begin{aligned}
w(k) &= x(k) - \theta(k) \\
&= d(k) + n(k)V \\
w(k) \bmod V &= d(k) \\
y(k) &= d(k) + \theta(k) \\
&= d(k) + \hat{x}(k) - d(k) - n(k)V \\
&= \hat{x}(k) - n(k)V \\
y(k) \bmod V &= \hat{x}(k)
\end{aligned}
\tag{2.6}
$$

The original data symbol x(k) is recovered at the receiver, free of postcursor ISI, with a simple modulo 2M reduction operation. Forcing ISI to zero using the error-free feedback values at the transmitter corresponds to an ideal DFE (no error feedback) using the ZF criterion.

2.6 A Feed-Forward Filter for Eliminating Precursors

Both the TH and DFE links require a feed-forward filter to remove precursors [Mazo, 349][Calderbank, 63][Belfiore, 1144-5]. This filter is necessary for complete elimination of ISI because the TH and DFE feedback filters cancel only causal postcursors. For optimal detection, the feed-forward filter should be located at the receiver where, in addition to eliminating precursors, it may whiten noise coloured by the receiver matched filter. Without this whitening operation, noise and signal power would tend to be concentrated at the same frequencies, reducing the accuracy of symbol detection [Gagliardi, 324-5].

In theory, there is no performance trade-off between precursor elimination and noise whitening functions. For a receiver filter perfectly matched to the joint transfer function of the combined transmitter filter and channel:

$$F(z) = H^*(1/z^*) \tag{2.7}$$

where F(z) is the receiver matched filter transfer function and H(z) is the combined transmitter filter and channel transfer function.

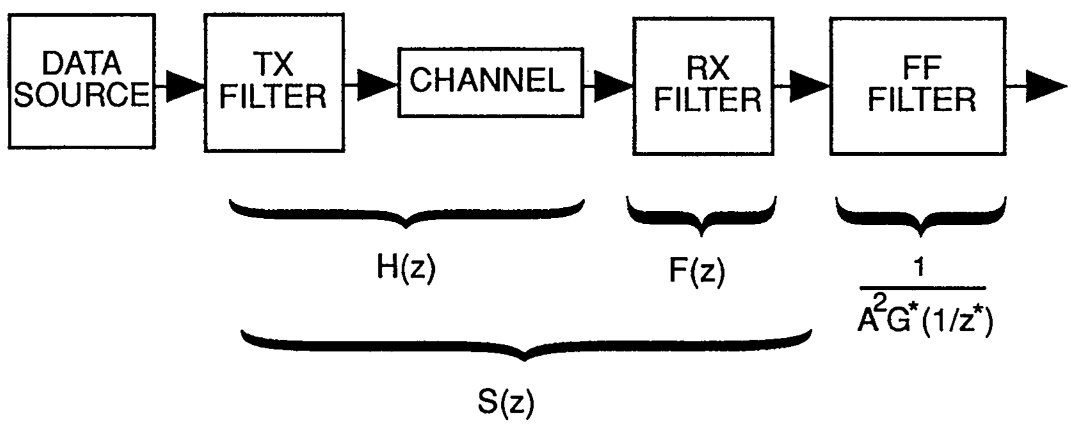

FIGURE 2.8 BASEBAND REPRESENTATION OF COMMUNICATION SYSTEM AND TRANSFER FUNCTIONS

The product of F(z) and H(z) is the inverse of the feed-forward filter transfer function, given by:

$$S(z) = H(z)F(z) = A^2G(z)G^*(1/z^*) \tag{2.8}$$

where A is a scaling factor equal to the geometric mean of S(z) about the unit circle [Lee, 31, 334]. The pair of functions F(z) and H(z) and the pair G(z) and G*(1/z*) are each formed by factoring the overall transfer function S(z) into two functions. Poles and zeros in one factored function are conjugate reciprocals of poles and zeros in the other pair member. Neither H(z) nor its matched transfer function F(z) is necessarily equal to AG(z).

A function with all its poles and zeros in the unit circle is called *minimum phase*. This property implies that the function is causal and, for all functions with the same frequency domain magnitude response, has the maximum concentration of energy around time zero [Oppenheim, 244-250]. A minimum phase response is more easily processed with a feedback canceller because precursors are already removed and there is minimum dispersion of energy in postcursors.

Neglecting the possibility of zeros on the unit circle, the allocation of poles and zeros between G(z) and G*(1/z*) is made so that G(z) is minimum phase. For F(z) and H(z), the allocation of poles and zeros is, in general, different than that between G(z) and G*(1/z*). The consequence of the foregoing is that the feed-forward filter can perfectly cancel precursors and whiten noise, at least in theory. Precursor cancellation occurs because the overall transfer function, including the feed-forward filter is:

$$G(z) = \frac{H(z)F(z)}{A^2 G^*(1/z^*)} = \frac{A^2 G(z) G^*(1/z^*)}{A^2 G^*(1/z^*)} \tag{2.9}$$

with G(z) a minimum phase function. Noise whitening occurs because white noise with single sided power spectral density (PSD) N_0 enters the system at the receiver input, encountering the transfer function

$$\frac{F(z)}{A^2 G^*(1/z^*)} \tag{2.10}$$

yielding a PSD at the feed-forward output of

$$\frac{N_0}{A^2} = N_0 \frac{F(z)F^*(1/z^*)}{A^4 G^*(1/z^*) G(z)} = \frac{N_0}{A^2} \frac{|S(z)|^2}{|S(z)|^2} \tag{2.11}$$

By equation 2.11, the PSD of the noise is scaled but retains its original flat shape.

In practice, there are a number of factors that inhibit effective precursor cancellation and noise whitening. *A priori* knowledge of the channel spectrum is generally not available; an adaptive algorithm, with attendant mean square error, is usually used to obtain feed-forward filter tap weights and compensate for mismatch between the overall impulse response, H(z) and F(z), the receiver filter. Often implemented as a transversal filter, the feed-forward filter may only approximate an ideal IIR feed-forward transfer function, assuming a spectral factorization of the signal transfer function into minimum and non-minimum phase functions is even possible. Length of the practical feed-forward filter is necessarily finite, creating the possibility of further divergence from the ideal filter function. Finally, alignment problems can arise. When these occur, the main sample of S(z) is incorrectly identified and, in addition to precursors, the feed-forward filter also attempts to cancel some postcursors or, alternatively, does not attempt to cancel every precursor. All of these circumstances will inhibit formation of the desired minimum phase function G(z) at the output of the feed-forward filter.

Unlike the ideal case, the practical feed-forward filter must trade-off the treatment of noise and precursor removal. An FIR filter will amplify noise power by the sum of the squares of the filter magnitudes [Hamming2, 12-18]. This contrasts with the noise power at the output of the ideal feed-forward filter, $\frac{N_0}{A^2}$, where A is fixed as the geometric mean of S(z) around the unit circle. In the practical case, adjustment of the feed-forward coefficients to reduce precursors can enhance noise. The converse is also true. The relationship between noise enhancement and precursor reduction is complex; calculation of their joint minimum requires, in addition to other steps, inversion of the autocorrelation function of the input sequence [Cowan, 16-17].

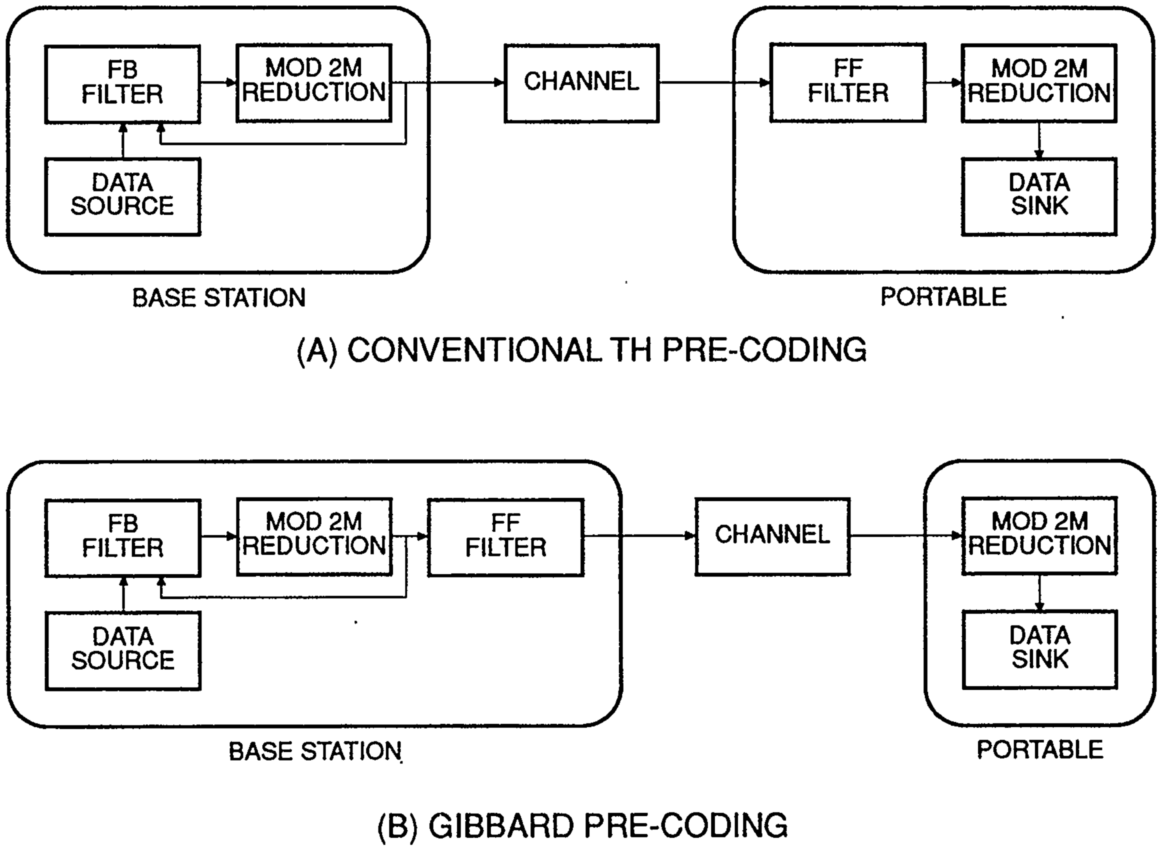

FIGURE 2.9 COMPARISON OF CONVENTIONAL TH AND GIBBARD PRE-CODING

To simplify portable receiver circuitry, Gibbard located the feed-forward filter at the transmitter instead of the receiver [Gibbard1, 41-3]. Allowing both precursors and postcursors to be removed at the transmitter, this innovation is consistent with the goal of asymmetric communication, namely concentration of processing complexity at the base station. The Gibbard structure shown in Figure 2.9 will be used for the study herein. To distinguish this structure from conventional TH pre-coding, the former will be referred to as a *Gibbard pre-*

coder, which may be regarded as a member of the general class of TH precoders.

With the feed-forward filter located at the transmitter, the opportunity for noise whitening at the receiver is sacrificed. Under this arrangement, noise need not be considered in the design of the feed-forward filter as noise is not present at the transmitter. At first blush, the ZF criterion may suggest itself for deriving the transmitter feed-forward filter coefficients, a criteria which attempts only to minimize peak ISI. Oddly enough, an feed-forward filter, derived at the receiver using the MMSE criterion, may also be helpful at the transmitter, providing the line of reasoning which follows below is accurate.

The usual weakness of the ZF criterion is it yields a feed-forward filter that attempts to compensate for precursor-causing selective fades in the channel spectrum by enhancing signal power at the fading frequencies. At the receiver, signal enhancement by the ZF feed-forward filter will also enhance noise. This suggests that, if moved to the transmitter, the ZF feed-forward filter will direct more signal power to the fades, power that may be wasted if the fade is sufficiently deep.

On the other hand, the MMSE criterion tends to avoid these drawbacks. Used at the receiver, this performance criterion will balance efforts to reduce ISI with the noise enhancement that may result from such reduction. An identical MMSE feed-forward filter, used at the transmitter, would restrain the expenditure of signal energy in selective fades by its tendency to avoid direct inversion of precursor caused selective fades. The objectives of noise minimization at the receiver and transmit power minimization at the transmitter are accomplished by the same MMSE feed-forward filter. For this reason, MMSE feed-forward receiver coefficients, if available, should be used by the TH pre-coding system to cancel precursor ISI and limit transmitter output power. Of course, as SNR becomes large, the ZF and MMSE criteria converge and this advantage would be lost. Simulation results will be presented in Section 5.6.2 to help justify this conclusion.

2.7 TH Pre-Coding Performance

2.7.1 Error Performance

The bit error probability for data transmitted over a TH link is determined by a variety of coupled, sometimes nonlinear, phenomena. The complexity of the system behaviour precludes the derivation of a closed form expression for error probability. For the most part, the descriptions given here will be qualitative rather than quantitative.

Noise is the most obvious source of error and is usually modelled as having a random Gaussian amplitude distribution and a flat (white) frequency distribution. Although some practitioners of the art collect all sources of distortion under the rubric of noise, this study will distinguish between distortion which is deterministic, such as that due to ISI or spectral shaping by filters, and distortion which is random due to background radiation in the wireless channel, interference from other users as well as thermal, shot and partition effects in electrical components [Jeruchim, 480][Stremler, 192]. Only the latter distortion will be referred to as noise.

The effect of noise on bit error probability is easily calculated for TH pre-coding using a square QAM signal constellation. At the receiver, the modulo 2M reduction operator accepts points y as input, defined as:

$$y = \{ y_x + a2M,\ y_y + b2M : a,b \in Z,\ -M < y_{x,y} \le M \} \qquad (2.12)$$

where a and b are taken from the set of integers, Z. Points y are mapped to points x where

$$x = \{ y_x, y_y \} \qquad (2.13)$$

Prior to modulo 2M reduction, the two dimensional interval $(-M,M]^2$ containing the signal constellation is repeated periodically in an infinite 2D grid; the reduction operator translates all these subspaces to the interval centred at the origin. A subset of the extended constellation, at the input to the modulo 2M reduction operator, is shown in Figure 2.10 for a 4 QAM constellation.

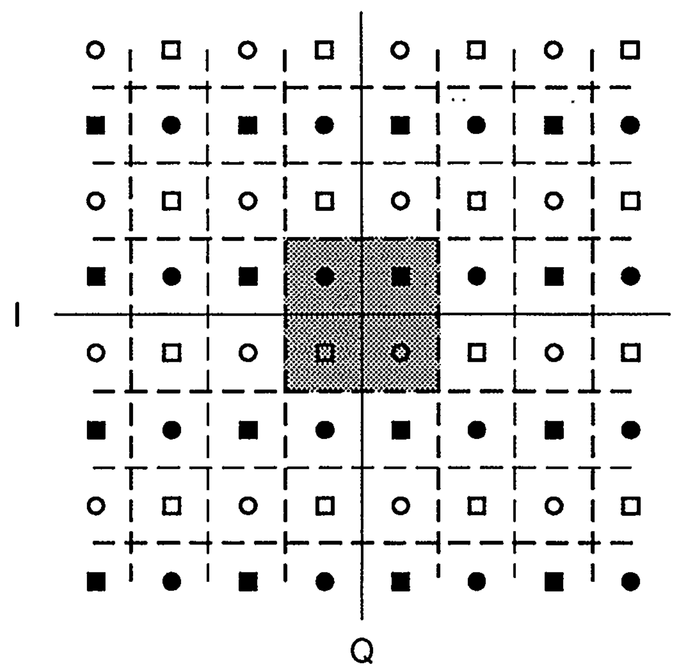

FIGURE 2.10 4 QAM SIGNAL CONSTELLATION (SHADED) SHOWING VORONOI CELLS AND PERIODIC EXTENSION

Each ideal symbol has a surrounding Voronoi cell, consisting of all points at least as close to it as to any other symbol [Conway, 33]. Received symbols are classified according to the Voronoi cell of the ideal constellation in which they lie. The probability of error is simply the probability that a noise sample will have sufficient power to push a received symbol into the Voronoi cell of another symbol, as represented in Figure 2.11.

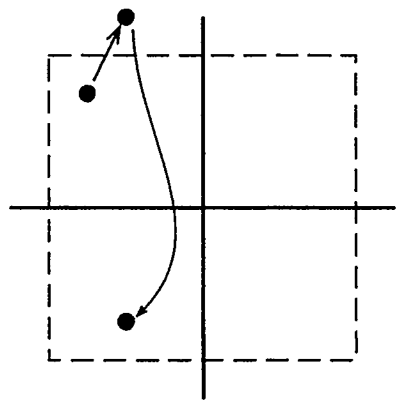

FIGURE 2.11 DATA FLIPPING CAUSED BY MODULO 2M REDUCTION

In TH pre-coding, the phenomenon of "data flipping" occurs when noise pushes a symbol outside the boundaries of the $(-M,M]^2$ interval. In this event, the modulo 2M reduction operator 'flips' the symbol about one or both axes and an error occurs because the symbol falls outside its own Voronoi cell. If TH pre-coding and the modulo 2M reduction operator are not used, the signal constellation is aperiodic. In the aperiodic case, symbols on the perimeter of the constellation have greater immunity from noise because of their lower *kissing number,* the number of nearest neighbours. For a non pre-coded constellation, the kissing number of a *perimeter* symbol is two for corner symbols and three otherwise, as shown in Figure 2.12. For TH pre-coding, the kissing number of a symbol, perimeter or not, is always four. Larger constellations, where there are proportionately fewer symbols on the perimeter of the constellation, have a smaller likelihood of data flipping and the advantage of non pre-coded over pre-coded transmission is diminished.

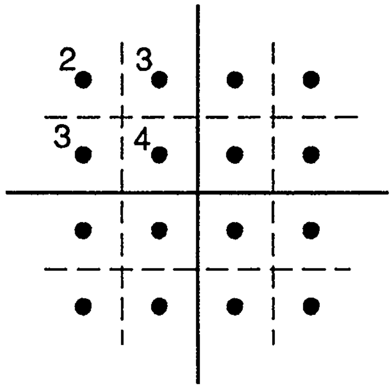

FIGURE 2.12 16 QAM WITH KISSING NUMBERS

Correcting for an omitted square root function and neglecting a filter efficiency factor, an estimate of the BER for non pre-coded QAM transmission over a Gaussian noise channel is given by [Korn2, 366]:

$$P_b(e) = \frac{2(1-\frac{1}{M})}{\log_2 M} Q\left(\sqrt{\frac{3\log_2 M}{M^2-1}\frac{2E_b}{N_0}}\right) \quad (2.14)$$

Where

$P_b(e)$ is the bit error probability;
M is the number of symbol levels in each dimension;
Q(x) is the Gaussian distribution tail probability; and
$\frac{2E_b}{N_0}$ is the SNR per bit.

This formula applies to Gray coded symbols from the set {±1,±3,±5±, ...,±(M-1)}. The $1-\frac{1}{M}$ value in the leftmost term accounts for the lower kissing number of symbols on the constellation perimeter. By omitting this term, the probability of errors caused by noise is given, for a TH pre-coded system, by:

$$P_b(e) \;=\; \frac{2}{\log_2 M}\, Q\left(\sqrt{\frac{3\log_2 M}{M^2-1}\,\frac{2E_b}{N_0}}\right) \tag{2.15}$$

Equations 2.14 and 2.15 differ by a factor of $1-\frac{1}{M}$, a factor due to TH data flipping. The non pre-coded error probability will be lower than the TH error probability by this factor, equal to 3/4 for the case of 16 QAM (M=4).

Despite a reduced noise margin, TH has a compensating advantage over DFE at the receiver, immunity from error propagation. A decision error made by the DFE will pass into the feedback filter where it will increase the probability of errors in subsequent decisions. This raises the possibility of a long sequence of incorrect decisions. These error sequences are unlikely to continue indefinitely. For moderate ISI and high SNR, the maximum increase in error probability for binary signals has been shown to be, at most, 2^N, where N is the number of feedback taps [Gitlin2, 508]. This upper bound is based on the number of random feedback symbols needed to produce the correct symbol sequence in the feedback filter. Using the 2^N bound, a BER increase exceeding one order of magnitude may result from error propagation in a feedback filter of length greater than three. In practice, the problem of error propagation is less than suggested by this bound. The BER performance disadvantage of a DFE compared to a TH pre-coder, which is immune from error propagation, has been found to disappear at low bit error rates ($<10^{-5}$) [Aman, 881].

Along with noise, a major source of error in a TH pre-coded system is uncancelled ISI. Some, but not necessarily all, ISI is eliminated by the TH pre-coder and feed-forward filter at the transmitter. Residual ISI persists for two reasons. The feed-forward and pre-coder feedback filter may not have sufficient length to invert or cancel ISI. In addition, their coefficients may be noisy and therefore suboptimal.

Recognizing the origin of residual ISI, it becomes evident that neither its probability distribution nor its contribution to the bit error rate is easily calculated, especially with the added complication of a time varying channel. In such circumstances, computer simulation is an accepted means of determining bounds on system performance [Tranter, 26]. Results of such simulations are presented in Chapter 5. However, general performance characteristics can be noted based on the preceding discussion. With larger signal constellations that reduce the impact of 'data flipping' and in the absence of error propagation, TH pre-coding and DFE will have approximately the same performance [Eyuboglu2, 13][Eyuboglu1, 301][Messerschmitt, 1251].

2.7.2 Power Performance

Boundedness of the transmitted signal power is guaranteed by the modulo 2M reduction operator. This operator confines its output to the half-open plane $(-M,M]^2$. For a fixed constellation, reducing the boundaries of this half-open plane also reduces the area of the Voronoi cells for symbols on the constellation perimeter, resulting in a decreased noise margin. To provide some protection against unwanted data flipping, the modulo 2M reduction half-open plane must at least exceed the size of the ideal symbol constellation. The larger dimension of this region leads to an increase in transmit power compared to the non pre-coded case.

For equiprobable, independent symbols, upper and lower bounds on average power transmitted from a TH pre-coder were established by Mazo and

Salz [Mazo]. Transmitted TH pre-coded symbols can be regarded as a modulo 2M reduced version of the ideal signal constellation from which a random variable, θ, representing postcursor ISI from previously transmitted signals, has been subtracted. The probability distribution of *transmitted* symbols about each symbol in the *ideal* signal constellation, given by θ, will be identical. The minimum possible transmitted energy results when θ is zero; the maximum occurs when θ is sufficient to push the signal constellation to the boundaries of the $(-M,M]^2$ region. Minimum and maximum energy transmitted signal constellations are shown in Figure 2.13 for 16 QAM.

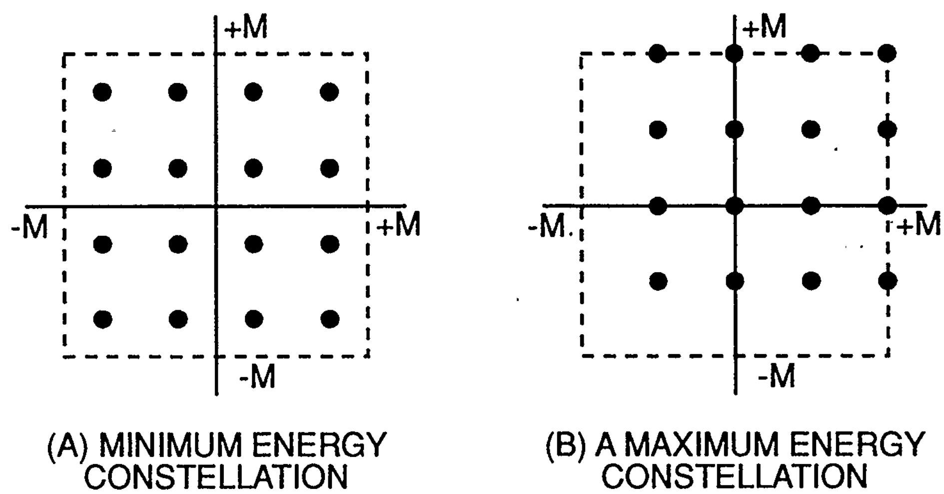

FIGURE 2.13 MODULO 2M REDUCTION
OPERATOR OUTPUT CONSTELLATIONS

Other possible maximum energy constellations can be achieved by rotating the constellation in Figure 2.13 (B) through multiples of 90°.

For rectangular M-level QAM subjected to TH pre-coding, the upper and lower bounds on average transmitted power are:

$$2\left(\frac{M^2-1}{3}\right) \leq P \leq 2\left(\frac{M^2-1}{3}\right) + 2 \tag{2.16}$$

The lower bound corresponds to the power in a non pre-coded signal constellation, indicating that savings in average transmit power are not possible with TH pre-coding when symbols are equiprobable and independent. The upper bound represents only a modest increase in transmitted power for a large constellation. For 16 QAM, the interval is [10,12]. Thus, the maximum increase in the transmitted power of TH pre-coded symbols over non pre-coded symbols at the output of the modulo 2M reduction operator is 0.79 dB. The lower bound can be reached for certain partial response channels and for channels in which the precursors and postcursors are integer multiples of the main sample. In these cases, the signal constellation will be identical before and after pre-coding [Kasturia, 1087]. Tightness of the average transmitted power bound demonstrates that power distribution at the pre-coder output is nearly independent of the channel impulse response [Harashima, 778].

If the constellation of the pre-coder *input* signal has a shape other than square, the shape cannot be preserved. The redistribution of the signal over the $(-M,M]^2$ boundary region by the pre-coder will make the increase in transmitted power even more significant than a square input constellation [Eyuboglu1, 306]. Efforts to overcome the restriction of the transmit signal space to a square region and overcome this region's relatively high peak-to-average transmit power ratio are described in Section 2.7.3 on *shaping.*

Pitstick and Cruz have developed an algorithm for calculating the increase in transmitted power for the case when the symbol distribution is not uniform [Pitstick]. These bounds are looser than those of Mazo and Salz, tightening as the variance of the symbol probability distribution increases. This makes intuitive sense because non-uniform symbol probability distribution permits the distribution of symbols to be concentrated in either higher or lower energy regions of the domain $(-M,M]^2$. The method of Pitstick and Cruz applies to independent symbols. For coded systems, where independence between symbols may not exist, bounds on average transmitted power have not been established.

The issue of Gibbard pre-coding's transmit power is also unresolved. This structure is realized with the addition of a feed-forward filter directly at the output of a conventional TH pre-coder. In compensating for precursor ISI, the feed-forward filter may amplify the signal. The amplification factor is determined by the filter coefficients, themselves derived from the channel impulse response. A bound on Gibbard pre-coder transmit power is thus channel dependent. Simulation results, presented in Chapter 5, will provide an indication of the power amplification that might be expected, with a feed-forward filter at the transmitter, for transmission over the indoor channel.

An important figure of merit for the Class A or B transmit power amplifiers generally employed for amplitude modulation is the peak-to-average power ratio ξ. Efficiency of a Class A amplifier is inversely related to ξ by the equation [Krauss, 510]:

$$\eta = \frac{1}{2\xi} \tag{2.17}$$

For a Class B amplifier, efficiency is still affected by the peak-to-average ratio, albeit less strongly. The equation for a Class B amplifier is [Krauss, 511]:

$$\eta \approx \frac{\pi}{4}\frac{1.048}{\sqrt{\xi}} \tag{2.18}$$

Peak-to-average transmit power measurements will also be presented in Chapter 5 as an indicator of the power amplifier efficiency associated with Gibbard pre-coding.

At the receiver, symbols undergo a modulo 2M reduction operation to restore the ideal signal constellation. By mapping the received symbols into a smaller domain, the modulo 2M reduction operator sacrifices some of the received signal power. This is an unavoidable consequence of the need to undo the modulo 2M reduction applied at the transmitter. As a result, the increased transmit power required for TH pre-coding does not in itself lead to any reduction in error probability. While noise power, too, is bounded by the modulo 2M reduction operator, in practice, this effect is of little consequence because SNR would have to be well below any reasonable operating level (noise standard deviation approaching 2M) for modulo 2M reduction to restrict its power.

2.7.3 Shaping

Shannon's classic equation for channel capacity on a Gaussian noise channel provides the theoretical basis for shaping gain.

$$C = B\ \log_2(1+\mathrm{SNR}) \tag{2.19}$$

Capacity, in bits per second, is given for a channel with a specified bandwidth B and SNR [Stremler, 505]. A more complex relation exists for the capacity of an ISI channel, but the expression above will suffice as it shows capacity increasing with SNR, a generally true result [Gitlin2, 129].

The objective of shaping is to narrow the gap between channel capacity and actual data rate by altering the signal constellation, without sacrificing BER performance. If the average transmit power can be lowered by rearranging the signal constellation without reducing the Euclidean distance between symbols, error performance will be preserved while SNR, and consequently channel capacity, will decline. An alternate means of narrowing the gap between the actual data rate and the maximum rate C is through coding to reduce the BER, but this falls outside the realm of constellation shaping.

Reductions in average transmit power can be accomplished by moving symbols, as much as distance requirements permit, towards (0,0), the lowest energy point in 2D signal space. In the optimum case, the symbol probability distribution will be Gaussian about the origin. For two signal constellations occupying the same space, the maximum possible shaping gain is $\pi e/6$ or 1.53 dB. This is achieved by a spherical constellation in a signal space of infinite dimensions [Lee, 666]. In the two dimensional case, the maximum possible shaping gain for a *fixed* constellation area is only 0.2 dB. Performance gain beyond this figure is possible if constellation area can be reduced without sacrificing distance properties.

Attention has been focussed on the apparently meagre gains available from constellation shaping because the opportunity for more easily achieved performance improvements, such as through trellis coded modulation, have been exhausted. In some cases, shaping gain is the path of least resistance on the journey towards Shannon's theoretical channel capacity [Eyuboglu1, 32].

Shaping gain and TH pre-coding have often been considered incompatible because of modulo 2M reduction [Laroia, 1460][Forney4, 32]. Regardless of the signal constellation at the pre-coder input, the boundary regions of the transmit signal space are square at the pre-coder output, nullifying any attempt to achieve constellation shaping. Kasturia and Cioffi have proposed alternative boundary regions for the TH transmit signal space, using an hexagonal lattice. This lattice is an approximation to a circular distribution, the optimum distribution for shaping gain [Kasturia]. Points outside the shaded region V_0, shown in Figure 2.14, are mapped into V_0 with a modulo V_0 reduction.

A disadvantage of the hexagonal lattice is the difficulty in implementing a modulo V_0 reduction operator. The input to the modulo V_0 operator at the receiver and transmitter will not be neatly distributed at the discrete points shown in Figure 2.14 but will have a continuous distribution over R^2. Linear combinations of integer scaled lattice basis vectors can be used to translate a point **w** from a region V_k ($k \neq 0$) to the corresponding point in V_0. However, this requires the identification of the V_k to which the point **w** belongs. This is not an easy task when the distribution of points is continuous and especially when **w** lies close to the boundaries between regions. In contrast, a modulo 2M reduction is easily implemented as a simple overflow or shift operation performed on a binary number to extract least significant bits [Messerschmitt, 1254].

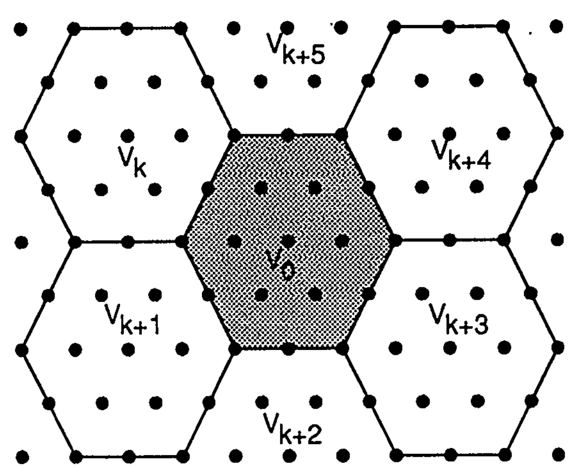

FIGURE 2.14 HEXAGONAL TH BOUNDARY REGIONS

In the configuration proposed by Gibbard, where the feed-forward filter is placed in the transmitter, at the output of the pre-coder, shaping gain is particularly unfeasible. Even if TH shaping gain could be realized at the pre-coder output using hexagonal boundaries, the feed-forward filter would alter the signal distribution and eliminate the gain.

2.7.4 Spectrum

In the absence of modulo 2M reduction, the TH pre-coder would be a simple feedback filter, subtracting weighted values of previously transmitted signals from the pre-coder input. This simple structure would implement an autoregressive process with a concomitant correlation between neighbouring elements of the filter's output sequence and shaping of its spectrum.

When modulo 2M reduction is present, there is a non-linear, randomizing effect which tends to remove correlation introduced by the filter as well as any correlation already present in the input sequence. The spectrum of the pre-coder output sequence will thus be, to some degree, flattened and spread [Tomlinson, 139]. In the extreme case of independently and uniformly distributed input the pre-coder output will also be independently and uniformly distributed [Mazo, 349] [Harashima, 778]. Put simply, the pre-coder will not alter an already flat spectrum at its input. In the practical case of input data drawn from a discrete signal constellation, the effect of pre-coding on the spectrum is less certain, although it is thought the spectrum of signals based on large constellations is not significantly altered [Eyuboglu1, 313][Trachtman, 821].

For the case of a feed-forward filter placed at the pre-coder output, the signal spectrum may undergo significant shaping prior to transmission. The shaping is dependent upon the spectrum of the channel and the precursors it creates. As described in Section 2.6, the feed-forward filter will attempt to invert that part of the channel transfer function responsible for precursors. The signal spectrum created by the feed-forward filter at the transmitter, although not identical, will bear some similarity to the inverse channel.

2.7.5 Hardware Requirements

Moving the equalizer from receiver to transmitter with TH pre-coding allows the signal processing burden to be shifted without an appreciable impact on the overall signal processing requirement. A minor increase results from the modulo 2M reduction operators required at both transmitter and receiver. Modulo reduction is easily accomplished by extracting the least significant bits of a value stored in binary format, the reverse of a slicer, which quantizes by extracting the most significant bits.

An additional overhead is imposed by the continuous distribution of transmitted signals over the $(-M,M]^2$ region. The pre-coder feedback filter requires sufficient numerical precision to represent these continuous values. In contrast, the feedback filter of a receiver-based DFE accepts input from a slicer, inputs quantized to the discrete values of the ideal signal constellation and representable by fewer bits [Messerschmitt, 1251][Kryzmien, 24]. If the filter is short, the requirement for increased numerical precision in the feedback section is not a significant burden as the signal processing architecture of the feed-forward filter, which requires numerical accuracy to deal with continuous input values, can simply be extended to the feedback section.

2.8 Relationship of TH Pre-Coding and Partial Response Signalling

Partial response signaling is a form of frequency efficient pulse shaping. Compared to a Nyquist pulse shape, with zeros at every symbol spaced interval from its centre, a partial response pulse shape is integer valued at multiple symbol spaced intervals, thus introducing controlled levels of ISI between transmitted symbols. So-called because a single symbol period only partially covers the non-zero sampling intervals, partial response signalling introduces a correlation between transmitted symbols that reduces the bandwidth required by the data signal at the price of increased transmit power [Korn2, 144][Sklar, 106] [Gitlin2, 59].

At the receiver, the partial response pulse shape is known and its value at symbol spaced intervals can be used as coefficients in a decision feedback filter. With past decisions as its input, this filter can subtract ISI from incoming data signals, yielding the desired ISI-free symbol. As in the case of a DFE, this arrangement is subject to error propagation, providing motivation for partial response pre-coding.

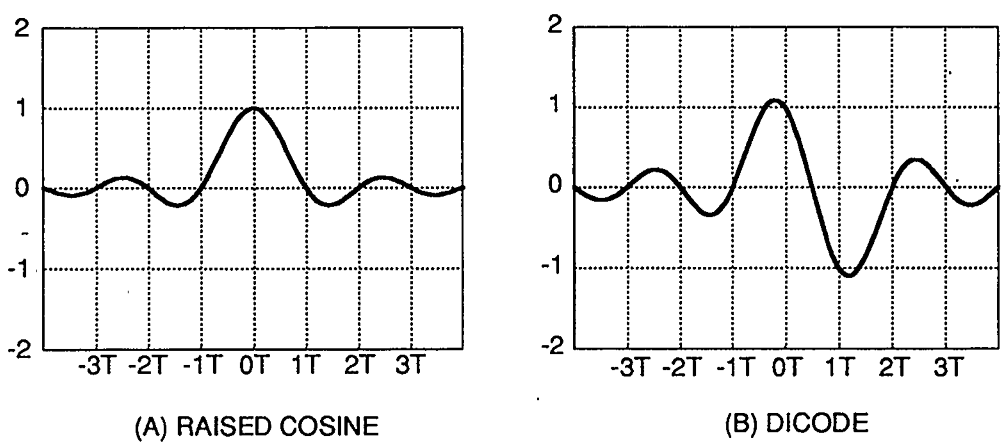

FIGURE 2.15 NYQUIST AND PARTIAL RESPONSE PULSE SHAPING

Like the TH case, partial response pre-coding uses a feedback filter at the transmitter, storing past transmitted signals to subtract anticipated ISI, in this case the ISI that will be introduced by the partial response pulse shape. A modulo reduction operator, previously shown to be invertible at the receiver, can be used to ensure boundedness of transmitted symbols [Sklar, 107]. Unlike the TH case, this modulo reduction operator fits the strict mathematical definition of the modulo function, meaning it maps to the range [0,n), $n \in Z$. Partial response pre-coding can be replaced with the more sophisticated pre-coding of Tomlinson-Harashima. In this case, the "channel" ISI removed by TH pre-coding is extended to include ISI caused by partial response signalling and other filters. Tomlinson-Harashima pre-coding has been shown to achieve bandwidth efficient, low error probability performance in removing partial response pulse shaping ISI when multipath effects from the wireless channel itself are neglected [Trachtman].

The transmitted partial response signals can only have integer values at sampling intervals as a result of the integer valued ISI introduced by the pulse shape. This can also be true of TH pre-coding, in the unlikely case of integer valued channel ISI with modulo 2M reduction along integer valued boundaries, although TH pre-coding is also applicable to the continuous valued case [Harashima, 774]. Partial response pre-coding can be regarded as a special case of TH pre-coding, and TH pre-coding is sometimes called "generalized partial response" [Mazo][Messerschmitt].

A common feature of both partial response signalling and TH pre-coding is the increase in average transmit power resulting from increased dimensions of the transmit signal space. TH pre-coding does not, however, possess the spectral advantages of partial response signalling. Unlike partial response signalling, the ISI in TH pre-coding is not strictly controlled and generally does not produce a smooth, gently-sloping pulse shape. Tomlinson-Harashima transmitted signals are usually continuous-valued over the range $(-M,M]^2$ in a pseudo-random distribution that inhibits both power and spectral efficiency [Tomlinson, 139][Forney4, 30].

2.9 TH Pre-Coding and Trellis Coding

The cascade of a trellis encoder and an ISI channel can be regarded as a finite state machine. As such, MLSE can provide accurate recovery of transmitted data. For optimum MLSE, a whitening matched receiver filter is needed to maximize signal power and flatten the noise spectrum [Forney2, 366-67]. For a channel impulse response that is not known *a priori*, the whitening, matched filter characteristic can be provided by an adaptive equalizer. Additional equalization may be necessary to simplify the joint encoder/ISI trellis by reducing ISI. Alternatively, equalization may be needed to force the channel to an impulse response used by the Viterbi algorithm or, if a joint encoder/ISI trellis is not desired, to eliminate ISI altogether.

A linear equalizer in front of the Viterbi decoder can result in significant noise amplification for a channel possessing spectral nulls. Noise amplification by a DFE will be much less significant but a combination of a DFE and Viterbi decoder is difficult to achieve. If the input to the DFE feedback filter is taken from the output of the Viterbi decoder, the input will not be available soon enough for subsequent DFE calculations because of the decoder's processing delay. If the input to the DFE feedback filter is taken directly from the output of the DFE decision device, errors will reduce the distance properties of the trellis and degrade performance of the Viterbi algorithm [Aman, 876]. Decision errors and error propagation due to the DFE are especially likely if trellis coding is used because the expansion in the signal alphabet reduces the Euclidean distance between individual symbols. Various remedies, implemented at the receiver, exist for these problems, at the price of increased complexity and possible performance degradation [Krzymien, 21]. Another solution, implemented at the transmitter, is available in the form of TH pre-coding.

The combination of TH pre-coding and trellis decoding has significant advantages. TH pre-coding allows accurate elimination of ISI without the problem of error propagation. Apart from the TH pre-coder, the Viterbi algorithm and the DFE feed-forward filter, retained at the receiver to perform whitening matched filtering, no additional complexity is required to join these structures. With the exception of an increase in transmit power due to the pre-coder, the combination of TH pre-coding and trellis coding realizes the full processing gain available from each structure individually [Aman, 879]. Furthermore, the signal set expansion due to trellis coding narrows the difference, for small signal constellations, between the transmit energy of pre-coded and non pre-coded signals [Pottie, 868].

A potential complication stems from the modulo 2M reduction operator at the receiver. Placing this operator after the Viterbi decoder adds to complexity by increasing the number of sequences which the decoder must account for. Placing this operator prior to the decoder raises the possibility of unwanted modulo 2M reduction operations, or data flipping, due to noise. Such an event would affect distances between sequence paths and cause errors to propagate to other symbols, somewhat akin to the consequences if an incorrect decision from a receiver DFE is fed into the Viterbi decoder. A simple and effective remedy is to wrap the $(-M,M]^2$ boundary region back onto itself, effectively joining opposite borders of the boundary region, by calculating branch metrics modulo 2M [Pottie, 868].

Researchers at both AT & T Bell Labs and Motorola Codex have implemented a combined TH pre-coding and trellis decoding for data transmission over a copper HDSL line, verifying that this configuration offers significant gains in performance [Aman][Pottie].

2.10 Other Forms of Pre-Coding

2.10.1 Trellis Pre-Coding

Trellis coded modulation, combined with TH pre-coding and techniques for achieving shaping gain yields a system known as a trellis pre-coder. The

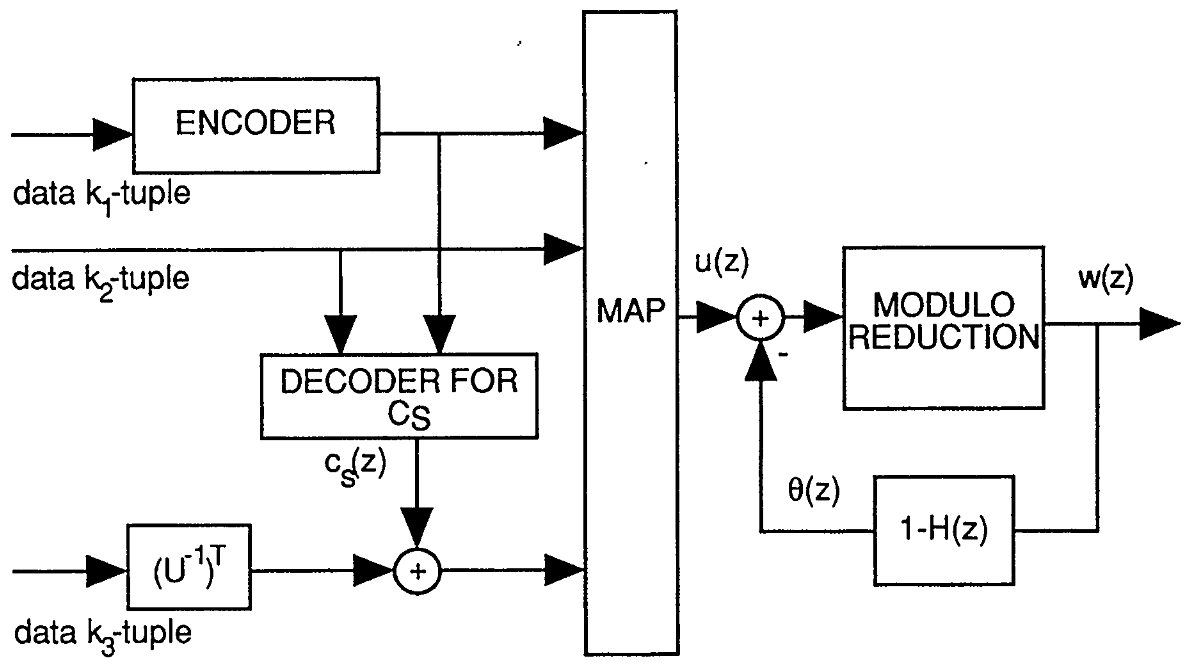

FIGURE 2.16 TRELLIS PRE-CODING TRANSMITTER

motivation for this system is to achieve the advantages of trellis coding and TH pre-coding with the added benefit of shaping gain to minimize transmit power. Apart from the fact that TCM is an essential component, trellis pre-coding is distinguished from TH pre-coding by the introduction of a shaping decoder. Trellis pre-coding is described in [Eyuboglu1] from which the following explanation is derived.

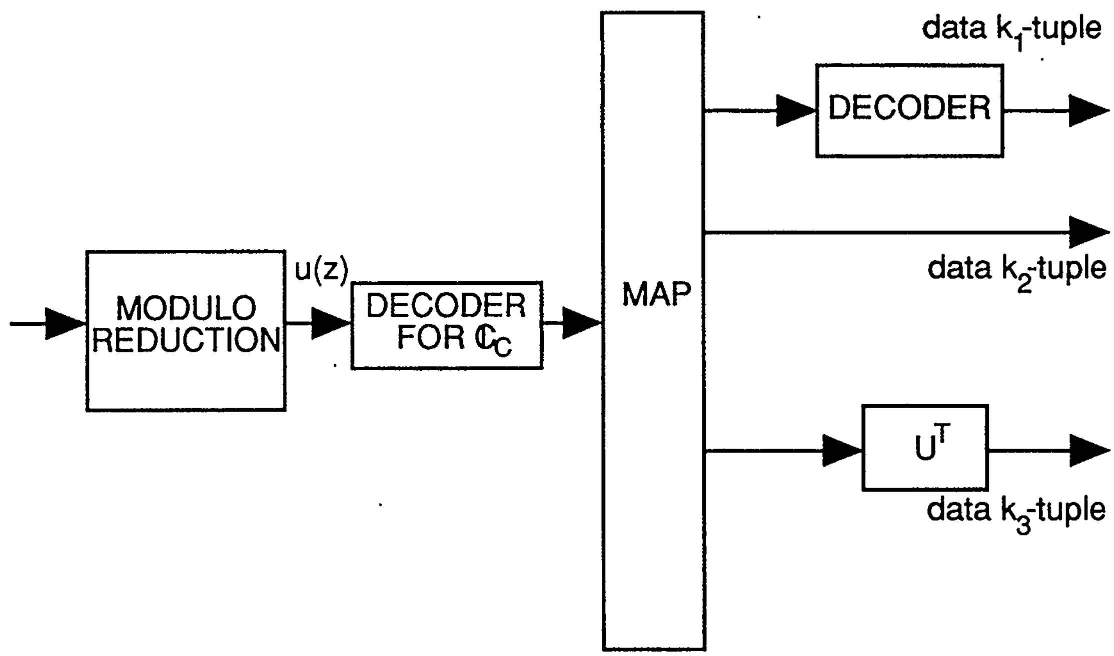

FIGURE 2.17 TRELLIS PRE-CODING RECEIVER

The shaping decoder shown in Figure 2.16 chooses a shaping sequence $c_S(z)$ from a shaping code C_S. The shaping sequence is used to modify the mapper's input bit sequence, itself taken from a trellis coset code $\mathcal{C}_C$. The bit sequence is changed to minimize the transmit energy of w(z) while ensuring that the bit sequence will still belong to $\mathcal{C}_C$. Due to the latter constraint, a Viterbi algorithm, configured for $\mathcal{C}_C$, can be used at the receiver to decode the bit sequence, as shown in Figure 2.17. Following the Viterbi decoder, the effect of the shaping code $c_S(z)$ can be reversed by running the decoded bit sequence through a syndrome forming matrix U^T. This matrix and the shaping code C_S are designed to be orthogonal. Trellis pre-coding may be regarded as a generalized form of TH pre-coding. Tomlinson-Harashima pre-coding can be arrived at simply be setting the trellis pre-coding shaping sequence $c_S(z)$ to zero.

A drawback of trellis pre-coding is the enormous search times required to identify the shaping sequence $c_S(z)$ that minimizes average transmit energy. The search must consider the possible mapper output sequences u(z) that result from each shaping sequence $c_S(z)$, the precursor cancellation feedback sequences $\theta(z)$ that result from u(z) and the resultant output sequence w(z). A sequence estimator, such as the Viterbi or a reduced state sequence estimation (RSSE) algorithm, is needed just to find the shaping sequence.

An additional feature of trellis pre-coding is its ability to achieve fractional changes in data rates. This is possible because, in the case of a square transmit signal space, a 45° rotation of the space will allow the same trellis codes to be used with an additional coset. One more bit per symbol can be transmitted with this extra coset. The pre-coding system can switch between rotated and unrotated spaces at a selected rate; the proportion of time spent in each will determine an average, fractional bit rate.

Despite its complexity, implementations of trellis pre-coding have inspired significant interest. In 1991, Motorola Codex demonstrated a one-third improvement in data rate over V.32bis, a 1991 modem standard supporting data rates of up to 14400 bps [Forney4, 32][Read, 41]. Trellis pre-coding carries out much of its processing at the transmitter but is not consistent with the goal of asymmetric communication because significant processing, in the form of a sequence estimator, is also required at the receiver.

2.10.2 Flexible Pre-Coding

Trellis pre-coding has limited compatibility with general coding schemes; it can achieve shaping gain only with a trellis coded sequence. Complexity of the search for a shaping code, which increases with the number of trellis states, is also a drawback. An alternative system, known as *flexible pre-coding* allows general encoding and also shaping methods to be used [Laroia][Eyuboglu2].

In brief, a data sequence, coded and shaped by any desired method, passes through a flexible pre-coder with only minor modification and is transmitted across a channel. At the receiver, a linear equalizer is used to cancel channel ISI. The coloured noise spectrum at the output of the linear equalizer is flattened with a noise whitening filter. This filter does not affect the signal adversely as the flexible pre-coder has pre-compensated for its effect. The output of the whitening filter enters a general detection algorithm. Following this, only a residual postcursive ISI from the pre-coding process remains which is easily cancelled, yielding the original data sequence.

The flexible pre-coder operates by calculating a cancellation term, $\theta(k)$, to subtract from the data $x(k)$ at its input. Unlike TH pre-coding, $\theta(k)$ is not equal to the postcursor ISI that will be created by the channel. Instead, it cancels ISI that will be created by a receiver noise whitening filter with transfer function $K(z)$. The cancellation term is made up of two components:

$$\theta(k) = c(k) - d(k) \tag{2.20}$$

The term c(k) is a quantized version of θ(k), so that x(k)+c(k) will be the nearest to x(k)-θ(k) member of the same set of coded data symbols as x(k). As in TH pre-coding, the dither sequence d(k) alone is combined with the ideal data x(k). The remainder of the postcursor cancellation term c(k) can be accounted for at the receiver. Transmitted data, w(k), is equal to:

$$w(k) \quad = \quad x(k) + d(k) \tag{2.21}$$

Regular TH pre-coding quantizes the postcursor cancellation vector via modulo 2M reduction, ensuring the transmitted data lies somewhere within the half-open square boundary region designated by the Cartesian product $(-M,M]^2$. Quantization in flexible pre-coding is much more subtle. If members of the set of ideal data symbols {x(k)} are equally spaced, the dither value d(k) is necessarily

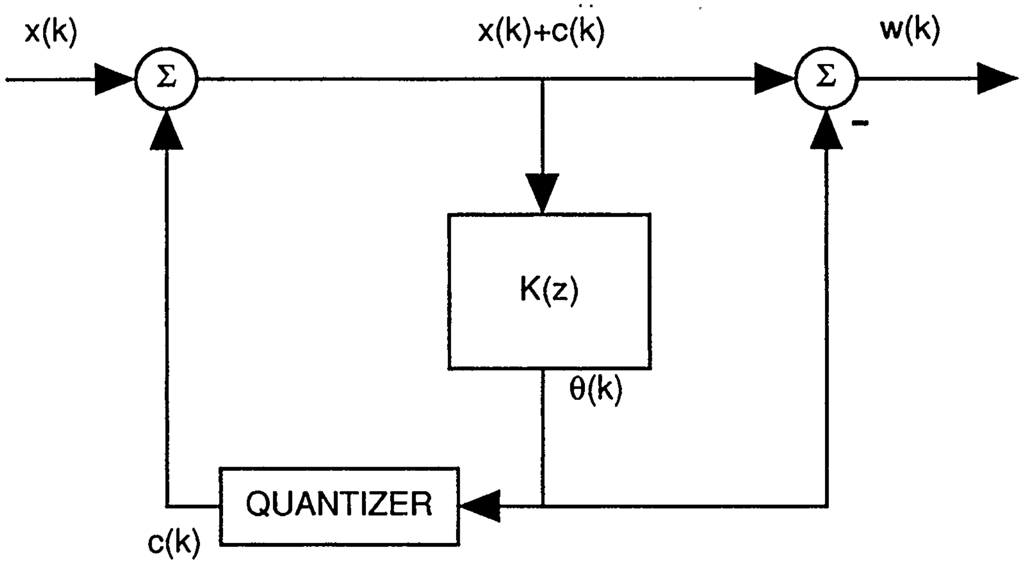

FIGURE 2.18 FLEXIBLE PRE-CODING TRANSMITTER

less than the distance between the ideal symbol x(k) and its nearest neighbour. Transmitted data w(k) must lie somewhere within a cell surrounding the ideal x(k), a cell small enough that x(k) is the only ideal data symbol included. Instead of one large transmit boundary $(-M,M]^2$ surrounding the entire ideal constellation, as in TH, each ideal data symbol x(k) has its own boundary region. These intricate boundaries ensure the dispersion of the ideal symbols by the pre-coder is much less than the general case of TH. Shaping gain is also not greatly compromised.

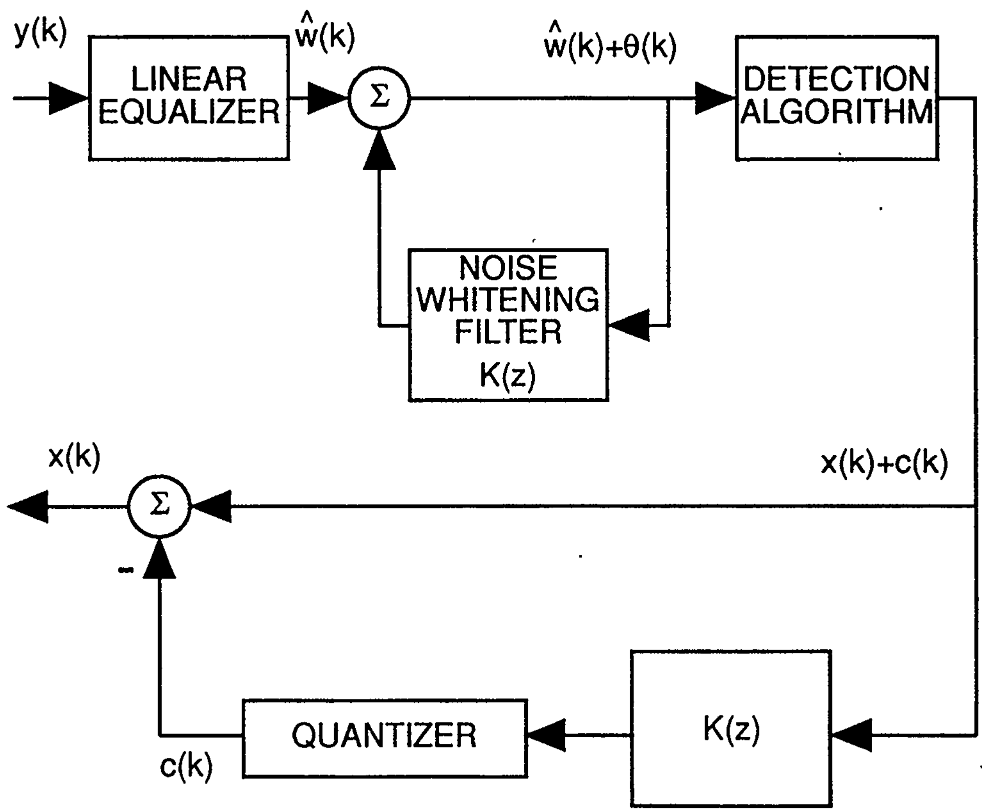

FIGURE 2.19 FLEXIBLE PRE-CODING RECEIVER

At the receiver, the noise whitening filter adds the postcursor term θ(k) to the received and equalized signal. Detection algorithm input will be equal to:

$$\begin{aligned} \hat{w}(k)+\theta(k) &= \hat{x}(k)+d(k)+\theta(k) \\ &= \hat{x}(k)+d(k)+c(k)-d(k) \\ &= \hat{x}(k)+c(k) \end{aligned} \tag{2.22}$$

After the whitening filter, a detection algorithm yields x(k)+c(k). The term c(k) is postcursive and easily calculated as the quantized output of a feed-forward filter. Following subtraction of c(k), receiver output is the original sequence x(k).

Flexible pre-coding, a significant departure from TH, allows both coding and constellation shaping gains to be realized. There is an ultimate limitation to this approach: attempts to realize further coding gain with more powerful trellis codes will expand the signal set, enlarging the signal constellation, increasing the transmit power and compromising shaping gain [Laroia, 1462]. This limitation prevents the full theoretical channel capacity from being realized with flexible pre-coding. Performance gains that are realized come at the expense of a complexity largely determined by the sophistication of the detection algorithm. If a Viterbi algorithm is used for detection, the receiver complexity increases well beyond that required by the receiver feedback filter and linear equalizer. In any case, the processing requirements at the receiver are sufficient to render flexible pre-coding inconsistent with the goal of asymmetric communication.

2.11 Structure of Pre-Coder Selected for Study

Tomlinson-Harashima pre-coding can be implemented in a variety of system configurations. Most commonly, coefficients for the TH pre-coder are derived at the receiver and communicated, across a sometimes noisy and dispersive channel, to the transmitter. An alternative approach is possible by using both a DFE and a TH pre-coder. A conventional adaptive DFE can be trained for equalization of received signals and make its coefficients available to the TH pre-coder for use in signal transmission, all at the same end of a two-way communication link. Because of its asymmetry, this structure will be used in this study. Common equalizer coefficients require a TDMA protocol for the DFE and pre-coder to share the same channel. The DFE will be adaptively trained with the RLS algorithm.

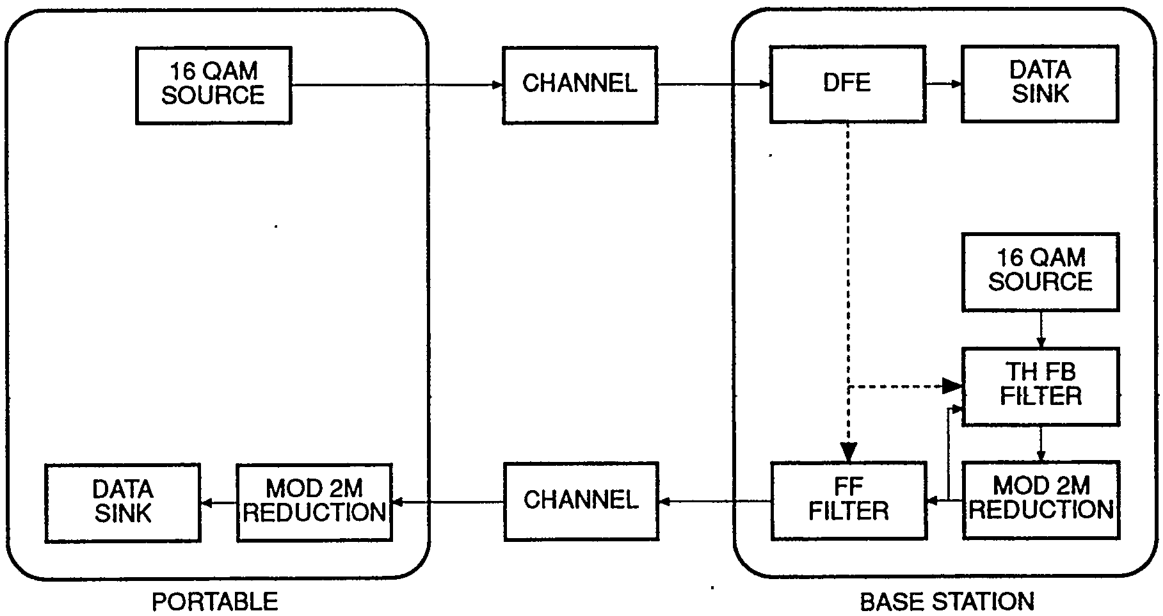

FIGURE 2.20 SIMULATION MODEL

Another design decision concerns the location of the TH pre-coder's feed-forward filter. The TH pre-coder cancels only postcursors from the transmitted signal and a feed-forward filter is required, to remove precursors, either at the transmitter or receiver. Placing the filter at the transmitter produces a structure called a Gibbard pre-coder. This arrangement sacrifices the opportunity for noise whitening and produces a further increase in transmit signal power. Despite these drawbacks, Gibbard pre-coding will be investigated, again because of asymmetric characteristics. A representation of the configuration used in this study is given in Figure 2.20.

Although the immunity of a TH pre-code from error propagation makes it suitable for use with trellis coding, a Viterbi algorithm must be implemented at the receiver for trellis decoding. The complexity of this algorithm is inconsistent with the goal of asymmetric communication, requiring excessive processing at the receiver, and will not be investigated further. Trellis and flexible *pre*-coding will also be rejected for this reason.

A final issue is the signal constellation. Hexagonal or other constellation shapes could be used instead of the customary rectangular QAM constellation if conventional TH pre-coding was used. With Gibbard's variation of TH pre-coding, the transmit feed-forward filter would likely redistribute the transmit constellation, annihilating any shaping gain from an alternative constellation shape. This study will use a rectangular QAM constellation customarily associated with TH pre-coding. Earlier work by Gibbard has investigated the performance of pre-coding with 4 QAM [Gibbard1, 59]. In this study, 16 QAM will be used to see if pre-coding can equalize a larger, higher bit rate constellation.

2.12 Conclusion

Placing a TH pre-coder at a communication link's transmitter stage can avoid some difficulties that arise with conventional equalization, such as noise enhancement, error propagation and processing delay. These improvements come at the expense of an increase in transmit power and reduced noise margin, but the performance loss is small and diminishes with increasing size of the signal constellation.

As DSP capabilities improve, more sophisticated extensions are being made to TH pre-coding in order to move towards the theoretical channel capacity with higher bit rates, lower error rates and reduced transmit power. These extensions, such as trellis and flexible pre-coding, produce limited performance gains at a significant increase in complexity, indicating that the elegant simplicity of conventional TH pre-coding is not easily improved upon.

Chapter 3
Error Rate Reduction with Diversity and Coding

3.1 Introduction

Tomlinson-Harashima pre-coding is used to reduce signal distortion introduced by ISI. Additional techniques may be required to overcome other types of signal distortion. For example, equalization cannot overcome the destructive interference between multipath arrivals, known as flat fading. For this phenomenon, diversity techniques may be needed. By creating alternate routes by which a message may travel to the receiver, diversity may allow fading channels to be bypassed.

Diversity duplicates the transmitted message, introducing a form of redundancy. Another type of redundancy which may be used to compensate for signal distortion is created by coding. By the introduction of additional check bits, coding imposes predictable patterns upon transmitted data. These patterns permit, to some degree, error identification and error correction. Coding makes possible further reductions in the bit error rate, beyond those already achieved through equalization.

The effectiveness of diversity and coding depend on the characteristics of the communication system to which they are applied. The severity and frequency of fades will determine the BER reduction which a diversity method may achieve. Similarly, the statistics of error events and the selection of a coding method will determine whether coding can yield performance gains sufficient to justify its use.

Diversity and coding are recurring topics in the communications literature but there is little published work on the application of these techniques to TH pre-coding, with the noted exception of trellis coding [Aman][Eyuboglu1][Laroia]. To determine the viability of TH pre-coding for practical wireless communication systems, it is worthwhile to analyze its performance in combination with diversity and coding methods. As a prelude, this chapter will examine various means for achieving diversity and coding gains and discuss the suitability of these methods to TH pre-coding and asymmetric communication systems.

3.2 Diversity

3.2.1 Purpose

In essence, diversity is the use of multiple redundant channels to mitigate channel related impairments. Severe distortion on a single channel can be overcome, or bypassed altogether, if additional uncorrelated channels are available. A commonly used measure in communications is *outage probability*, the probability that the bit error rate will rise above a specified threshold level. If the outage probability of a single channel is P_O, the probability of simultaneous outages on N independent channels is $(P_O)^N$ [Acampora, 17]. Significant improvements in signal quality are possible by using diversity to create a low overall outage probability. These gains become particularly significant if the outage probability of a single channel P_O is already small [Vannucci, 313].

The performance improvements made possible by diversity are in addition to those achievable through other techniques, such as equalization. Simple forms of diversity combining can be used on top of other distortion-combating methods [Winters2, 1740]. Where equalization alone may be insufficient, the addition of diversity to a communication system might make reliable communications possible [Lo, 644].

In general, diversity has been regarded as a means of overcoming flat fading, an impairment that equalization cannot correct [Mitzlaff, 25]. Diversity also has application to other types of channel-related problems. By appropriate diversity branch selection or combining, ISI can be reduced [Balaban2, 885]. Sufficient physical distance between channels allows diversity to overcome the problem of shadowing created by physical obstruction of signals [Arnold, 277] [Chang, 89]. If an antenna array is used, appropriate diversity combining can overcome the interference created by other users of the spectrum [Vaughan, 181]. The channel redundancy created by diversity also reduces the need for careful antenna alignment as misalignment of two or more antennas is less likely than misalignment of a single one [Cox]. By reducing various impairments, diversity may lower a system's bit error rate or enable an increase in the rate of data transmission [Nix, 1869][Smulders, 2154].

3.2.2 Classifications

There are five means by which diversity can be achieved. These are [Jakes, 310-313]:

1) space diversity;
2) polarization diversity;
3) angle diversity;
4) frequency diversity;
5) time diversity.

Space diversity achieves channel redundancy by the use of multiple antennas at the receiver. Polarization diversity uses orthogonal signal polarizations to provide access to a redundant channel. The directional properties of antennas permit angle diversity to receive signals traveling over different channels.

Frequency and time diversity deliberately send multiple copies of the same message (as opposed to the implicit diversity of multipath), either on different frequency subchannels or at different times.

The remainder of this section will focus on space diversity although the combining and detection methods also apply to polarization and angle methods. With the exception of the implicit time diversity of channel coding, frequency and time diversity will not be examined because of their inherent inefficiency. Frequency diversity is wasteful of spectrum, usually a limited resource, while long processing delays are introduced by time diversity.

3.2.3 Antenna Separation

Space diversity can exist at two levels, *macro* and *micro*. The former is the result of a relatively large physical separation of antennas which, in addition to combating multipath effects, can also be used to overcome shadowing [Chang, 89]. This type of diversity is often neglected because of the inconvenience of separating antennas by large distances, particularly antennas connected to a portable communication device. Micro-diversity is characterized by smaller distances between antennas and is used to combat flat and frequency selective fading. Small separations are feasible because the wireless channel varies significantly over short distances [Winters1, 871]. Usually a distance of one-quarter to one-half wavelength is given as an adequate distance between antennas to ensure channels are uncorrelated [Acampora, 13][Balaban1, 347]. At 1100 MHz, this amounts to a distance of 6.8 to 13.6 centimetres.

3.2.4 Testing Signal Quality

To take advantage of channel redundancy, a method is needed to select or combine the signals from the different antennas. This generally requires some measure of signal quality to determine the best signal or signal combination

[Mitzlaff, 25]. One measure of quality is the received SNR. This is difficult to determine directly so received power is often used instead, an equivalent measure if the noise power is the same at all antennas [Chyi, 80]. In the extreme, when there is significant interference or when noise and ISI are particularly severe, signal power cannot provide an adequate measure of signal quality [Chang, 89].

Other measures of signal quality include the mean square error. The *ALTAIR*™ system, Motorola's wireless LAN product, uses the difference between the received and expected signal to determine the best transmit-receive antenna combination [Mitzlaff, 25]. Other possibilities are the bit error rate or, for coded data, the Hamming distance between received data and codewords [Chang, 90].

3.2.5 Combining Methods

Switched diversity is the simplest method of diversity implementation. With this method, a receiver takes the signal from just one antenna at a time. When signal quality falls below a threshold, the receiver switches to a different antenna [Acampora, 14]. Circuitry at the receiver remains relatively uncomplicated with switched diversity [Vaughan, 187]. If used in combination with adaptive equalization, the equalizer must be retrained after each switching operation in order that equalizer weights reflect the new channel characteristics. Otherwise, performance will degrade over the non-diversity case [Fattouche, 407].

An increase in complexity yields *selection diversity.* In this, the quality of signals from all antennas is continuously monitored and the best signal selected. A receiver for each antenna signal is required unless the signal quality measure can be applied directly at the antenna output prior to receiver circuitry [Jakes, 313].

The combination of diversity signals is accomplished with *equal gain combining*. In this, signals are summed either before or after demodulation. Pre-detection combining is performed prior to demodulation, and circuitry to match the phases of the signals is required. Post-detection combining, performed at baseband, avoids co-phasing but results in a minor performance degradation [Adachi, 196]. If a weighted sum of signals is created, *maximal ratio combining* is realized. The weights can be determined by relative signal power. Performance improvements using these combining methods rather than selection diversity are generally not large [Acampora, 14].

A significant performance gain is possible with *optimum combining* [Winters1, 871]. Signals are joined in an equalizer structure with weights chosen to minimize the MSE [Balaban2, 885][Scott, 107-34]. This is a multi-dimensional optimization problem which may be implemented only at the expense of signal processing complexity [Acampora, 18][Vaughan, 187]. Flat fading, ISI, interference and diversity combining are addressed jointly, producing an output that is optimal in the linear sense [Clark, 174].

Non-linear diversity combining may be implemented with maximum likelihood sequence detection. One possibility is to calculate path metrics separately for signals from each antenna. A decision is made on the data sequence using the sum of metrics across all signals [Liu, 247]. Performance of non-linear combining is superior to linear methods but complexity is considerably greater [Winters1, 871].

3.2.6 Performance

Anticipated improvements from diversity are difficult to predict. The gain depends on factors such as channel, data rate, number of antennas and combining method. For both indoor and mobile radio channels, using various combining methods and performance measures, reported results show an improvement of between one and three orders of magnitude for dual branch diversity with a tendency toward a single order of magnitude improvement [Chang, 93][Cartledge, 170][Wu, 433][Nix, 1869][Balaban3, 895][Pahlavan, 168].

3.2.7 TH Pre-Coding and Diversity

As mentioned in Section 3.2.5, an equalizer using switched or selection diversity must be retrained whenever a new channel is chosen. A single set of equalizer weights cannot remove ISI from multiple uncorrelated channels. Similarly, in the case of TH pre-coding, ISI can be suppressed on only a single channel at a time.

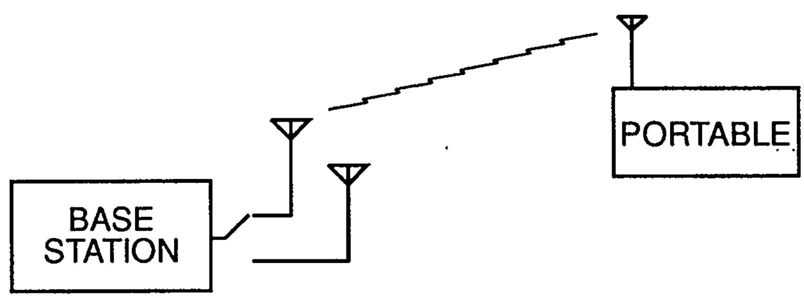

FIGURE 3.1 SWITCHED DIVERSITY AT
BASE STATION ONLY

More sophisticated forms of diversity combining, such as equal gain, maximum ratio, optimum and maximum likelihood, form a hybrid channel by merging the signals from multiple antennas. The pre-coder's task of establishing an ISI free channel to the receiver is complicated if these combining methods are used. In this case, the pre-coder must compensate for ISI at the output of a hybrid channel, requiring knowledge of the combining procedure as well as the impulse response of each individual channel to calculate an overall impulse response. These sophisticated forms of combining are also inconsistent with the asymmetric communication concept because they require additional signal processing complexity at the receiver.

Based on the complications that arise from using advanced types of diversity combining, it would seem that switched or selection diversity are most naturally used with TH pre-coding. Simplicity at the portable unit can be assured by using switched diversity *at the base station only* [Acampora, 17]. Because of channel reciprocity the best portable-to-base station path will also be the best return channel. The base station can select this channel and use it for transmission and reception with only a single antenna required at the portable. Reciprocity will hold if both the portable and base station, using TDMA, transmit at the same frequency [Mitzlaff, 26][Acampora, 13].

3.3 Coding Methods

3.3.1 Purpose and Performance Measures

The term *coding* has multiple meanings. As used here, the word refers to *channel coding*, or the introduction of redundancy to a message for error control. This is distinct from *source coding* , also known as compression, which removes redundancy from a message in order to maximize entropy or information content [Biglieri, 2]. In the current context, coding is also distinguished from *encryption,* an operation that is used to enhance message privacy.

Error control is an objective shared by both coding and equalization but these methods are fundamentally different. Coding is a constructive process, introducing controlled redundancy to a message which may be used at the receiver to detect and correct errors, regardless of their source. Redundancy is not a requirement for equalization nor does equalization possess the generality of coding. Equalization is aimed specifically at the problem of ISI, although noise averaging and whitening are related, but subordinate, objectives. Tomlinson-Harashima *pre-coding* is therefore a misnomer because it is an equalization process, used to create an ISI-free channel, although customary usage here prevails. Another difference is evident when hard-decision detection is used at the receiver. In this case decoding is a post-mortive process, applied to examine the metaphorical entrails of a message whose vitality has already been extinguished by hard decision detection. This differs from equalization, a pre-emptive process that attempts to remove ISI before decision errors are made. When soft-decision decoding is used, this difference between coding and equalization may become obscure.

Coding for error control can be implemented for a variety of reasons. *Detection* of errors may be used to determine if a message is faulty and should be re-transmitted [Rice, 1413]. Monitoring of the BER may also determine if system parameters, such as the choice of a diversity antenna, should be changed. Another application is error *correction* which reduces the BER by correcting message errors at the receiver [Berlekamp4, 46]. Reductions in the BER may seem like the ultimate goal of any coding method. In fact, coding may be used simply to maintain a constant BER while other hardware is downgraded to reduce cost. For example, coding may be used to overcome non-linear distortions introduced by a transmit amplifier [Friederichs].

Redundancy, introduced by coding, creates a correlation between transmitted bits[1]. The entropy of a message, a measure of its information content, is thereby reduced [Gitlin2, 109]. This is most evident with the parity bits created by systematic codes. For a sequence of information bits of length k,

---

1 Some codes, such as Reed-Muller and Reed-Solomon, may use non-binary symbols. For brevity, terminology will reflect the binary case except where otherwise specifically required.

parity bits are formed by linear combination of the information bits. Parity bits are determined completely by the information bits. They do not, themselves, carry any new information and are thus aptly described as redundant [Williard, 87]. Together, the information and parity bits make up a codeword of length n. Customarily given the description (n,k) the code has an information rate of k/n [Bhargava, 11]. As the number of parity bits (n–k) increases relative to information bits k, the rate of the code, an indicator of its information-bearing efficiency, declines [Kanal, 725].

A reduction in information-bearing efficiency is the price paid for the increased reliability of information in a coded system. Several measures can compensate for this decline. Increased bandwidth can be used to transmit codewords more quickly [Bhargava, 11]. Another possibility is greater transmit power to permit a larger signal constellation with more bits per symbol. A third alternative is to increase the signal constellation without an increase in transmit power, as in trellis-coded modulation, by using decoding complexity to offset the reduction in Euclidean distance between individual symbols [Ungerboeck2, 5]. A final possibility is to use longer codewords. For a fixed error detection and correction capability, longer codewords require proportionately fewer parity bits but decoding complexity is greater [Chien2, 744].

Parity bits make error detection and correction possible by restricting n-length codewords to a subset of all possible n bit combinations. Received words that do not belong to the set of codewords are obviously in error. Depending on the code, identification and correction of the specific error might be possible [Longo, 25]. The utility of parity bits can be easily understood by a geometric visualization of code space. Figure 3.2 shows a two dimensional representation of four possible signals {00,01,10,11} but only two permissible codewords {00,11} taken from a simple repetition code.

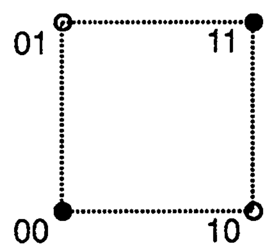

FIGURE 3.2 TWO DIMENSIONAL
REPETITION CODE {00,11}

Hamming distance D^H is the number of co-ordinates in which two codewords disagree [Hamming1, 11]. The Hamming distance between the codewords shown in Figure 3.2 is two. In general, given the minimum Hamming distance in a code D^H_{min}, the maximum number of errors that can be *detected* is $\lfloor D^H_{min} / 2 \rfloor$ [Biglieri, 4]. For the code shown in Figure 3.2, one error can be detected. A single error will yield one of the words from the set {01,10} which are not recognizable as codewords. However, two errors will yield a valid codeword and the error will not be detectable.

Illustration of error correction can be seen by carrying the repetition code of Figure 3.2 into three dimensions, as in Figure 3.3. In the higher dimension, the minimum Hamming distance D^H_{min} is three and up to two errors can be *detected.* If a single error occurs, the received word will lie within the Voronoi region (or decoding sphere) of a codeword and can be *corrected* [Chen1, 1809]. The Voronoi region of codeword {000} includes {100,010,001} while the set {101,011,110} belongs in the Voronoi region of codeword {111}. Any word containing a single error will be decoded to the nearest codeword. For two or three errors, the received word will be decoded to the wrong codeword. In general, the maximum number of errors that can be *corrected* is $\lfloor (D^H_{min} - 1)/2 \rfloor$ [Biglieri, 3].

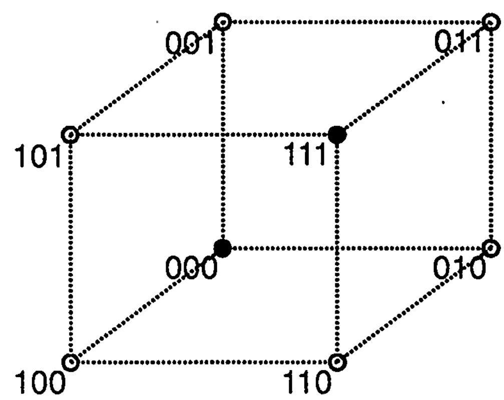

FIGURE 3.3 THREE DIMENSIONAL REPETITION CODE {000,111}

The foregoing demonstrates the importance of the concept of distance for error control. Error detection and correction capabilities are a function of a code's distance properties. Distance requirements for correction exceed those of detection. In addition, it has been shown that error patterns are not always correctable or detectable [Longo, 32].

Hamming distance is not the only distance measure used in coding theory. Another common measure is Euclidean distance. Rather than measuring the bit differences between codewords, Euclidean distance measures the difference in phase and amplitude between modulated signals. This is helpful in soft-decision decoding which employs information about symbol reliability. Maximizing the Euclidean distance or metric between symbol sequences improves error control properties for trellis coded modulation, just as Hamming distance improves these properties in the case of block codes [Ungerboeck2, 7].

Distance is an indicator of a code's efficacy. This raises the question of the maximum theoretically achievable code performance. Shannon's channel encoding theorem shows that, for transmission at a rate below channel capacity, a code with unlimited length codewords can bring the decoding error arbitrarily close to zero [Biglieri, 27]. Channel capacity depends on channel bandwidth, frequency response and SNR [Gitlin2, 130]. For a fixed capacity, the ultimate limitation is not accuracy but the rate of data transmission [Bhargava, 11]. In theory, coding can be used to make the channel completely reliable [Berlekamp4, 45].

Shannon's performance bound neither specifies the required codes nor limits their complexity. While practical codes can be assessed on their closeness to this bound, considerations of encoding and decoding complexity are also important. For example, a turbo code has been reported that achieves performance within 0.7 dB of the Shannon bound using two parallel, recursive convolutional encoders at the transmitter. At the receiver, decoding requires two probabilistic decoders which perform multiple iterations on the data [Berrou]. This level of complexity, both in hardware and processing delay, may be excessive for some practical applications.

Constraints on complexity can be imposed by focussing attention primarily on codes that fall into two analytically tractable classes. The first such class consists of *linear* codes. In this class, parity bits are formed by addition of data bits, simply accomplished with the exclusive or (XOR) operator [Longo, 13][Bhargava, 11]. In a linear code, the addition of any two codewords yields another codeword. Closure under addition reduces complexity of the algebra involved in decoding.

For linear codes, the distances between one codeword and all others is independent of the chosen word [Blake, 82]. As a result, error detection and correction capability are identical for all codewords. While these and other characteristics simplify the analysis and manipulation of linear codes, other performance measures are sacrificed. Compared to the linear case, encoding and decoding of non-linear codes is generally more difficult but some possess superiority in rate and distance properties over comparable linear codes [Berlekamp2, 68].

The second analytically tractable class consists of *systematic* codes. For any particular code in this class, all codewords are the same length and identical parity check equations are applied to each codeword, independent of the value of individual information bits [Hamming1, 12]. For every systematic code, either the code itself or an equivalent will form a codeword divisible into information bits and parity check bits [Goldie, 150]. The consistent structure imposed upon systematic codes simplifies encoding and decoding. Selection of a code that is both systematic and linear narrows the scope of a search for practical coding methods.

3.3.2 Coding Strategies

Error patterns and design constraints may suggest a coding strategy. One possibility is forward error correction (FEC), an approach which uses relatively complex codes to correct errors at the receiver. The alternative is automatic request for retransmission (ARQ). In a Type 0 ARQ strategy, the transmitter resends blocks of data if the receiver has detected an error [Berlekamp4, 46][Longo, 32].

The ARQ method, used extensively in data networks, requires less complicated codes because error detection alone is required [Deng, 700]. Additional redundancy, in the form of retransmitted data blocks, is used only when needed [Longo, 32]. In general, ARQ can deliver a consistent quality of data, unlike FEC which may be unable to correct all errors, particularly if channel conditions become severe. The greater reliability of ARQ data is achieved by placing system throughput at risk [Rice, 1413]. In a heavily used system, repeat requests may become too numerous to handle if the BER degrades [Kallel, 1472]. In contrast, a FEC strategy can guarantee constant throughput although data quality is less certain [Rice, 1413].

An error-free feedback channel is required in an ARQ system to ensure accurate reception of repeat requests [Vucetic, 654]. In addition, extensive storage may be needed at the transmitter to record previously transmitted data blocks in anticipation of a retransmit request. Alternatively, data must be transmitted at a slower rate to avoid overrunning a small storage buffer [Berlekamp4, 47-48].

The strengths of FEC and ARQ can be combined in a hybrid system to increase performance. In a Type I ARQ system, FEC is used to correct small numbers of errors. If the number of errors is too large, ARQ is called upon to obtain reliable data [Harbour, 657]. There are many varieties of Type II ARQ systems. In one variation, check bits for error *detection* only are sent with the initial block of data. If an error is detected, ARQ is used to obtain further check bits for error *correction* [Kallel, 1474]. In this method, both the number of initially transmitted redundant bits and the length of repeat-requested data blocks are kept small.

Selection of a FEC, ARQ or hybrid error correction strategy is conditioned by the amount of traffic on the channel and the degree to which delay and error can be tolerated. Another significant factor in the selection of a coding system are error statistics. Coding theory's orthodox approach to error statistics is based on the *binary symmetric channel.* In this model, the channel is without memory and the probability of error is identical for every bit. Errors are regarded as completely random, occurring with a binomial probability distribution [Williard, 86]. This model is often employed for its analytic simplicity [Kanal, 724].

In some channels, burst errors are more likely than random errors [Kanal, 724][Berlekamp4, 49]. Instead of the binary symmetric channel, a Markov model, representing a channel with memory, can be used to simulate the increased probability of error if a bit occurs in the vicinity of other errors [Drukarev, 513]. Some codes have greater resistance to burst errors than others and knowledge of error statistics is an important factor in code selection.

Burst errors are more predictable than random errors and, at least in theory, a channel memory can be exploited to provide increased channel capacity [Kanal, 727]. In practice, this memory is not utilized and burst errors are regarded as more deleterious than random errors [Berlekamp4, 50]. To overcome the problem of burst errors, interleaving can convert a burst error distribution to a random error distribution [Bhargava, 19][Chen1, 1807]. Interleaving rearranges the order of transmitted bits to disperse burst errors and achieve an error pattern consistent with a binary symmetric channel model [Vucetic, 654]. One method is to store data arriving at a transmit buffer row-by-row but transmit the data column-by-column. At the receiver, this pattern is reversed [Seshadri, 54]. Interleaving introduces a delay and requires buffers at the transmitter and receiver to accumulate data for rearrangement [Bhargava, 19]. Overhead can become large when significant depths of interleaving are required [Berlekamp3, 581].

An additional type of data manipulation that may be incorporated into a coding strategy is the addition or deletion of check digits. These modifications are known, respectively, as *extending* and *puncturing* a code [Berlekamp1, 333-34]. A code may be extended by calculating additional parity checks for an existing codeword. The increased distance between codewords can improve a code's error detection and correction capability [Williard, 92]. Puncturing a code deletes some of the check digits and reduces distance between codewords. In terms of error control, deleting check digits may be counter-productive but can assist in decoder simplification. Puncturing is also useful when a variable rate system is desired; check digits may be removed in order to increase the rate of information transfer [Yasuda, 316]. An additional application for puncturing is in adaptive coding systems.

Ordinarily, codes must be designed to compensate for worst-case conditions on a non-stationary channel. Redundancy is wasted when worst-case conditions do not prevail. With an adaptive coding system, the number of check digits can be varied according to channel severity [Berlekamp4, 52]. For example, with punctured convolutional codes, redundancy can be added or removed as conditions warrant. This is possible without altering the basic structure of the encoder and decoder, a significant benefit in a case where decoding overhead may already be significant [Vucetic, 653].

3.3.3 Encoding and Decoding

Amongst paradigmatic methods for implementing and manipulating codes, a frequently used approach is algebraic coding. This method can be used for Hamming, Bose-Chaudhuri-Hocquengham (BCH) and Reed-Solomon (RS) codes. In a simple form of algebraic coding, a *generator matrix* is used for encoding and a *parity check matrix* for decoding. In this approach, a vector composed of information bits is multiplied by a generator matrix to produce a codeword vector, consisting of both information and parity check bits. For decoding, the received word is multiplied by a parity check matrix to produce information bits and *syndrome* bits [Hoffman, 45-68]. In the binary case, operations on each bit are carried out modulo 2.

The syndrome of a decoded word provides the means for error detection and correction. It is independent of the information bits and depends only on the pattern of errors. Clues about error location and magnitude are derived by interpretation of the syndrome [Longo, 35][Bhargava, 16]. Syndrome identification can be a complicated process and decoding is correspondingly more difficult than encoding, in the general case [Blake, 220]. Decoding is also an uncertain process. In cases where decoding does not yield a correct result, two alternatives are possible. The first is called *decoding failure* and occurs when the code recognizes that the message cannot be correctly decoded. The second, potentially more harmful outcome, occurs when an incorrectly decoded message is mistaken for a correct message, an event known as *catastrophic error* [Berlekamp3, 590-91].

For codes with long words, the use of matrices for encoding and decoding can be cumbersome. More flexible and powerful algebraic manipulation is achieved by representing codewords as polynomial elements of a Galois field, denoted $GF(p^k)$, where p^k is the order of the field [Berlekamp1, 104]. Like the real or complex numbers, the Galois field is a set for which the operations of addition and multiplication are defined. The field is closed under these operations, the associative and commutative properties hold and each element has an additive and multiplicative inverse [Berlekamp1, 87]. In short, the field possesses all the attributes necessary for algebraic manipulation.

The Galois field is useful in coding theory because it is finite. Operations on polynomial *coefficients* are always carried out modulo a fixed number and operations on polynomials themselves are carried out modulo an irreducible polynomial [Hoffman, 123]. These constraints prevent the size and complexity of algebraic expressions from growing without bound. In fact, algebra using a Galois field with binary symbols corresponds to the operation of simple digital logic circuits. Addition and subtraction are accomplished by applying an XOR operation to codewords. Multiplication and division require repetitive XOR operations, accomplished with simple feedback shift registers [Gitlin2, 190].

With algebra defined over the Galois field, encoding no longer requires a generator *matrix*. Instead, a codeword polynomial is generated by multiplying a message polynomial with a generator *polynomial*. Information bits make up the coefficients of this message polynomial. At the receiver, the decoder divides the received word by the generator to retrieve the message polynomial and a syndrome polynomial. Further algebraic manipulation can convert the syndrome to an error polynomial which can be used to identify and correct errors [Ramabadran, 64][Gutman, 989-90]. The *cyclic* codes are the class of codes created with a generator polynomial and Galois field algebra [Ramabadran, 64][Proakis1, 386]. In this class, the cyclic shift of any codeword produces another codeword [Longo, 20].

Algebraic decoding is suboptimum with respect to utilization of the full minimum distance properties of a code [Longo, 37]. By employing hard decisions, algebraic decoding also sacrifices information about the reliability of various bits [Bhargava, 18]. Despite these drawbacks, algebraic techniques are widely used and have made complex and powerful codes practically possible [Berlekamp2, 67].

Several options present themselves with respect to implementation of algebraic decoding techniques. As mentioned above, simple digital logic circuits can be used to implement the Galois field algebra of binary symbols, a hardware implementation of decoding. The obvious alternative is a software implementation [Whiting]. Another design choice is whether to explicitly derive the error polynomial from the syndrome using algebraic techniques. Because each syndrome uniquely corresponds to the most likely error polynomial, another possibility is to map syndromes to errors using memory lookup. This is less complex than explicit derivation but impractical when codewords and syndromes become long [Gutman, 990][Bhargava, 15].

Algebraic decoding is only one amongst many decoding methods. Majority logic decoding is another. In this method, parity checks are orthogonal and bits are tested for error by taking a majority vote amongst several decoding circuits [Longo, 40-46]. Reed-Muller codes are an example [Rice, 1413]. Complexity of majority logic decoding is relatively moderate and error correction capability can sometimes exceed the minimum guaranteed level [Drukarev, 519]. Decoding can also be implemented at relatively high speeds [Rice, 1413].

All coding methods involve trade-offs and majority logic is not an exception. Its drawbacks are an error correction capability that may be less than other codes of comparable rate [Longo, 62-63]. There are also few short length, cyclic codes that are majority logic decodable [Drukarev, 519].

The voting procedure involved in majority logic decoding is compatible with soft decision decoding. With soft decisions, reliability as well as redundancy is used to determine information bits [Bhargava, 11-12]. Unlike the discrete, either-or symbol representations of hard decision decoding, soft decision decoding assigns bits a confidence level. In majority logic decoding, the confidence level can be indicated by the extent of the voting majority. If the results of the vote are insufficiently conclusive, a request for retransmission can be made [Rice, 1413].

Soft decision decoding can also be extended to algebraic decoding techniques [Friederich, 1572][Bhargava, 16]. A bit detected close to a detector's decision threshold can be regarded as being of dubious reliability. If reliability information is exploited, code performance may be improved or comparable performance can be maintained with a reduced amount of redundancy [Longo, 56][Berlekamp4, 47]. Although soft decision decoding is possible, reliability information is difficult to incorporate into conventional algebraic decoding techniques which are more naturally suited to hard decisions [Bhargava, 16].

The Viterbi algorithm is a decoding method, often used for trellis codes, that makes effective and natural use of soft decisions. Distances between a received signal sequence and possible codeword sequences are calculated. These calculations produce distance measures that are both real-valued and, by nature, incorporate reliability information [Berlekamp4, 48]. Accuracy of this maximum likelihood estimation method improves as symbol sequences become longer but the already significant complexity of the Viterbi algorithm becomes prohibitive at longer lengths [Bhargava, 17]. Another limitation of the Viterbi algorithm is its vulnerability to burst errors, a vulnerability which can be mitigated with interleaving of data [Vucetic, 653].

The Fano algorithm, a sequential decoding method, is an alternative to the Viterbi algorithm for convolutional codes [Longo, 46-48]. A likely sequence is traced through a branching sequence tree. If the wrong path has been followed, a dead-end will eventually be reached when the path will fail to branch to a likely decoded symbol. The decoder will then have to back up and search other possible paths for the most likely sequence [Bhargava, 17]. Although fewer total computations are required because the algorithm searches only paths near the current decoded path, the number of computations can vary significantly on any single iteration, making throughput unpredictable and unsteady [Longo, 51].

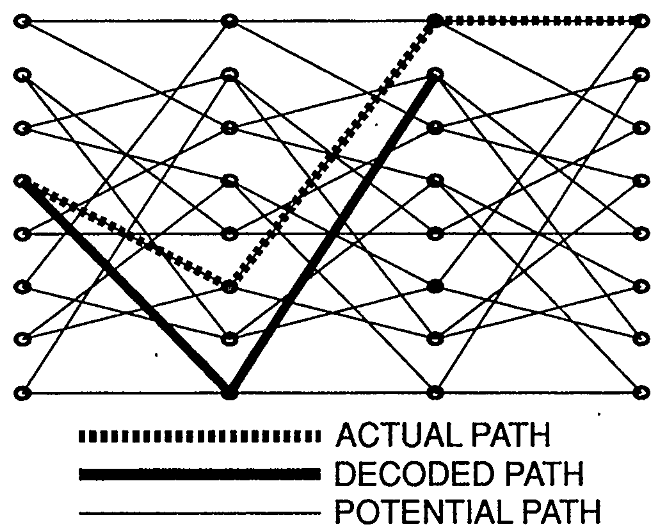

FIGURE 3.4 SEQUENTIAL DECODING ERROR

3.3.4 Block Codes

The above description of encoding and decoding methods, coding strategies and performance measures has given a broad overview of some issues in coding theory and provided the background for an examination of some specific codes. Bifurcation of the coding world into block and convolutional codes provides a convenient basis on which to proceed with this examination.

Block codes, as their name implies, process data on a block-by-block basis. A message is divided into finite length segments which are encoded and decoded independently from each other [Ramabadran, 63][Longo, 10]. This is in contrast to the "sliding block" structure of convolutional codes in which symbols are transmitted in a continuous sequence [Longo, 10-11]. Redundancy is not confined to independent blocks, instead each symbol in a convolutional encoded sequence has a redundancy relationship with neighbouring symbols [Berlekamp4, 46].

Block codes are simpler to decode than convolutional codes, requiring fewer operations for each decoded bit. In addition, the hard decision arithmetic generally used with block codes is easier to implement than the real number arithmetic of soft decisions [Berlekamp4, 49]. For these reasons, block codes are well suited for high speed operation [Berlekamp4, 51]. Block codes are also appropriate for TDMA systems which require transmitted data that is partitioned into frames [Bhargava, 18].

A simple type of block code are the *repetition codes*. With these, an information bit is simply repeated multiple times [Williard, 87]. Encoding and decoding are easily implemented and error control can be readily improved by increasing the repetition length. The simplicity of this method is achieved at the expense of efficiency; the information rate of repetition codes is low.

For non-trivial cases, the first example of error correcting codes were the *Hamming codes* [Blake, 6]. This class uses parity check equations to correct single bit errors [Williard, 89]. Hamming codes are easily decoded and are widely used. For example, Ethernet, the IEEE 802.3 LAN standard, incorporates shortened Hamming codes [Fujiwara, 987].

A (23,12) Hamming code, also known as the Golay code, is an example of a perfect code. Perfection denotes the effective utilization of all combinations of parity check bits. Each syndrome corresponds to a single error pattern so capacity is not wasted on ambiguous parity bit combinations [Williard, 91]. Stated another way, in a perfect code, every received word falls within the Voronoi region of some codeword [Biglieri, 40]. Given the efficiency of perfect codes, one might wonder why any other type of code would be considered. In fact, there are very few perfect codes. For binary symbols, certain types of Hamming and repetition codes are the only perfect codes possible [Longo, 62].

Hamming codes are a subset of the BCH codes [Clairborne, 82]. The class of BCH codes is distinguished by multiple error correction capability [Williard, 96]. Understandably, the greater capability of multiple error correcting codes makes the decoding process more complex than the single error correcting Hamming codes [Berlekamp1, 11]. In general, decoding is a three stage process. First syndromes are computed, followed by conversion of the syndromes into an error locator polynomial. Finally, the roots of this polynomial, which indicate error locations, are found [Hoffman, 135][Kraft, 1721].

For correction of one or two errors, BCH decoding is relatively easy to implement but becomes more complex as the number of errors increases [Williard, 97-98]. Solution of non-linear equations is generally required to obtain the error locator polynomial but these equations need not be solved directly [Kraft, 1721]. The Berlekamp-Massey algorithm is an iterative procedure for finding the error locator polynomial that can be implemented in both the frequency and time domains [Blahut, 299][Ferguson, 305] [Shayan, 1535]. Once the error locator polynomial is determined its roots may be identified without actual factorization using a Chien search which cycles through potential roots [Chien1]. .

Reed-Solomon codes are a popular subset of BCH codes found in deep space probes, compact disc players and digital audio tape recorders [Berlekamp4, 45][Morii, 1801]. These codes use a multi-level, rather than binary, symbol alphabet although symbols can ultimately be rendered in binary form [Chen1, 1808]. A RS decoder corrects symbol errors regardless of the number of bits each symbol represents [Berlekamp4, 52]. Bursts of bit errors can therefore be absorbed by the symbol alphabet [Bhargava, 15]. Another advantage of RS codes is their maximal distance property. For a given length and number of parity check digits, RS codes achieve the maximum possible theoretical distance between codewords [Blake, 154]. The multi-level alphabet complicates the decoding process. In addition to finding and solving an error *locator* polynomial, an *evaluator* polynomial must be solved to find error magnitudes [Morii, 1802].

3.3.5 Convolutional Codes

The alternative to block codes are codes of the convolutional type. Unlike block encoders which map blocks of information bits to codewords, convolutional encoders take the form of a tree which branches according to the value of incoming data [Berlekamp4, 46]. If branches eventually merge, the number of paths through the tree is finite and the structure is called a trellis [Bhargava, 17]. In this form, convolutional codes represent a finite state machine [Ungerboeck2, 7].

Redundancy in a convolutional code relates each member of a symbol sequence to neighbouring symbols. Continuous correlation across a transmitted sequence enables decoding with relatively powerful maximum likelihood sequence estimation [Longo, 11]. Continuous correlation also allows errors to have far-reaching effects. The problems of error propagation and vulnerability to burst errors are particularly acute in the case of convolutional codes [Berlekamp4, 46]. Although the codes readily support soft decision decoding, the decoding process is also a weakness of convolutional codes because of complexity and delays [Bhargava, 18][Berlekamp4, 49].

The relative strengths of convolutional and block codes can be combined through *concatenated coding.* In this method, two different types of encoder-decoder pairs are used in series, one pair called an outer and the other called an inner code [Forney1, 91]. At the receiver, the incoming message is first processed by the inner decoder which might use a Reed-Solomon code to convert a low quality message to medium quality. This could be followed by an outer convolutional decoder to turn medium quality data to high quality [Berlekamp4, 50]. Powerful coding combinations can be realized in this manner although complexity can become significant.

3.3.6 Coded Modulation

Convolutional coding and modulation have been combined into a joint operation known as trellis coded modulation [Ungerboeck2, 5]. This is a very powerful and bandwidth efficient form of coding in which the encoder maximizes the Euclidean distance between potential symbol sequences [Biglieri, 69-72]. Like other convolutional codes, this can be decoded using the Viterbi algorithm [Forney3, 642].

Coded modulation can also be used for block codes. Partitioning the signal constellation into cosets allows large *effective* distances between symbols in a relatively compact signal constellation. This is achieved by constructing cosets from symbols separated by a large Euclidean distance. A series of bits is encoded to select the coset, thus narrowing the decoding operation to symbols with good distance properties. Uncoded bits choose a particular element from within the coset [Forney3, 639].

A less sophisticated form of coded modulation is known as Gray coding. This is a mapping of binary words to the signal constellation which ensures that adjacent symbols differ in only one bit [Proakis1, 259]. Using this method, the most likely symbol errors will produce only single bit errors [Gitlin2, 326].

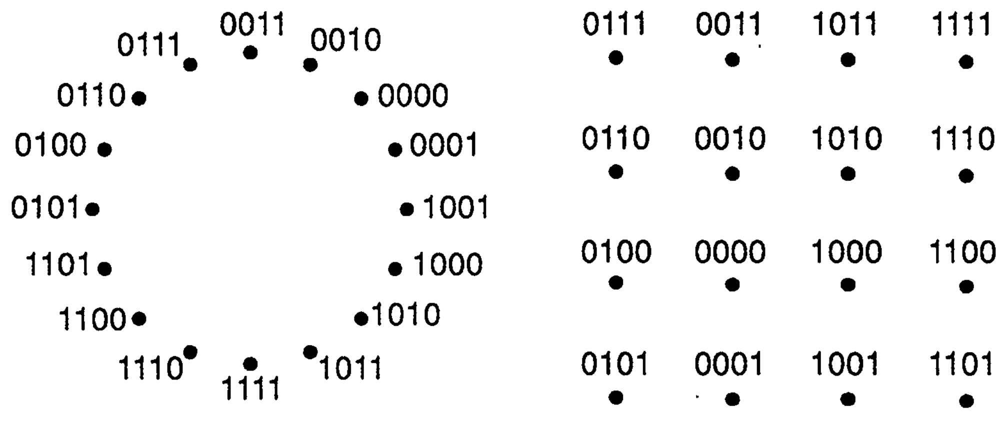

FIGURE 3.5 GRAY CODED CONSTELLATIONS

As shown in Figure 3.5, Gray coding of a rectangular signal constellation will be effective even when the TH pre-coding data flipping phenomenon occurs, a phenomenon discussed in Section 2.7.1. If excessive noise or ISI pushes a symbol outside the $(-M,M]^2$ boundary region, causing the modulo 2M reduction operator to flip the symbol to the region's opposite side, the symbol will still fall within the Voronoi cell of a codeword that differs in only one bit. Gray coding is inherently circular, a feature that accommodates the TH constellation which wraps back on itself as a result of modulo 2M reduction.

3.3.7 Code Selected for Simulation

Having examined some specific codes as well as aspects of coding theory, it is now possible to select a code appropriate for a TH pre-coding asymmetric communication system. The logic of such a system clearly militates against any method that will require substantial processing overhead, both because the system must operate at high speed and because the processing requirements at the portable receiver must be small. On this basis, convolutional codes can be rejected.

The Viterbi algorithm is too complex for the asymmetric communication system and introduces a processing delay. Although TH pre-coding is compatible with trellis decoding, the asymmetric communication link uses a DFE in one direction. As shown in the Section 2.9, the processing delay of the Viterbi algorithm is incompatible with the requirement of a DFE for immediate reliable decisions at its feedback filter input [Aman, 876]. Sequential decoding is an alternative to the Viterbi algorithm, but processing requirements, although less than the Viterbi algorithm, are still substantial. Constant throughput is also not guaranteed.

Of the block codes, Reed-Solomon possesses resistance to burst errors that are possible, if not inevitable, on a wireless channel [Kanal, 724]. The non-binary symbols used by the code are also easily mapped to a non-binary transmit signal constellation. Upon closer examination, these features lose some of their attraction. Burst error protection is achieved because this type of error is absorbed by the symbol structure [Berlekamp4, 52]. In other words, because a symbol represents multiple bits, a short burst of bit errors may only involve a small number of symbols. Errors are corrected at the symbol level, so bit error bursts can be overcome. This capability is unnecessary in a Gray coded system where one symbol error will likely represent only a single bit error. The multi-level symbol alphabet of RS codes is also a processing burden and requires solution of a significant system of equations to decode a Reed-Solomon encoded message.

Repetition codes are easily implemented, but are inefficient at carrying information. Hamming codes, also relatively easy to implement, are already used in high speed LANs but their single error correction capability may be insufficient for a wireless channel. Of all the codes examined, this leaves only the BCH class. Processing of these codes can become burdensome, but judicious selection of a short, simple version should mitigate complexity problems. A (15,7) BCH code can be defined over GF(2^4), a Galois field with only fifteen four-bit elements. This code has distance five and can correct two errors [Hoffman, 132]. Some patterns of three errors are detectable but cannot be corrected [Berlekamp1, 17]. The codewords are multiples of following generator polynomial [Chien1, 130]:

$$g(x) = 1 + x^4 + x^6 + x^7 + x^8 \tag{3.1}$$

Calculation of the error polynomial is relatively simple for a double error correction capability. For two syndromes, denoted S_1 and S_3, the error locator polynomial is given by [Chien1, 131]:

$$x^2 - S_1 x + (S_1^2 + \frac{S_3}{S_1}) = 0 \tag{3.2}$$

The roots of this equation can be found with a Chien search or, because the Galois field is small enough, by memory lookup. Once found, the logarithms of these roots will indicate the error locations [Hoffman, 135].

The 7/15 rate of the selected code is inefficient, a consequence of the simplicity of the decoding operation and a typical feature of short codes [Chien2, 744]. However, a large number of errors can potentially be corrected as a result of the code's short length. A double error correcting code of length fifteen can tolerate an average of one error for every 7.5 transmitted bits. The low rate will also allow the relative merits of uncoded narrow-band wireless data transmission to be compared with high overhead, wide-band transmission.

The performance of this code is difficult to predict. Examination of the differences between random and burst errors indicates that coding gain depends on the error statistics of the channel [Longo, 70]. Because the indoor radio channel is vulnerable to error bursts, the code may be swamped when these bursts occur, by error vectors with distances exceeding the correction and detection capability of the code. With sufficient interleaving, burst error locations may be randomized. The effectiveness of these measures at reducing the error rate may be estimated through computer simulation of the coded communication system.

Although ARQ schemes have also been discussed, these will be only a peripheral part of this study. Repeat request systems may be a necessity in a wireless LAN system to ensure a high standard of data integrity, but the channels used in this study involve spatial rather than temporal variations. Temporal variation is necessary for a Type 0 or Type I ARQ system so that errors in the original block of data are not simply duplicated in the retransmitted block. A more extensive discussion of channel modelling issues is contained in the next chapter.

3.4 Conclusion

Apart from wind, one theme to emerge from this chapter is the existence of numerous diversity and coding methods. The requirements of TH pre-coding and asymmetric communication help to reduce the set from which diversity and coding methods will be selected. For example, sophisticated diversity combining is ruled out by the inability of TH pre-coding to create multiple ISI-free channels simultaneously. Asymmetric communication also requires simplified signal processing at the portable. As a result, switched antenna diversity will be used at the base station. Using this approach, the base station will select a channel with the smallest mean square error, after equalizer training, and use only that channel for subsequent transmission and reception. This diversity method may be implemented entirely at the base station only and is invisible to the portable, not adding to its signal processing requirements.

The selection of a coding method is less obvious. Convolutional codes and codes with non-binary alphabets can be ruled out by their decoding complexity. Many other options exist, but a short two-error correcting (15,7) BCH code was selected because of its low complexity and significant error protection capability. A drawback of this code is a relatively low information rate, but this should help illustrate the extent to which bandwidth, processing overhead and data integrity may be traded-off.

Chapter 4

Simulation of Tomlinson-Harashima Pre-Coding

4.1 Introduction

Previous chapters have explained the motivation for asymmetric communication and provided the theoretical basis for an asymmetric communication system using Gibbard pre-coding. Attention can now turn towards performance evaluation. As a prelude to the results presented in Chapter 5, the present chapter will examine how performance measurements were obtained.

Short of actual implementation, a communication system may be evaluated either analytically or through simulation modelling. In general, analytic techniques are more accurate but simulation is the only feasible method for systems of moderate to high complexity [Woerner, 43][Tranter, 26, 34]. Modelling avoids the need to solve potentially vast systems of equations but presents its own set of difficulties, requiring substantial effort to ensure that simulation methodology and functional representations yield accurate results. This chapter will explain the choices and approaches that have been taken in developing and running a simulation model of an asymmetric communication system.

4.2 Simulation Approach

4.2.1 Monte Carlo Analysis

System BER performance was measured using Monte Carlo analysis. In this approach, waveforms and noise levels are modelled as they are expected to appear in an actual communication system (or its lowpass equivalent) and error probability is estimated by counting error events. Of all simulation methods, this is regarded as the most accurate, but also the most costly in terms of simulation time [Jeruchim, 530][Tranter, 34].

Simulation time may be reduced by adopting one of the variance reduction methods, including semi-analytic analysis, importance sampling and tail extrapolation [Tranter, 30-33][Jeruchim, 503-30]. These possibilities were rejected for several reasons, including the fact that simulations for this study were carried out over a large number of channels. For each channel, it is necessary to train the adaptive DFE, pass its coefficients to the Gibbard pre-coder and transmit data. Using Monte Carlo analysis, only 1000 symbols were transmitted over every channel, perhaps a computational burden no greater than would be required if each channel was subjected to a variance reduction technique. A greater risk of inaccurate results is also a consequence of the assumptions about error distribution necessary to apply variance reduction [Tranter, 31]. The alternative, Monte Carlo analysis, avoids these assumptions and possesses the additional advantage of replicating signal waveforms as they are expected to actually appear in a real communication system, enabling verification of the simulation's accuracy and measurement of parameters such as signal and noise power [Tranter, 30].

An exact BER can be found with Monte Carlo analysis only by letting the number of simulation iterations become infinite [Jeruchim, 492]. As even the most patient of graduate supervisors is unlikely to tolerate such a long wait for results, simulations must be truncated to a finite length. This length should be adequate to yield accurate results without requiring excessive simulation time. As shown next, balancing these objectives may not be simple.

4.2.2 Confidence Limits

Simulation is a means for estimating performance parameters. These parameters are random variables with confidence limits that can be established if the variable's distribution is known [Tranter, 26]. Since error events are relatively rare, it was assumed that the number of transmitted symbols required to estimate the BER would significantly exceed the number needed to estimate signal and noise power. Attention was therefore focussed on finding a simulation duration appropriate for BER estimation.

A binomial distribution is often assumed for error events in communication systems, allowing confidence limits to be easily established with Poisson or normal binomial approximations [Jeruchim, 498-500]. In an early attempt to minimize the simulation time required for this study, a BER estimate, assumed to be accurate within ±22% of the actual rate, 95% of the time, was obtained by running each simulation for a duration sufficient to generate 100 error events [Crow]. Transmitted data was partitioned into frames and, for each frame, a new channel was randomly drawn from a pool of channel models.

The results generated using this procedure were disappointing. One drawback was the difficulty in estimating simulation run time. At high SNR, some simulations would consume days of computer time before being terminated, without producing a BER estimate, when it became apparent that weeks or months would actually be required for the requisite 100 error events to be counted. The main drawback of this procedure was that BER measurements were not commensurable from one simulation to the next. Bit error rate plots, as a function of SNR, were highly irregular, quite different from the smooth curves ordinarily found in the literature. Error events in the asymmetric communication system are not, in fact, binomially distributed and some channels are much worse than others for generating errors. Bad channels, although few in number, were responsible for most of the errors. In essence, this initial simulation procedure consisted of transmitting frames of data over different channel models until a few bad channels were encountered, sufficient to drive the error count above the 100 error event threshold. A small number of channels determined the error count, yielding a BER estimate with a high variance.

The next approach was to run each simulation until a fixed number of bad channels was encountered, determined by counting the number of frames with errors. This procedure treated bad channels as the binomially distributed variable. Irregular BER curves persisted because the set of bad channels changed at different SNR levels, as some bad channels ceased to cause errors when SNR was increased. Different sets of bad channels produced incommensurable BER performance because of considerable variation in multipath severity, even between bad channels. Finally, it was recognized that meaningful comparison between BER measurements at different SNR levels, various data rates, diversity or non-diversity configurations and coded or uncoded configurations requires that every simulation be carried out over an identical set of channels, regardless of the number of error events, as long as a minimum error event threshold is satisfied.

A set of 600 randomly selected channels was chosen for use in every simulation. Each of these had an associated channel, in case dual antenna diversity was being modelled, making 1200 channels in all. For every simulation, or point on a BER curve, a frame of 1000 data symbols was sent over each of the 600 channels, for a total of 600 000 transmitted symbols or 2.4 million transmitted bits. The smallest detectable BER, for the case of a single bit error, is 4.17×10^{-7}. The range of SNR values for the simulations was chosen so the lowest BER would be above this minimum, roughly between 10^{-4} and 10^{-5}, to provide a level of confidence in the results.

Actual confidence bounds are difficult to determine. For the binomial distribution, confidence bounds are readily available but this distribution does not hold for the errors encountered in this study [Crow, 635][Jeruchim, 499]. Errors are dependent and confidence levels will be less tight than the binomial case [Jeruchim, 502]. Determination of exact confidence bounds for the BER estimates in this study requires a model for the error distribution [Jeruchim, 502]. Because of the anticipated difficulty in finding a model that accounts for the variation in error frequency across 600 channels, determination of exact confidence bounds was not attempted.

Approximate confidence levels were determined by recognizing that a greater number of error events in this study would need to be counted for confidence limits comparable to the limits with a binomial error distribution. By controlling the SNR levels, the lowest anticipated number of errors for any simulation, 120 bit errors, would produce a BER estimate of 5×10^{-5}. Guessing that, for the same confidence limits, the number of error events counted would need to exceed by a factor of ten the number of errors in the binomial case, the actual BER would then lie in the range 2.5 x 10^{-5} to 9.0 x 10^{-5} (±50%, approximately) with 95% confidence. For most results, these bounds would be tighter because, at lower SNR, the number of error events would exceed the number anticipated for the minimum BER.

Confidence bounds were needed to help determine an appropriate duration for the simulations. Because of their inexactitude and speculative origin, these bounds will not be included with the plotted or tabulated results presented in Chapter 5.

4.2.3 Verification

In addition to confidence limits based on the adequacy of sample size, assurances are needed that results have been derived from accurate models. Verification was carried out by matching waveforms and coefficients from SPW™, the primary simulation platform, with corresponding values obtained from programs written for the MATLAB™ numeric computation system. These tests included comparing channel impulse responses taken from the simulation with MATLAB™ calculated responses. In addition, coefficients from the adaptive DFE were compared both with Wiener coefficients and with coefficients from the same adaptive algorithm implemented in MATLAB™. Another test was to match output of the SPW™ simulator's Gibbard pre-coder with the output of a MATLAB™ pre-coder version.

Additional tests were performed without resorting to MATLAB™. A coarse check on accuracy was obtained by matching SPW™ derived BER performance curves with theoretical curves for 16 QAM over an AWGN channel. To test for systematic mistakes in recording errors, error distribution was also examined to ensure there was no obvious pattern to single and burst error events.

Proof of a simulation's accuracy may be unattainable, but system components were tested, individually and collectively, to ensure performance satisfied expectations. Implementation details for these components are provided below.

4.3 Simulation Design Details

4.3.1 Simulation Platform

Modelling was performed with SPW™, version 3.0, a commercial CAD package for communication system design and simulation[1]. Several features of this package facilitated system design, such as a graphical interface and functional block organization. These features allow a communication system model to be assembled and reconfigured by connecting or reconnecting functional blocks in a system block diagram. To speed up design, SPW™ includes a standard library of blocks that perform signal generation and storage, modulation and demodulation, filtering, equalization, logical and mathematical functions and other common communications-related operations [Comdisco, 1-11]. Blocks can be organized hierarchically, enabling advanced functions to be assembled from standard library blocks [Comdisco, 1-1]. For functions that are unavailable or not readily derivable from standard blocks, SPW™ permits custom blocks, written in FORTRAN or C, to be incorporated into the design, an aspect

---

[1] SPW is a registered trademark of the Alta Group of Cadence Design Systems, Inc., of Foster City, California, USA (formerly Comdisco Systems).

of SPW™ used frequently in creating a model of the asymmetric communication system [Comdisco, 1-3].

Once the design is in place, the details of running a simulation are handled by SPW™. For every simulation iteration, the internal state and output of each blocks are updated according to a block's function, previous state and input. Simulations operate at a discrete waveform level and signals may be sampled at relevant points in the system for subsequent analysis, a helpful debugging feature. For the simulations carried out in this study, double precision arithmetic was consistently used.

4.3.2 Simulation Overview

Major functional blocks of the asymmetric communication system are shown in Figure 4.1. The asymmetric communication system consists of a base station, a portable and a two-way radio link between them. The base station and portable share the same channel using TDMA and the channel impulse response will be identical in both directions due to reciprocity [Morrison2][Acampora, 13]. As intended, signal processing requirements, in the form of a DFE and Gibbard pre-coder, are concentrated at the base station. Coefficients for the Gibbard pre-coder are taken from the adaptive DFE.

The system model is intended for use in estimating performance of a Gibbard pre-coder and DFE communication links for a particular user, not for estimating performance of an overall network [Woerner, 42]. Bit error rates, frame error rates, average transmit and receiver signal power, peak transmit signal power and noise power are measured. Noise is modelled with an average distribution that is Gaussian in the time domain and white in frequency (AWGN).

No attempt has been made to account for interference that might originate with other users of an asymmetric communication system nor have attempts been made to determine an overall system capacity.

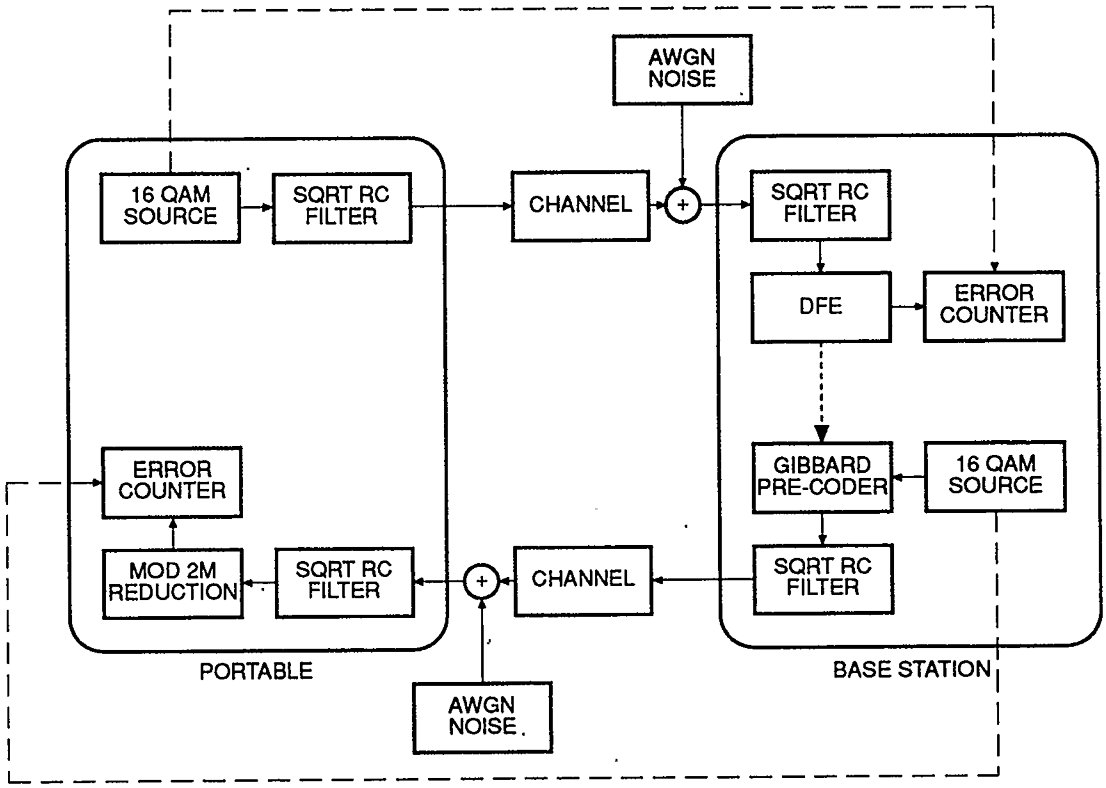

FIGURE 4.1 MAIN FUNCTIONAL BLOCKS OF THE ASYMMETRIC COMMUNICATION SYSTEM SIMULATION MODEL

Discrete waveform-level simulations, as used in this study, require a sampling rate sufficiently high to avoid aliasing [Jeruchim, 268]. To avoid excessive sampling requirements, signals are modelled as their lowpass equivalents. Modulation and demodulation of information signals with a carrier frequency is avoided by using lowpass equivalents, without inhibiting the ability of the simulation to represent relevant channel phenomena such as flat and frequency selective fading [Tranter, 27]. The minimum sampling rate is twice the highest signal frequency component [Stremler, 122]. The highest frequency component after raised cosine filtering is given by [Feher, 322]:

$$f_{max} = (1+\alpha)\,\frac{f_{symbol}}{2} \tag{4.1}$$

In equation 4.1, f_{symbol} is the symbol transmission rate. For a normalized symbol rate of 1, using a finite roll-off of α=0.35, f_{max} is 0.675. At the minimum, the simulation sampling would need to be at twice this rate, or 1.35. To accurately reproduce waveforms in the time domain and ensure accurate functioning of all blocks, the sampling rate should exceed this minimum [Jeruchim, 268]. In this study, the frequency of sampling was four times greater than the symbol rate.

4.3.3 Gibbard Pre-coder

The Gibbard pre-coder was implemented using custom-coded SPW™ functional blocks. With coefficients taken from the DFE at the conclusion of DFE training, pre-coder operation consists of calculating feedback and feed-forward filter output and performing a modulo 2M reduction operation every symbol interval. During development of the simulation, a separate channel estimator was tested. Pre-coder feedback filter coefficients were taken from this estimator. Tests showed the computational burden could be reduced without sacrificing performance by eliminating the estimator and taking all pre-coder coefficients directly from the DFE. Pre-coder operations and signal flow are shown in Figure 4.2

Filter dimensions for the Gibbard pre-coder and DFE are identical to permit sharing of coefficients and for performance comparison. The adaptive DFE coefficients are trained to jointly minimize ISI and noise. Unlike the DFE, the Gibbard pre-coder is not susceptible to noise enhancement because it operates at the noise-free transmitter. However, the selection of equalizer dimensions solely on the zero forcing basis of ISI cancellation by the pre-coder would neglect the dual role of the equalizer coefficients in noise and ISI minimization. In order that the coefficient vector will be sufficiently long for both purposes, dimensions were determined based on DFE MMSE performance criteria.

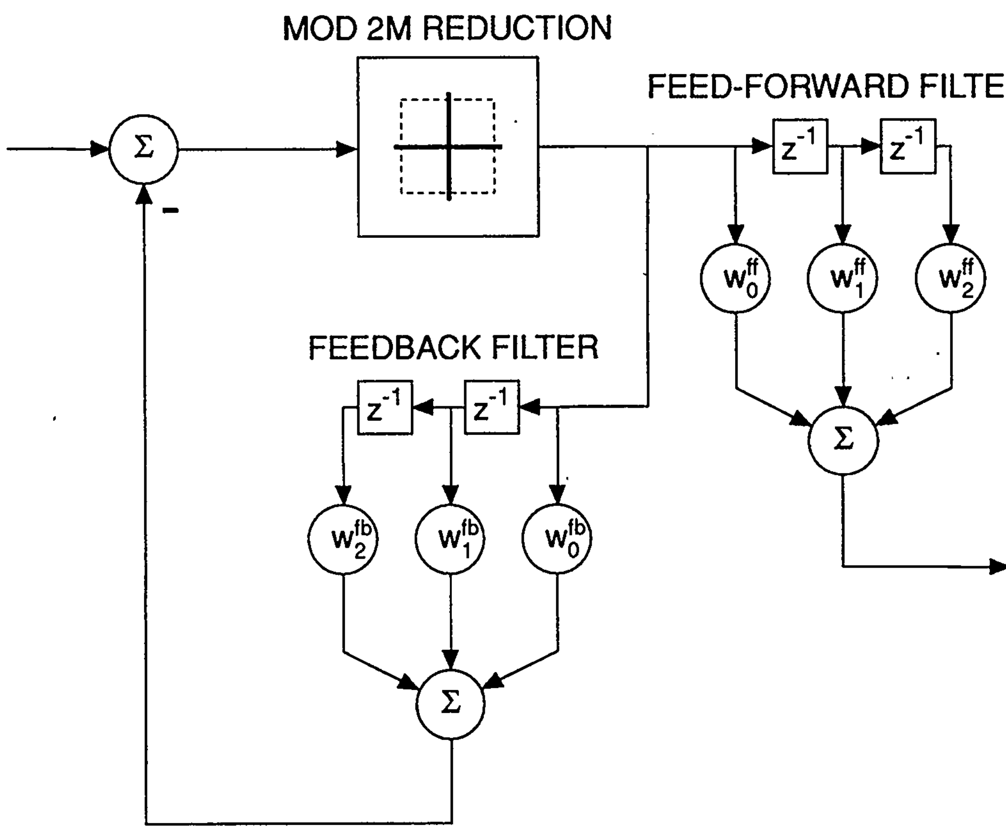

FIGURE 4.2 FUNCTIONAL DIAGRAM OF GIBBARD PRE-CODER WITH DIMENSION (3,3)

4.3.4 Decision Feedback Equalizer

A general formula does not exist to determine an appropriate length for the feed forward and feedback dimensions of a DFE, although the dimensions depend, in some way, on the channel impulse response [Bingham, 277]. As a starting point for testing various equalizer lengths, one suggestion is to use a length slightly in excess of a truncated channel impulse response [Bingham, 277]. This truncated impulse response is determined by removing a small portion of the leading and trailing data points of the full impulse response, comparable to the acceptable error at the equalizer output.

This approach does not significantly clarify the question of DFE length because it leaves unresolved the distribution of the length between feed-forward and feedback filters and is unclear on how much the length should exceed that of the truncated channel impulse response. A different and more direct approach, used in this study, is based on a priori knowledge of the channel and extensive calculations in MATLAB™ computation software. Every channel used in simulations was convolved with the impulse response of the transmit and receive raised cosine filters to determine an 'overall' impulse response. At different SNR levels and feed-forward and feedback filter lengths, Wiener equalizer coefficients were calculated from the overall response, sampled at the symbol rate. By applying Wiener coefficients to the sampled, overall impulse response, residual ISI and noise amplification were determined and a signal-to-distortion performance measure calculated with the following formula [Amitay, 598]:

$$\rho_D = \frac{P_s}{P_i + P_n} \tag{4.2}$$

In this formula, P_S is the received power of a bipolar pulse, excluding ISI and noise, P_i is the mean square ISI and P_n is the mean square noise. The ρ_D performance criterion provides an upper bound on BER, given by the equation [Amitay, 598]:

$$\text{BER} \leq 2\exp(-\rho_D/2) \qquad (4.3)$$

Performance curves, as a function of feed-forward and feedback filter length, may be plotted using the signal-to-distortion performance measure, averaged across all channels. The crest of the curve, where the gradient is small, gives a DFE dimension which balances performance and complexity. Due to the small gradient beyond the crest of the curve, performance gains are insufficient to justify additional equalizer taps, especially because the number of computations required to train an RLS equalizer increases as a function of length squared [Gitlin2, 591]. An example of an error performance surface is shown in Figure 4.3.

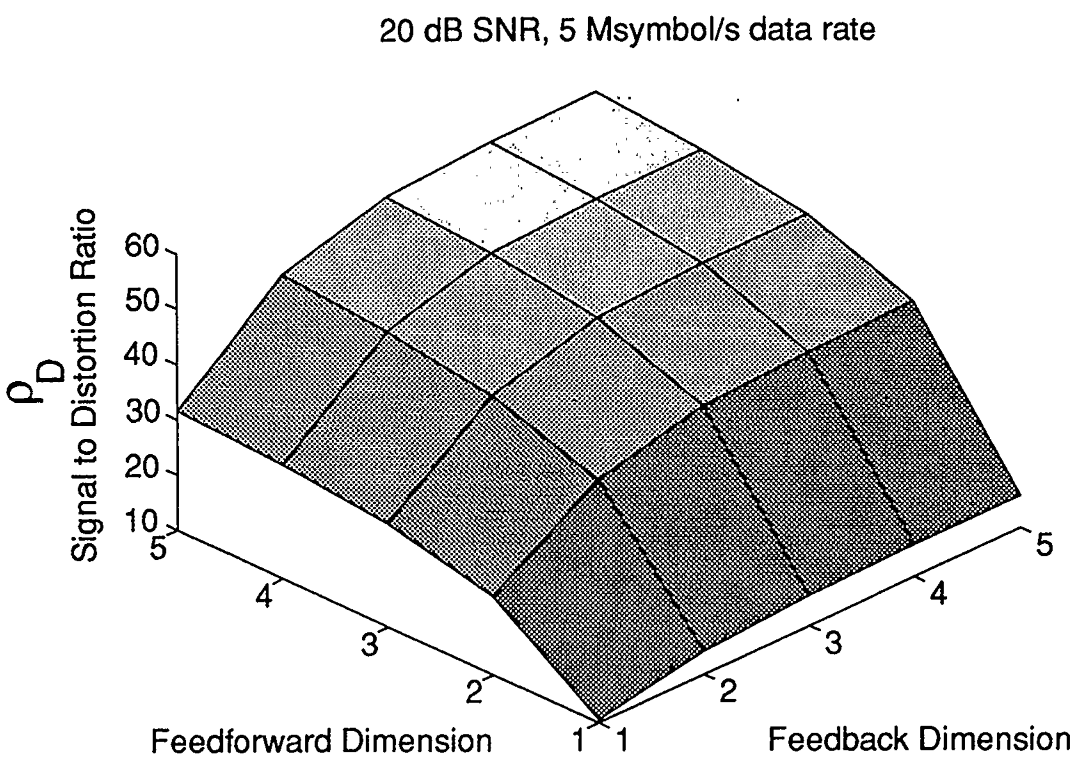

FIGURE 4.3 DFE SIGNAL-TO-DISTORTION PERFORMANCE SURFACE

Performance curves are based on the average signal-to-distortion ratio and neglect variance in the performance statistics. Simulation test runs were necessary to ensure satisfactory overall performance given the possibility of channels with performance indices that deviate from the mean. A strict relationship was also imposed between equalizer dimensions at different data rates. For valid comparison of results, dimensions were scaled in proportion to the data rate, reflecting changes, relative to the symbol period, in the length of the channel impulse response at different rates. In the end, the equalizer dimensions given in Table 4.1 were adopted.

TABLE 4.1 DFE SIZES

DATA RATE (Msymbol/s)	EQUALIZER DIMENSION (FF,FB)	LENGTH OF TRAINING SEQUENCE
5	(3,3)	50
10	(6,6)	100
20	(12,12)	200

The DFE was trained with a complex-valued RLS algorithm. Lengths for the training sequences were chosen to guarantee coefficient convergence for all channels. Convergence time for the RLS algorithm increases in direct proportion to equalizer length so training sequence length was also scaled in proportion to data rate, as shown in Table 4.1 [Gitlin2, 591]. Frame length was increased to accommodate the training sequences and provide a constant number of transmitted data symbols for every simulation.

Coefficient convergence was improved in speed and accuracy by training the feedback filter using ideal, error-free symbol values. The alternative, passing feed-forward filter output to the feedback filter while training, yields an error statistic too imprecise for satisfactory coefficient convergence. Error-free training feedback may render the equalizer output excessively dependent on the feedback filter during regular data transmission, increasing vulnerability to error propagation. This risk was outweighed by the number of errors that result when the feedback filter coefficients are trained with non-ideal symbols. Furthermore, the Gibbard pre-coder is immune from error propagation and error-free training of the feedback filter in the DFE will yield coefficients well suited for the pre-coder's feedback filter.

4.3.5 Channel Modelling

The channel plays an important and central part in the evaluation of the asymmetric communication system. Indeed, the channel provides the raison d'être for the Gibbard pre-coder and DFE, for it is channel-induced ISI which these components are designed to defeat. Channel modelling cannot be approached lightly; care must be taken to ensure that its effects are modelled realistically [Woerner, 43].

Four possible approaches to channel modelling are given in [Woerner, 43]. First, there are analytically-based approaches, using path strength distributions such as Rayleigh, Ricean, lognormal and Nakagami. Second, there are models derived from measured channel statistics. Simulated channels taken directly from actual channel measurements are a third possibility. Fourth, with ray-tracing a channel model can be derived from knowledge of the environment in which the communication system is intended to operate.

For this study, the third option was selected, taking the model directly from channel measurements. Analytic channels were rejected to avoid dealing with questions about the accuracy and suitability of a selected model. The second approach, a simulated channel derived from measurement statistics, was ruled out because an appropriate model was not available. Deriving a channel model from knowledge of the environment, the fourth approach, would be too time-consuming, specific to only a few locations, potentially inaccurate and unnecessary given the availability of a large database of channel measurements.

Channel measurements used in this study were taken in two Calgary office buildings using a network analyzer connected with two antennas, to produce frequency domain data over the 900 to 1300 MHz bandwidth. Seventy-five measurements were taken at twenty sites in each building for antenna separations of 5, 10, 20 and 30 metres. The creation of this database was undertaken by Morrison and Tholl; details of the measurement system and methodology may be found in [Morrison1] and [Hashemi3].

Before measurements from this database could be used in SPW™, several processing steps were necessary. To begin, 600 channels were randomly chosen to be used in every simulation. This number provides a large sample size without causing prohibitively long simulation time. To provide for antenna diversity, an additional channel, measured at a distance of 20 cm from the first, was matched to each of the 600 randomly selected channels. All of the selected channels were measured at 30 metre antenna separations, the largest available distance. Multipath effects, measured in terms of RMS delay spread, are severest at this separation [Hashemi3, 115]. Severe multipath is desirable for rigorous testing of the Gibbard pre-coder.

In this study, the oversampling factor was held constant over different data transmission rates. An alternative approach is to use the same channel model at all data rates and vary the oversampling factor [Gibbard2, 286]. This alternative reduces the required amount of channel pre-processing but simulation time becomes excessive when oversampling is high. Instead, different pools of channel models were generated for every data rate by taking an appropriate bandwidth for each of the 600 selected pairs of channel measurements. These bandwidths are given in Table 4.2

TABLE 4.2 BANDWIDTHS OF CHANNEL MODELS

DATA RATE (Msymbol/s)	SAMPLING RATE (Msamples/s)	CHANNEL BANDWIDTH (MHz)	CHANNEL FREQUENCY RANGE (MHz)
5	20	20	1090-1110
10	40	40	1080-1120
20	80	80	1060-1140

The channel measurement database was pre-processed using MATLAB™ computation software. First, frequency domain data was taken from the database corresponding to the 600 selected channel pairs and the frequency ranges specified in Table 4.2. Regardless of bandwidth, the energy of every extracted data vector was scaled in proportion to the energy in the 80 MHz frequency bandwidth to compensate for path loss and shadowing. Path loss is a reduction in signal energy due to distance and, even at the constant 30 m antenna separation, can vary considerably, depending on the measurement environment [Woerner, 43-44]. By compensating for large scale signal attenuation, performance results largely depend on flat and frequency selective fading. Unlike large scale attenuation, these are phenomena which equalization, micro-antenna diversity and coding can combat. By focussing on these phenomena, the potential performance of the asymmetric communication system can be better assessed. Scaling in proportion to the energy in the 80 MHz band preserves relative power differences between narrow and wideband channels so that variations in the severity of frequency selective fades are maintained.

Following energy scaling, the data vector extracted from the measured channel database is multiplied by a Hamming window to reduce truncation artifacts that would otherwise arise when an Inverse Fast Fourier Transform (IFFT) is applied to the finite length data sequence [Oppenheim, 446]. By taking the IFFT of the windowed data, frequency domain data is converted to a time domain impulse response. The first half of this impulse response is relevant while the latter consists of 'negative time' measurements, representing the period before application of an impulse to the channel, and is ultimately discarded. Noise statistics, taken from this negative time measurement are used to reduce noise in positive time. A noise threshold, 2.5 standard deviations above the mean noise power, was calculated and any impulse response components below this threshold were regarded as noise and removed [Morrison1, 10]. Components 30 dB below the largest component were also eliminated, restricting the dynamic range of the measurements to a level achievable with a 30 metre antenna separation [Hashemi1, 113].

In addition to discarding the negative time measurements, the positive time impulse response was also truncated, a necessary step to limiting the number of required computations for each simulation. To avoid sacrificing accuracy, the truncated impulse response length was determined only after looking at the time domain distribution of significant multipath components. As shown in Figure 4.4, there are very few significant multipath components, defined as components within 20 dB of the largest component's power, after 800 ns, the selected truncation length. Discarding data from beyond 800 ns produced sequences of length 16, 32 and 64 for 5, 10 and 20 Msymbol data rates, respectively, lengths which are powers of 2 and therefore suited for FFT/IFFT calculations used in frequency domain filtering.

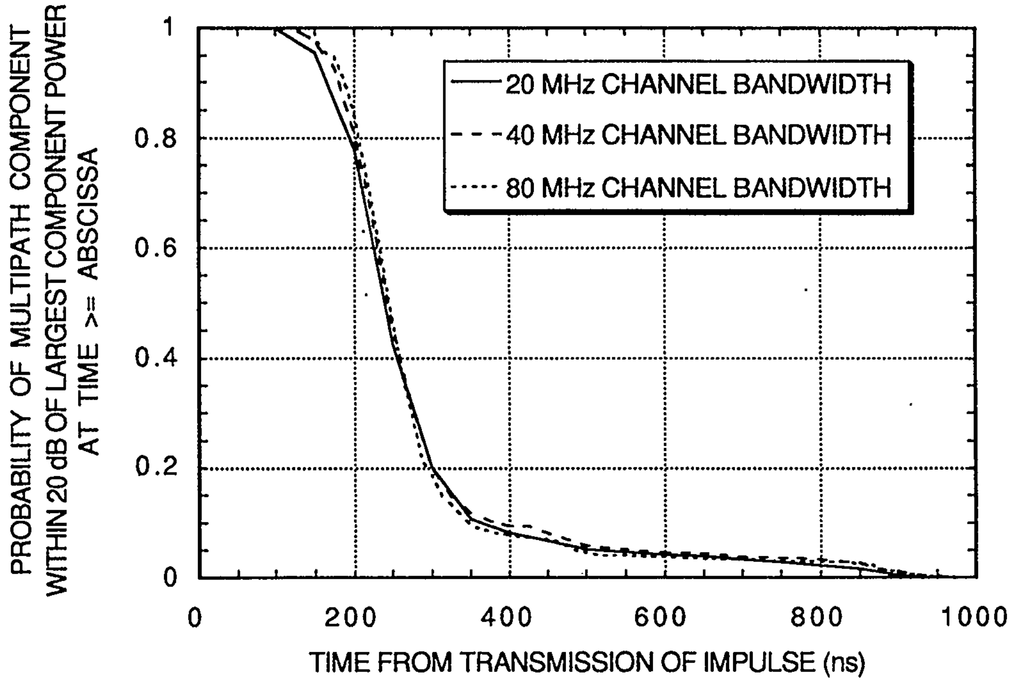

FIGURE 4.4 DISTRIBUTION OF SIGNIFICANT MULTIPATH COMPONENTS IN CHANNEL IMPULSE RESPONSE

A statistic for measuring the severity of a channel's multipath effects is the rms delay spread, τ_{RMS}, given by the equation [Hashemi2, 975]:

$$\tau_{RMS} = \sqrt{\frac{\sum_k (t_k - \tau_m - t_A)^2 \, |h(k)|^2}{\sum_k |h(k)|^2}} \tag{4.4}$$

In this equation, t_k is a component's arrival time, t_a is the arrival time of the first component, $|h(k)|$ is the component's magnitude and τ_m is the mean excess delay, calculated with [Hashemi2, 975]:

$$\tau_m = \frac{\sum_k (t_k - t_A)\,|h(k)|^2}{\sum_k |h(k)|^2} \tag{4.5}$$

Table 4.3 provides the mean and standard deviation of τ_{RMS} before and after truncation. Truncation has caused a slight reduction in the mean of the RMS delay spreads. The standard deviation has been more significantly affected, showing that truncation has reduced the severity of multipath spread for more extreme channels. On the whole, accurate modelling of multipath effects has not been compromised by truncation. Table 4.3 also shows a decline in the mean τ_{RMS} as the data rate increases, possibly an indicator of the greater susceptibility of narrowband transmission to flat fading [Gibbard2, 286]. If the main component is relatively small as a result of flat fading, τ_{RMS} may become large.

TABLE 4.3 RMS DELAY SPREAD

	BEFORE TRUNCATION		AFTER TRUNCATION	
DATA RATE (Msymbol/s)	τ_{RMS} μ (ns)	τ_{RMS} σ (ns)	τ_{RMS} μ (ns)	τ_{RMS} σ (ns)
5	46.2	17.8	44.1	13.7
10	38.5	17.7	36.3	13.5
20	35.7	17.8	33.7	14.0

After truncation, the length of the remaining data sequence is doubled through zero padding to avoid corruption of the data during frequency domain filtering. Corruption is a possibility because the equivalent time domain convolution that results from frequency domain filtering is circular; the convolution will wrap back on itself, producing inaccurate results unless a buffer of zeros is provided [Blais, 16-17]. Following zero-padding, an FFT is used to take the time domain data back into the frequency domain. In this form, the data is stored for use by the SPW™ simulator.

Filtering in the frequency domain was chosen for its computational efficiency. During simulation, zero-padded blocks of transmitted data symbols are brought into the frequency domain with an FFT where element-by-element multiplication of the symbol data with the channel model is carried out. Data is then restored to the time domain with an IFFT, and blocks of data are recombined for further processing using the overlap and add method [Oppenheim, 558]. Even with zero-padding and FFT/IFFT transformation, frequency domain filtering requires fewer multiplications than equivalent time domain operations. For a block of length N, the FFT and IFFT operations each require [Brigham, 134]:

$$\text{multiplications} = \frac{N}{2}\log_2 N \tag{4.6}$$

An additional N multiplication operations are needed to multiply each data block by the channel model. The total number of multiplication operations is therefore:

$$\text{multiplications} = N(1+\log_2 N) \tag{4.7}$$

In the time domain, data sequences are not zero padded and a convolution operation would operate on a sequence of length N/2. The number of multiplications is given by:

$$\text{multiplications} = \left(\frac{N}{2}\right)^2 \tag{4.8}$$

From these equations, it can be shown that frequency domain filtering of a zero-padded 32 length sequence would require 192 multiplications compared to 256 multiplications for the equivalent non-zero padded 16 length time domain sequence. Gains become even more significant as the channel model length is increased for higher data rates.

This study uses a quasi-static approach to channel modelling [Jeruchim, 386]. Slow channel variations are completely ignored and the channel is assumed stationary during a transmitted frame. Between frames, a new channel model is loaded into the simulator. Quasi-static modelling allows simulation under a large number of channel conditions without requiring the excessive computation time needed to model transitions between channel states. Another deliberate omission from the channel is Doppler shift or frequency domain signal spreading [Kennedy, 12]. Relative motion of the portable and base station is assumed to be slow or non-existent, eliminating the need to model this effect.

4.3.6 Carrier Phase Recovery

Assuming coherent demodulation of the received signal waveform, carrier synchronization is defined as the alignment of a waveform generated by the receiver's local oscillator with the signal carrier wave [Jeruchim, 573]. For QAM, a phase difference between the local oscillator and carrier wave results in attenuation of the demodulated signal and crosstalk interference between the in-phase and quadrature channels [Franks, 1108]. Since modulation and demodulation do not occur in baseband communications, the effect of a phase difference between the carrier and local oscillator waveform will not be present unless a phase error is deliberately introduced into the simulation model [Jeruchim, 565]. This study will neglect the issue of carrier synchronization and assume perfect coherent demodulation in order to focus attention on the performance of Gibbard pre-coding rather than subsidiary operations in the asymmetric communication system, such as carrier recovery.

4.3.7 Symbol Timing Recovery

Symbol synchronization is the selection of timing for taking samples of the incoming signal at the receiver, also known as timing recovery [Proakis3, 596]. Performance of the DFE depends, in part, upon the choice of sample timing [Leclert2, 677]. This dependence is less than the case of a linear equalizer but greater than the case if fractional feed-forward tap spacing is used [Salz, 1471][Ungerboeck1, 863]. Because the Gibbard pre-coder takes its coefficients from the DFE, its performance will also be affected by a poor selection of timing phase.

Performance variations due to sample timing may be understood by examining the spectrum of the sampled impulse response. The roll-off factor of the raised cosine filter causes the spectrum of the received signal to extend beyond the Nyquist bandwidth (1/2T). Sampling at the Nyquist frequency (1/T) by the DFE will fold out-of-band signal components into the Nyquist bandwidth. If the selection of sample timing is poor, some aliased components will be out of phase with their in-band counterparts with which they will interfere destructively, producing frequency selective fades [Ungerboeck1, 857]. The spectrum of a selected channel response is shown in Figure 4.5 along with sampled spectra that result for different choices of timing phase. Timing offset B would be a poor choice, causing attenuation of signal components.

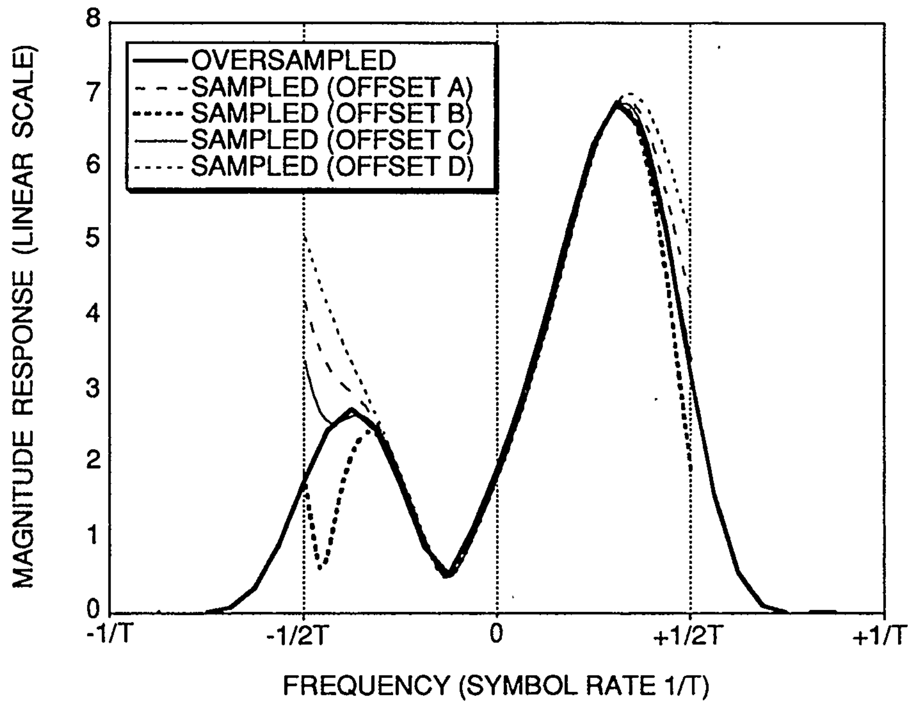

FIGURE 4.5 MAGNITUDE OF CHANNEL RESPONSE SPECTRUM BEFORE AND AFTER SYMBOL RATE SAMPLING

When distortion of the received waveform is minor, the optimal timing phase can be found at the maximal eye opening [Gitlin2, 434]. When distortion is significant, the best sample timing may not be obvious until equalization has actually been tried at various timing phases [Gitlin2, 434]. Because channel distortion is significant at the high data rates used in this study, symbol synchronization presents a challenge. Synchronization may be recovered from zero-crossings or through decision-directed maximum-likelihood parameter estimation [Franks, 1111-15]. However, explicit modelling of synchronization circuitry in the SPW™ communication system simulation was rejected because of the lengthy development time to produce a working model, the additional computations required for simulating synchronization circuitry and the risk that a flawed or sub-optimal model would distort measurement of the Gibbard pre-coder's performance. Instead, timing was derived from channel data prior to simulation.

A criterion is required to select appropriate symbol timing for each channel. This criterion must provide two pieces of information: the symbol-spaced instants at which the incoming waveform should be sampled and the identity of the 'main sample' of the sampled impulse response for alignment with the last tap of the DFE feed-forward filter. The first item, the sampling instant, is known as the *timing phase* [Proakis3, 596]. An obvious criterion for determining timing information is the BER, but this is difficult to calculate reliably [Proakis1, 554]. Instead of relying directly on BER estimates, other criteria were examined and promising choices evaluated using the upper bound on BER obtained with equations 4.2 and 4.3 above. One possible approach is to sample at the maximal eye opening, but this is suited for a system without equalization [Leclert1, 530]. For systems with equalizers, a more suitable criterion is to select the timing phase that maximizes the energy of the sampled impulse response [Bingham, 211][Godard, 518]. For a linear equalizer with constant average noise power and moderate channel distortion, it has been shown that maximal signal energy will yield a maximum SNR level which, in turn, will yield minimum mean square error at the equalizer output and a low BER [Godard, 522]. Although a DFE is less prone to noise enhancement than a linear equalizer, a maximal energy criterion may also be suitable for a DFE [Bingham, 211]. This is suggested by the expression for MMSE at the output of a DFE with an infinite number of feed-forward filter taps [Proakis1, 595]:

$$J_{min} = \exp\left\{ \frac{T}{2\pi} \int_{-\pi/T}^{\pi/T} \ln\left[\frac{N_0}{X\left(e^{j\omega t}\right) + N_0} \right] d\omega \right\} \tag{4.9}$$

In this equation, J_{min} is the MMSE, N_0 is the one-sided noise power spectral density, and $X(e^{j\omega t})$ is the received signal spectrum. Equation 4.9 implies that MMSE will be minimized by maximizing the denominator of the term within square brackets. This could be accomplished by maximizing $|X(e^{j\omega t})|^2$, the power of the received signal.

Adoption of the maximal energy criterion determines the timing phase but does not determine the main sample component of the sampled impulse response. As described in Section 2.2, this component separates precursors and postcursors. The main sample is aligned with the last tap of the DFE feed-forward filter. The DFE attempts to transform the main sample into a unity gain impulse and drive the remaining components towards zero. For a DFE link, this component should be chosen to jointly minimize ISI, noise enhancement by the feed-forward filter and the possibility of error propagation in the feedback filter [Bingham, 290-91]. For the Gibbard pre-coder, the selection of a main sample should also minimize ISI and inhibit the formation of large magnitude feed-forward filter coefficients that might increase transmit signal power.

In general, the obvious candidate to serve as the main sample is the component with greatest energy. Otherwise, the largest energy component would either have to be a precursor, which the feed-forward filter might have difficulty cancelling, or a postcursor, which might increase the probability of DFE error propagation. For cases where at least one precursor has energy comparable to the main sample, the feed-forward filter may be unable to adequately cancel all the precursive signal components. In this case, a significant precursor may have to be designated as the main sample, despite the increased risk of DFE error propagation [Bingham, 291]. Designation of a component as the main sample other than the largest energy component will be referred to as 'advanced timing.'

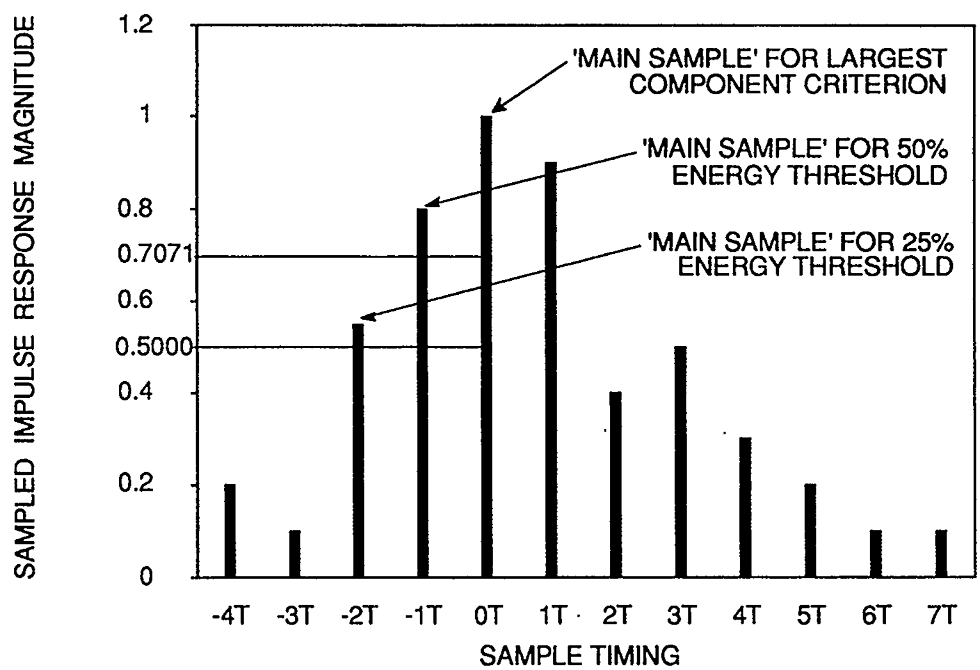

FIGURE 4.6 ADVANCED TIMING EXAMPLE

An evaluation of advanced timing was performed by calculating the distribution of ρ_D, the signal-to-distortion measure from equation 4.2, for 120 of the channel models used in system simulations, ten per cent of the total available channels. These calculations were performed, using MATLAB™, for the cases of no advanced timing, advanced timing for a precursor within 50 per cent of the power of the largest component and advanced timing using a 25 per cent power threshold, cases illustrated in Figure 4.6. A numerical search was also performed on each channel to determine the maximum possible value of ρ_D.

With the exception of the optimum ρ_D value, results are obtained with a timing phase using the maximal energy criterion. By comparison with the optimum value, the adequacy of the maximal energy criterion could also be assessed. A representative set of results from this evaluation is shown in Figure 4.7.

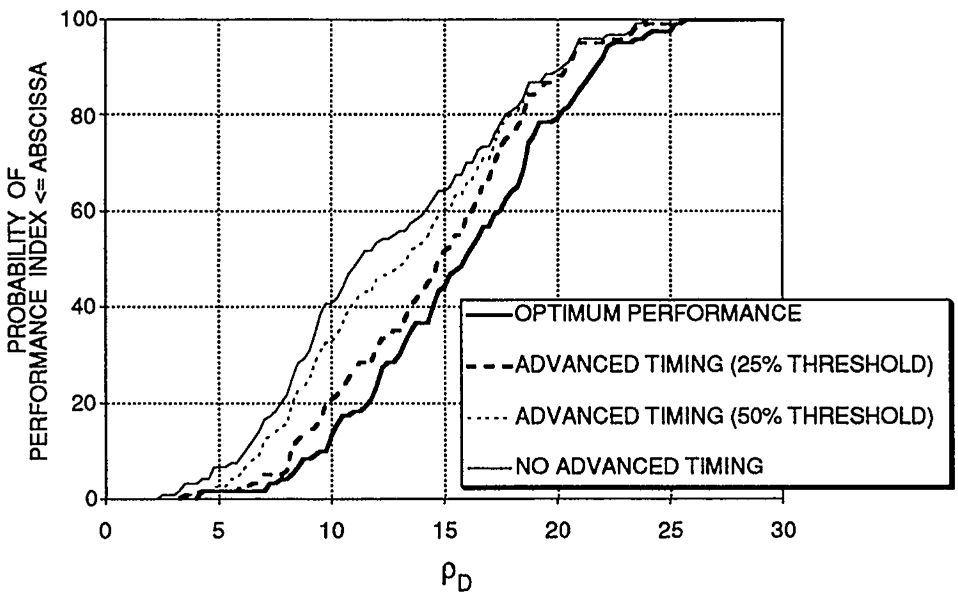

FIGURE 4.7 PERFORMANCE INDEX DISTRIBUTION
20 Msymbol/s, 20 dB SNR

The results of Figure 4.7 show that advanced timing is necessary to bring the signal-to-distortion ratio for the maximal energy criterion closer to the optimum signal-to-distortion value. While the value of ρ_D accounts for ISI and DFE noise enhancement, it neglects other factors which must be considered. Advanced timing increases the energy of DFE feedback filter coefficients, and thus increases the probability of error propagation in the DFE link [Bingham, 291]. Furthermore, as the power threshold for switching to an earlier but lower-than-maximum-energy main sample is reduced, the energy of the main sample can be relatively small. For the DFE to turn a small main sample into a unity gain impulse requires amplification of the small sample, achieved with large magnitude feed-forward filter coefficients. When these coefficients are used in the Gibbard pre-coder's feed-forward filter, the pre-coder's transmit power will be increased, an outcome which imposes greater demands on transmitter hardware.

To balance the improvement in ISI reduction obtained from advanced timing against increased DFE error propagation probability and pre-coder transmit power, a 50 per cent power threshold was adopted. For every channel used in simulations of the asymmetric communication system, timing information was pre-calculated, with timing phase selected to maximize energy in the sampled impulse response. The main sample is the largest energy component or, if existent, the first preceding component with at least 50 per cent of the largest component's energy. Additional testing of this advanced timing algorithm indicates the largest component will be designated as the main sample 88.3 per cent of the time for channels at 10 Msymbol/s and 20 dB SNR. This figure falls as the data rate increases, an indication of the relative severity of multipath effects, and the potential for large pre-cursors, at high data rates.

4.3.8 Automatic Gain Control

To compensate for path loss and shadowing, coefficients of each channel model are scaled in proportion to the energy in an 80 MHz bandwidth. Average received power for any signal that uniformly spans this bandwidth will be constant for all channels. Signals used in this study do not span this bandwidth; raised cosine filters restrict signal spectra to less than 80 MHz and transmission across different channels may therefore produce varying levels of average received signal power.

An automatic gain control (AGC), modelled at the pre-coder and DFE link receivers, amplifies the received signal to compensate for channel attenuation [Proakis1, 274]. For the DFE link, the AGC model used in simulations is perfect, amplifying filtered QAM signals at the receiver by a factor exactly compensating for power loss in the channel. For the Gibbard pre-coder link, transmitted signals are modified by the pre-coder in anticipation of attenuation and frequency selective fades, so amplification of the received signal power to transmitted power levels by the AGC is unnecessary. The AGC forms part of the overall channel response and the Gibbard pre-coder must encounter the same overall response as the DFE in order to accurately compensate for channel effects. For the pre-coder link, an AGC factor identical to that used in the DFE link is therefore required. Figure 4.8 shows the location of the AGC in relation to other functional blocks.

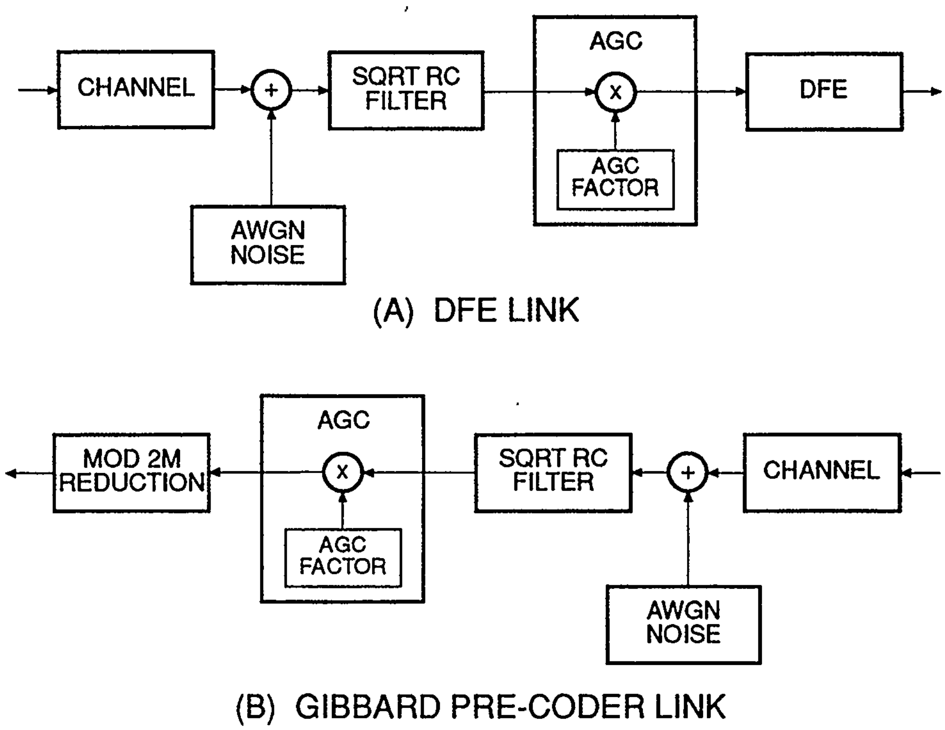

FIGURE 4.8 ROLE OF THE AGC

The AGC amplification factor is calculated, for each individual channel, from the energy in an impulse response formed by convolving channel and raised cosine filter responses. Mean and standard deviation of the AGC factors are given in Table 4.4 for the different data rates. As bandwidth shrinks, increasing susceptibility to signal attenuation from frequency selective fades is demonstrated by the larger average AGC amplification factors and larger variance at lower data rates.

TABLE 4.4 AGC AMPLIFICATION FACTORS

DATA RATE (Msymbol/s)	MEAN	STANDARD DEVIATION
5	137.7	54.0
10	124.6	39.7
20	115.3	36.1

4.3.9 Noise

As shown in Figure 4.8, average white Gaussian noise is added to the signal just prior to the receiver. Noise is complex and scaled to achieve a desired average SNR level at the output of the DFE link's receiver square root raised cosine filter. Noise with an identical power level is added to the received signal in the Gibbard pre-coder link, but signal power is dependent on pre-coder coefficients, so average pre-coder SNR may deviate from levels in the DFE link. Both signal and noise pass through the AGC, leaving SNR unaffected by AGC amplification.

Measurements of SNR are taken at the receiver, following the square root raised cosine filter. As explained in Section 2.7.1, noise, for the purpose of SNR measurements, is defined as random power variation. Signal distortion, such as that due to ISI or filter responses, is excluded from this definition.

Average noise power is constant throughout any single simulation but average received signal power may vary depending on channel severity. This approach preserves BER performance differences between channels with spectral nulls and channels without nulls. If frequency selective fading is present in a channel, signal energy is lost in the fades, SNR declines and the number of bit errors increases. Overall average signal-to-noise ratios are calculated from average SNR levels that prevail for each of the 600 channels used in simulations. A noise scaling factor K_N is obtained with the following formula:

$$K_N = \frac{1}{G_{RC}} \sqrt{\frac{1}{600} \sum_{i=1}^{600} \frac{1}{G^2_{AGC(i)}}} \tag{4.10}$$

In this equation, G_{RC} is the gain of the square root raised cosine filter and $G_{AGC(i)}$ is the AGC amplification factor for each channel. While SNR levels may fluctuate for any individual channel, this scaling factor ensures that SNR, averaged over all the channels, will achieve the desired level at the DFE receiver.

4.3.10 Diversity

Modelling switched antenna diversity at the base station was straightforward. There are 600 pairs of channel models used in this study, each pair derived from measurements at locations separated by 20 centimetres. Two decision feedback equalizers, one for each paired channel, are used at the base station in diversity simulations and trained simultaneously. At the conclusion of training, a channel is chosen for data transmission according to the smallest equalizer MSE, averaged over a short window. This choice represents the selection of one of the diversity antennas for subsequent data transmission and reception. Equalizer coefficients for the selected channel are then provided to the Gibbard pre-coder which also transmits over the selected channel, in an appropriate TDMA time slot.

4.3.11 Coding

A (15,7) BCH coder and decoder were implemented efficiently, as custom coded SPW™ functional blocks, using bit-wise shift and XOR operations available in the C programming language. For the selected BCH code, words are short enough to permit memory lookup of error correction vectors from syndromes, a means of speeding up the simulation process.

To overcome bursty errors, especially due to error propagation in the DFE, error locations were randomized with interleaving. Another error control design possibility is automatic repeat request (ARQ) to allow retransmission of frames with detected errors. Although ARQ was not implemented, a record was kept of decoding failure, described in Section 3.3.3, to assess potential benefit from an ARQ system.

4.4 Conclusion

The asymmetric communication system is represented in the SPW™ development and simulation software platform as a collection of functional operators connected in a signal-flow block diagram. Although SPW™ is a very effective platform for modelling communication systems, its library of standard functional blocks is too general to represent many of the operations required by this study. To create a system model, all but a few basic blocks were custom-coded in the C programming language. Well established techniques, such as decision feedback equalization and RLS adaptive algorithms were implemented with relative ease. Gibbard pre-coding, because of its simple transversal filter structure, was also amenable to implementation. Greater effort was required to design models where the number of design possibilities was large, as was the case for models of the channel and synchronization.

Channel models were created from a database of actual frequency domain indoor channel measurements. Data from these measurements was brought into the time domain, pre-processed and then restored to the frequency domain for computationally efficient signal filtering. Symbol synchronization was derived by searching for a timing phase that would yield the sampled channel impulse response with maximum energy. Once the timing phase was found, a component of the sampled impulse response was designated as the 'main sample' for equalization purposes. The largest component of the sampled impulse response was chosen as the main sample, unless there was an earlier component of significant energy.

When the model of the asymmetric communication system was fully complete and tested, simulations were run which allowed measurement of signal power, noise power and, using Monte Carlo analysis, estimation of the BER. Four configurations of the system were tested: one using a single channel, a second with switched antenna diversity, a third with (15,7) BCH coding and a fourth with both diversity and coding. Each of these configurations was simulated at three data rates (5, 10 and 10 Msymbol/s) and five SNR levels (15, 18, 21, 24 and 27 dB). The total number of simulation runs was 60 (4 systems x 3 data rates x 5 SNR levels) with each run taking approximately ten hours, for 600 hours or 25 days of continuous computer time. Results from these simulations are presented in the next chapter.

Chapter 5

Simulation Results

5.1 Introduction

The BER, as a function of SNR, is a common and fundamental figure of merit for a communication system, indicating the feasibility of reliable data transfer across a channel. Estimates of the BER will show whether or not Gibbard pre-coding might be an effective means of implementing a wireless LAN, and if performance can be significantly improved with switched antenna diversity and channel coding.

Unlike the transmitted waveforms in a DFE link, signals emerging from a Gibbard pre-coder are modified to compensate for channel multipath effects. In addition to the BER, transmitted power levels in the pre-coder link are important, determining if the Gibbard pre-coder is compatible with efficient and affordable transmit power amplifiers. Whether Gibbard pre-coding is an effective, and therefore *desirable*, equalization method is indicated, in part, by BER estimates. On the other hand, transmit power requirements will help determine hardware complexity, indicating if Gibbard pre-coding is *realizable*.

5.2 BER Performance

5.2.1 Performance of Basic System (Without Diversity and Coding)

Bit error rates for a simple Gibbard pre-coder, transmitting uncoded 16 QAM data without base station antenna diversity, are shown in Figure 5.1. In the legend, the pair of numbers following the data rate gives the feed-forward and feedback filter pre-coder dimensions, respectively. Performance at a 5 Msymbol/s data rate is inferior to performance at higher rates, a consequence of the narrower bandwidth of 5 Msymbol/s transmission. At narrower bandwidths, frequency selective fades tend to occupy a larger percentage of the signal bandwidth and thus annihilate proportionately more signal energy than with wider band signals, possibly causing envelope fading [Gibbard2, 286]. Greater immunity from envelope fading is balanced by more severe ISI when data rates increase from 10 to 20 Msymbol/s, shown by almost identical BER performance at these higher rates.

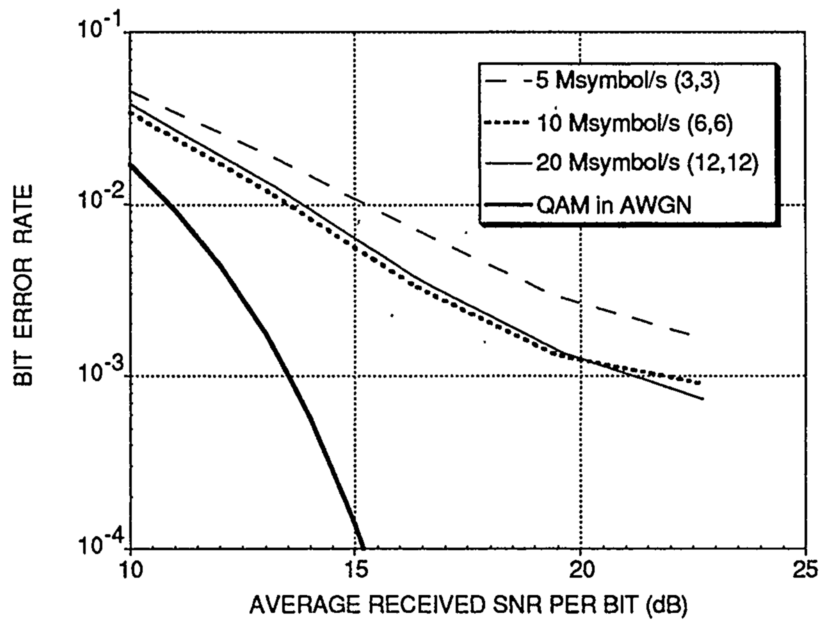

FIGURE 5.1 BER OF BASIC GIBBARD PRE-CODER

A BER of 10^{-8} has been cited as an acceptable level for a wireless LAN [Freeburg, 63][Morris, 2]. Even with a significant increase in transmit power, it seems unlikely that performance curves shown in Figure 5.1 could be extended to this level as the slope of the curves is flattening, seemingly in approach to an irreducible bit error rate. However, sluggish improvement of the BER performance curves shown in Figure 5.1 belies significant performance improvements for a large majority of channels over the range of simulated SNR levels.

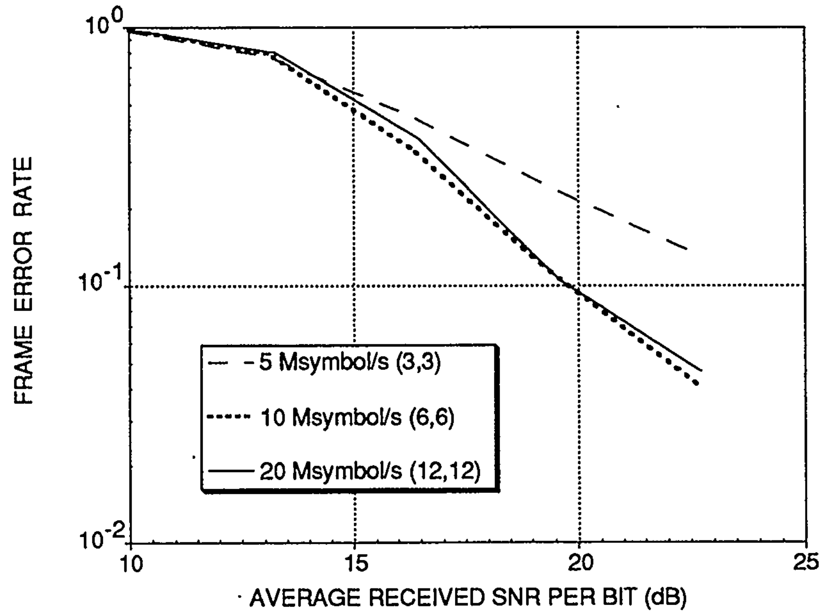

FIGURE 5.2 TRANSMITTED FRAMES CONTAINING ERRORS FOR BASIC GIBBARD PRE-CODER

For the simulations carried out in this study, a frame of 1000 random symbols, or 4000 bits, is transmitted over 600 different channel models. Figure 5.2 shows the proportion of data frames with errors to the total number of transmitted frames, indicating that, at high SNR, the pre-coder successfully removes inter-symbol interference from data transmitted over most channels. In the case of a 10 Msymbol/s data rate, almost 96 per cent of the frames are received without error. From the BER at this data rate, 9×10^{-4}, it may be shown that only 10 per cent of frames would be received without error, on average, if there were a uniform distribution of error events. These figures indicate that error events are highly concentrated in a small number of channels and suggest that satisfactory wireless LAN BER performance might be achieved with a basic Gibbard pre-coder link if the severest channels could somehow be avoided. The small number of severe channels might be avoided by notifying portable users their current location is unsatisfactory[1] or by delaying transmission until channel conditions are favourable. In either case, data transmission would proceed only if the MSE at the DFE output is below a certain threshold at the conclusion of the training sequence.

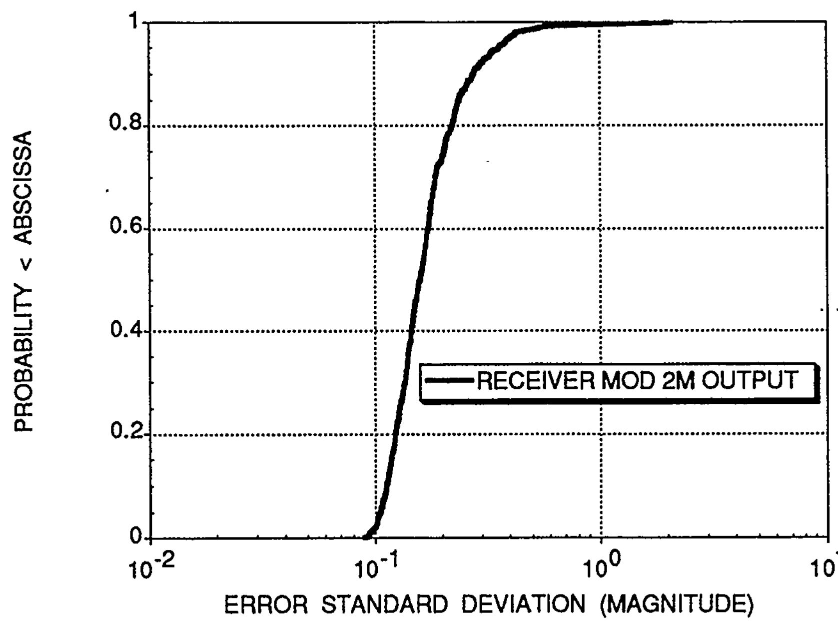

FIGURE 5.3 GIBBARD PRE-CODER LINK - MAGNITUDE OF ERROR STANDARD DEVIATION AT OUTPUT OF RECEIVER MOD 2M REDUCTION OPERATOR, 10 Msymbol/s, 22.6 dB SNR PER BIT

An illustration of the disparity in error susceptibility between channels is given in Figure 5.3. For each channel in turn, the error at the input of the receiver's decision device was calculated for all transmitted data symbols. The

---

[1] For example, NCR's *WaveLAN®* has diagnostic software for assessing the quality of a wireless link before logging onto a network [Muller, 116].

standard deviation of this error indicates the tendency of the symbols to swing about the mean error, which is almost always close to zero. A tendency towards large swings about the mean indicates that received symbols are more likely to be detected outside their Voronoi regions. Figure 5.3 gives the distribution of the error standard deviation for a 10 Msymbol/s data rate at 22.6 dB SNR per bit. At the top of the graph, the protrusion of a few channels into a domain of large standard deviation indicates the highly uneven distribution of error potential amongst the 600 channels. This protrusion is probably accentuated by a propensity towards data flipping under the worst channel conditions, a phenomenon described in Section 2.7.1. Data flipping occurs when errors in the Gibbard pre-coder link are sufficient to cause an unwanted modulo 2M reduction operation at the receiver.

5.2.2 Basic Gibbard Pre-Coding and DFE Performance Comparison

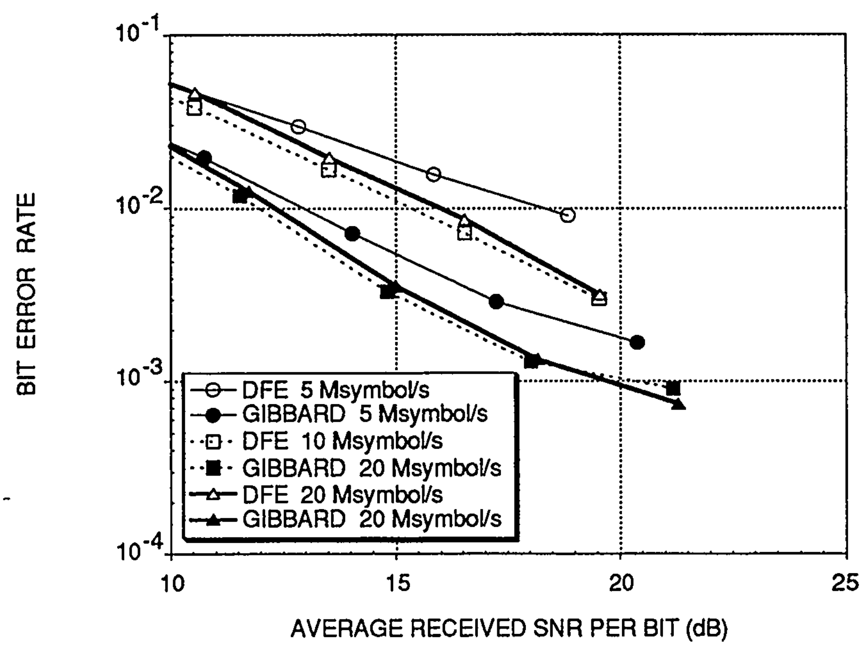

FIGURE 5.4 BER COMPARISON OF BASIC DFE AND GIBBARD PRE-CODER

Two data links are used in the asymmetric communication system, a Gibbard pre-coder link and a DFE link, an arrangement shown in Figure 4.1. A performance comparison highlights the relative advantages and disadvantages of the two equalization methods. From Figure 5.4, the DFE BER, as a function of receiver SNR, is inferior to the performance of the Gibbard pre-coder. The average maximum gap between identical DFE and pre-coder BER estimates for the same data rate is 4.7 dB SNR. Apart from this gap, the DFE and Gibbard pre-coder links behave in approximately the same manner, with poorest performance at the 5 Msymbol/s data rate and nearly identical performance at data rates of 10 and 20 Msymbol/s. For DFE and Gibbard pre-coder

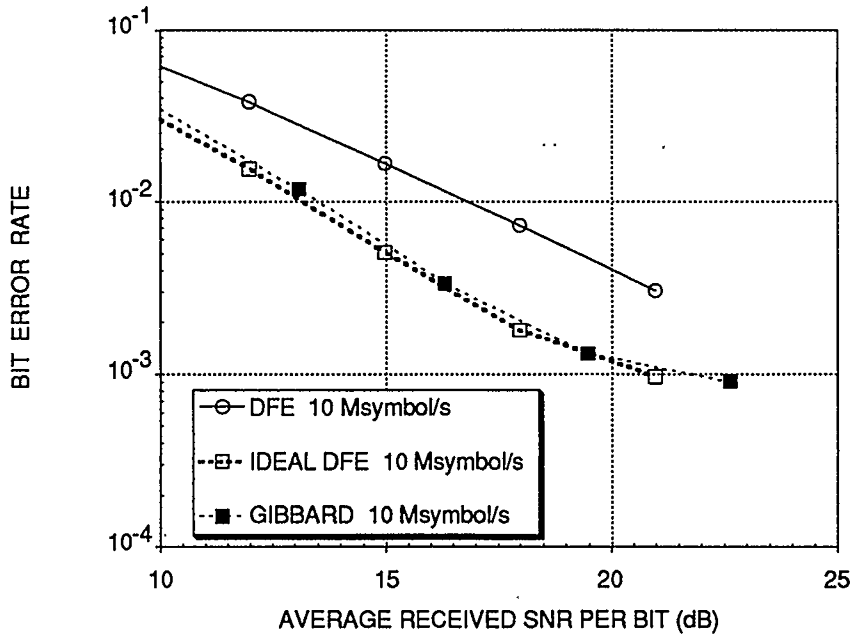

FIGURE 5.5 BER PERFORMANCE OF IDEAL DFE (NO ERROR FEEDBACK)

communication links, similarity in the relative position of BER performance curves reflects identical channel conditions encountered by the two equalization methods. Despite identical channels, a 4.7 dB performance gap between DFE and pre-coder links arises, a result of differences in transmit power and error sources for Gibbard pre-coding and decision feedback equalization.

A feature which distinguishes decision feedback equalization and Gibbard pre-coding is the possibility of error propagation. Incorrect decisions made by the DFE pass through the device's feedback filter where they may induce additional errors in subsequent decisions. The pre-coder is immune from this phenomenon because the pre-coder's feedback filter is located at the transmitter, where feedback is error-free. At simulated SNR levels, error propagation in the decision feedback equalizer is the main cause of the gap between DFE and Gibbard pre-coder BER performance, as demonstrated by Figure 5.5. For the 10 Msymbol/s data rate, Figure 5.5 gives the performance curve of an ideal DFE, which has

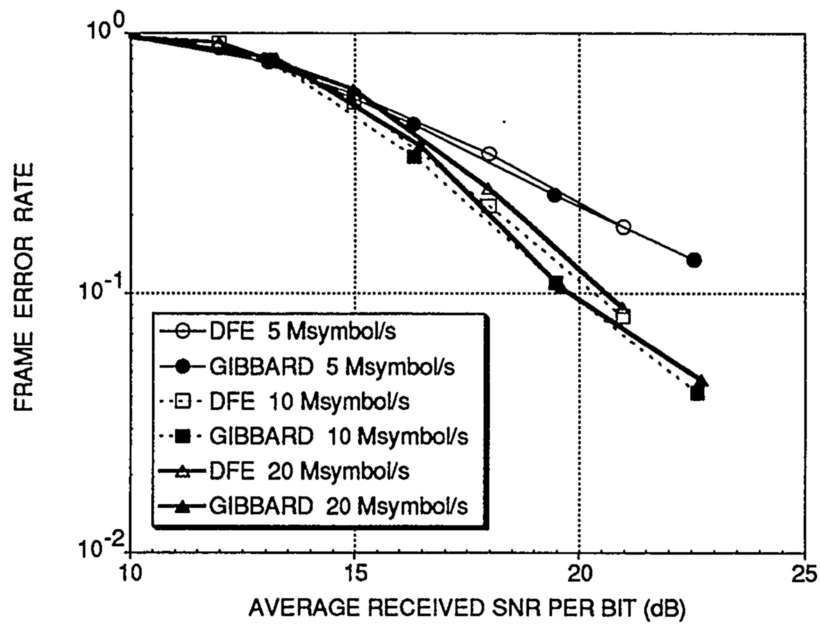

FIGURE 5.6 TRANSMITTED FRAMES CONTAINING ERRORS FOR BASIC DFE AND GIBBARD PRE-CODER

error-free decision feedback, and shows the disappearance of the BER performance gap when error propagation is eliminated. In fact, without error propagation, the DFE BER is slightly less than for Gibbard pre-coding.

Error propagation, although significant, is not the only source of performance difference between the DFE and pre-coder. In Figure 5.6, the probability of an error-bearing frame is shown. This statistic does not reflect the duration of an error burst, since a burst cannot extend across more than a single frame. Instead, the frame error probability is related to the probability of an initial error event. The results in Figure 5.6 suggest the Gibbard pre-coder link has a marginally lower probability of an initial error event.

Figure 5.5 shows Gibbard pre-coding has a slightly higher BER than an ideal DFE but Figure 5.6 indicates pre-coding has the lower frame error rate. Seemingly inconsistent, these results are explicable by two distinct phenomena, DFE noise enhancement and pre-coder data flipping. The former increases the likelihood of a DFE error-bearing frame, *broadening* DFE error events over a larger number of frames. The latter increases the likelihood of a pre-coder error event when a severe multipath channel is encountered, *deepening* the density of these events during error-bearing frames.

Convolution of incoming signals with DFE feed-forward filter coefficients amplifies noise present at the receiver input and increases the probability of errors by the decision device. In the pre-coder link, this problem is avoided because transversal filters are located at the transmitter where a lack of noise eliminates the possibility of enhancement. Figure 5.7 shows a narrowing of the gap between DFE and Gibbard pre-coder frame error rates with increasing SNR.

This narrowing indicates the declining impact of noise enhancement on DFE performance as SNR levels increase.

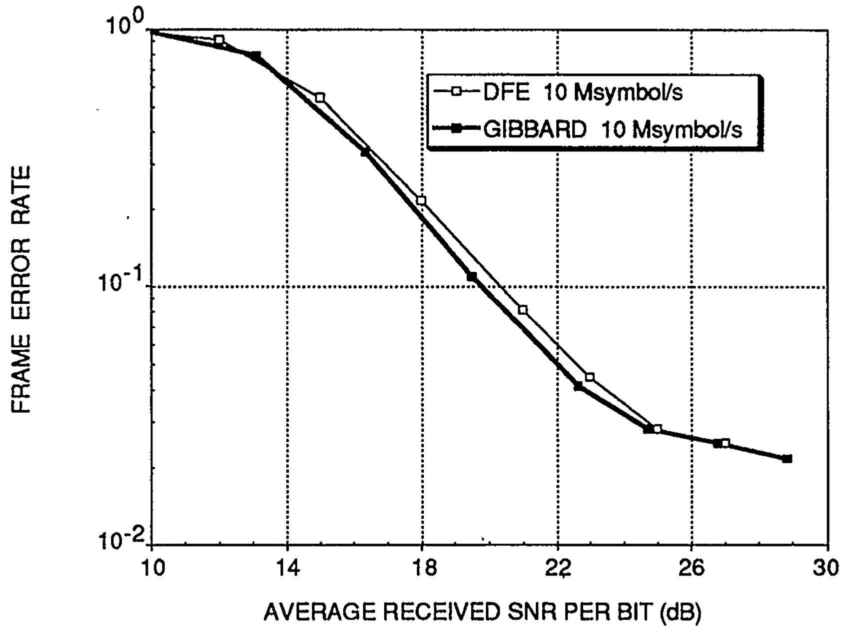

FIGURE 5.7 TRANSMITTED FRAMES CONTAINING ERRORS FOR BASIC DFE AND GIBBARD PRE-CODER, 10 Msymbol/s DATA RATE

The data-flipping phenomenon occurs when noise and ISI induce an unwanted modulo 2M reduction operation in the receiver of the Gibbard pre-coder link, an operation which translates a received symbol to the opposite side of the $(-M,M]^2$ region, causing a bit error. Without a modulo reduction operator of its own, the DFE is immune from the data flipping phenomenon. At low SNR, the effect of data flipping is manifested in the error magnitude probability distribution.

Error magnitude is defined as the Euclidean distance between a received symbol at the input to the receiver's decision device and the symbol's ideal value. A comparison of error magnitude probability distribution for the pre-coder and DFE is shown in Figure 5.8, with error measurements taken for every transmitted data symbol transmitted across 600 channels. Gibbard pre-coder and DFE measurements were taken from the same simulations using the same equalizer coefficients and average noise power. The SNR levels differ because, in modifying the transmit signal waveform, the Gibbard pre-coder also changes the pre-coder link's average received signal power.

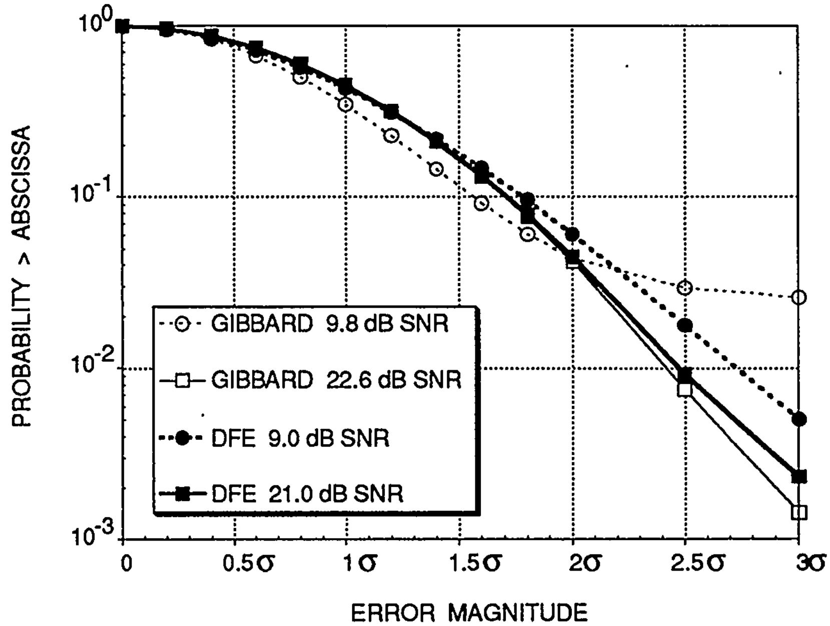

FIGURE 5.8 GIBBARD PRE-CODER AND DFE ERROR MAGNITUDE PROBABILITY DISTRIBUTION, 10 Msymbol/s DATA RATE

In Figure 5.8, the extended tail of the pre-coder's error probability distribution at 9.8 dB SNR is the result of data flipping. Because the Euclidean error needed to *trigger* an unwanted modulo 2M reduction operation is generally smaller than the error *resulting* from the reduction operation, errors are magnified by data flipping, increasing the proportion of errors with large Euclidean magnitude. A dip in the low SNR Gibbard pre-coder probability distribution between 0.5σ and 2.2σ is the result of errors in this range being magnified by data flipping into the range of this probability distribution's extended tail. At higher SNR levels, the BER declines, data flipping becomes less likely, and the error magnitude probability distribution for the pre-coder and DFE links more closely resemble each other. Data flipping occurs less frequently at high SNR levels but continues to degrade pre-coder BER performance relative to the DFE. A theoretical calculation in Section 2.7.1 shows a 4/3 increase in TH error probability from data flipping compared to DFE performance, although this effect will not be evident until the BER falls below the levels estimated in this study.

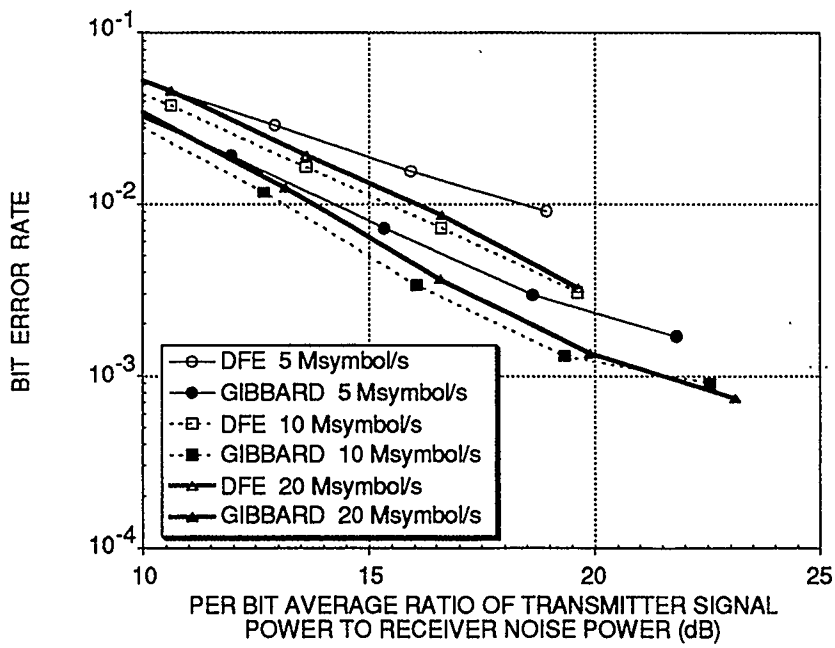

FIGURE 5.9 BER VERSUS TRANSMIT POWER - COMPARISON OF BASIC DFE AND GIBBARD PRE-CODER LINK

In addition to data flipping, a drawback of the Gibbard pre-coder is the sometimes significant transmit power expended to overcome spectral nulls. This problem is avoided by the DFE, which performs signal processing at the receiver, leaving average transmit power constant from channel to channel. Pre-coder transmit power characteristics are examined in Section 5.6, but BER performance is shown here, as a function of transmit power, to illustrate the differences in DFE and pre-coder transmit signal amplification. Figure 5.9 shows BER performance curves versus the ratio of *transmitter* signal power to *receiver* noise power. When viewed in this fashion, the comparative advantages of Gibbard pre-coding over decision feedback equalization are diminished. At identical data rates, the average maximum gap between non-ideal DFE and pre-coder BER curves narrows from 4.7 dB SNR, as in Figure 5.4, to 3.5 dB when differences in transmit power are accounted for.

5.3 Switched Antenna Diversity Performance

Base station switched dual antenna diversity was implemented, allowing selection of the channel producing the smallest MSE, as measured at a DFE output. Pre-coder transmission and DFE reception occur through the antenna representing the better of two channels so odious channels may potentially be avoided. Figure 5.10 illustrates the BER reduction which is achieved through switched antenna diversity. At receiver per bit SNR levels of 23 dB, the BER performance improvement from antenna diversity is at least a single order of magnitude. For the 10 Msymbol/s data rate, performance improvement is more significant, exceeding two orders of magnitude. A disproportionate number of severe fading channels at the 20 Msymbol/s data rate has accentuated the gap between performance at 10 Msymbol/s and 20 Msymbol/s in favour of the former, although diversity still brings an order of magnitude improvement for the 20 Msymbol/s case. This performance gap underscores the fickleness of the indoor radio channel and the difficulty in guaranteeing reliable wireless communication, even with antenna diversity. Despite this gap, BER curves from Figure 5.10 suggest that antenna diversity is a more effective means of lowering the BER than blasting additional signal power through the channel. However, diversity, as implemented for this study, requires the training of an additional DFE for the second channel and therefore involves a substantial increase in the complexity of signal processing hardware. In addition, the continued presence of error-inducing, severe ISI channels indicates that BER performance improvement is possible with diversity but the method is no panacea for the *Sturm und Drang* of the indoor radio channel.

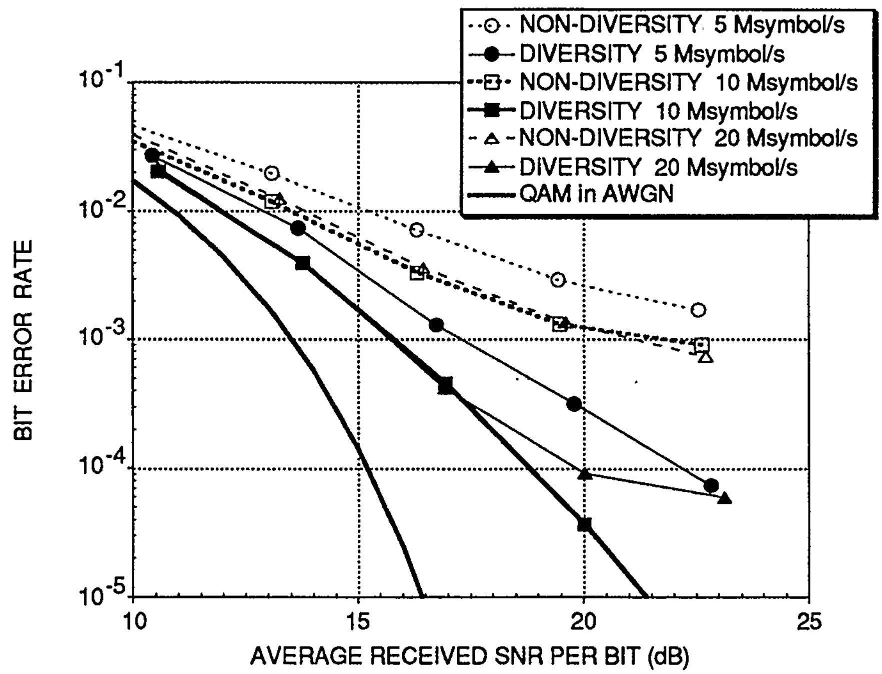

FIGURE 5.10 BER OF GIBBARD PRE-CODER WITH SWITCHED DUAL ANTENNA DIVERSITY

Corresponding to the BER reduction achieved through antenna diversity, the frame error rate has also declined. Figure 5.11 shows a reduction in the proportion of frames containing errors, for identical data rates, of approximately one order of magnitude at high SNR. With diversity, error events are further concentrated in a small number of frames transmitted over severe channels. Interestingly, the flattening of the 20 Msymbol/s diversity BER performance curve at high SNR, so evident in Figure 5.10, is absent from the frame error rate performance curves of Figure 5.11. The opening of a BER performance gap at high SNR favouring diversity transmission at 10 Msymbol/s over 20 Msymbol/s is not the result of a greater number of error-bearing frames at the higher data rate. Instead, there are proportionately more errors within a smaller number of error-bearing frames at 20 Msymbol/s.

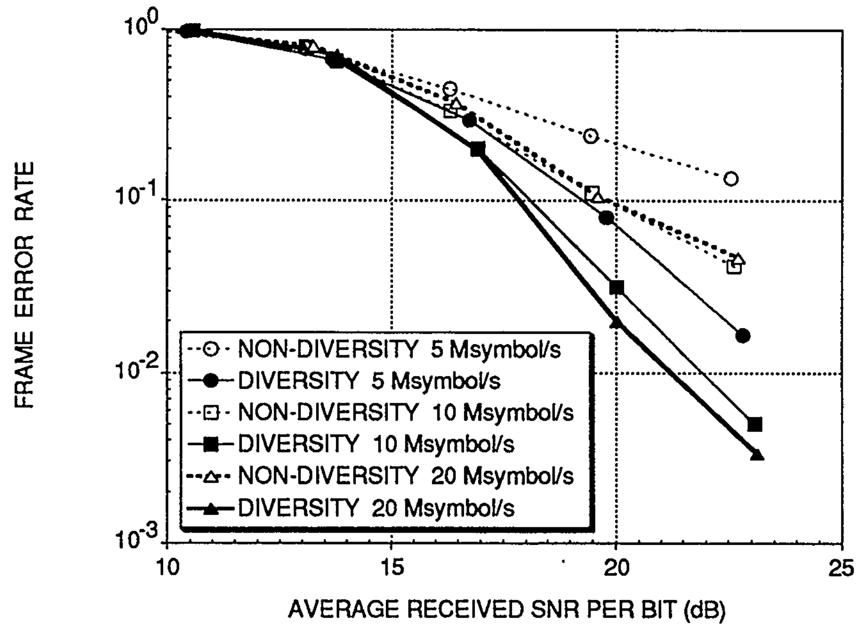

FIGURE 5.11 TRANSMITTED FRAMES CONTAINING ERRORS FOR GIBBARD PRE-CODING WITH SWITCHED DUAL ANTENNA DIVERSITY

Diversity's effect is evident in the error standard deviation at the output of the receiver's mod 2M reduction operator, an indicator of error susceptibility. For each channel, Figure 5.12 gives the error standard deviation for 10 Msymbol/s data transmission at a received SNR level of 22.6 dB, showing that error susceptibility is reduced by switched dual antenna diversity. Significantly, the shape of the standard deviation distribution is largely unaffected by diversity, meaning that errors continue to be caused by a small number of channels at high SNR. Although diversity may allow bypassing of severe multipath channels through an alternative channel, there is a possibility that the alternative channel may itself have sufficient ISI to cause errors. In this sense, diversity mitigates but does not completely surmount the problem of channel multipath effects.

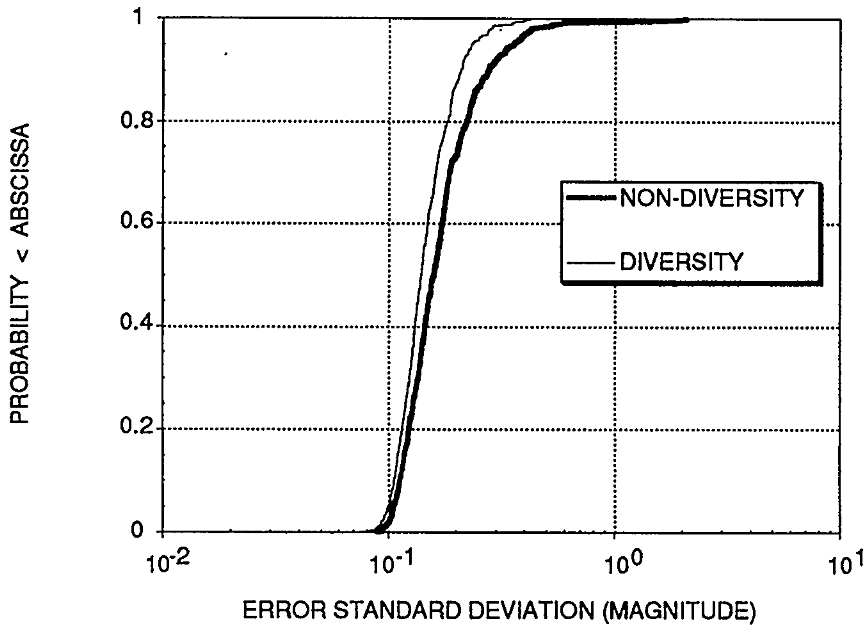

FIGURE 5.12 GIBBARD PRE-CODER LINK - ERROR STANDARD DEVIATION AT 10 Msymbol/s, 22.6 dB SNR PER BIT FOR SWITCHED DUAL ANTENNA DIVERSITY

5.4 Channel Coding

5.4.1 Error Correction

A (15,7) BCH code was used to estimate the effect of channel coding on Gibbard pre-coding's BER performance. Contents of the 4 Kbit data frames used in this study were interleaved to randomize error locations within a single frame. For pre-coding, intra-frame interleaving is largely ineffectual because the pre-coder is immune from error propagation, unlike the DFE, and stationary channel models are used for a frame's full duration. As a result of stationarity, momentary degradation of a channel, resulting in a short burst of symbol errors across a fraction of a frame, cannot occur. Instead, severe channel conditions will cause symbol errors throughout the frame and an attempt to randomize these error locations through interleaving is essentially futile. Nonetheless, interleaving was implemented because each symbol represents four bits in 16 QAM and a single symbol error may cause a bit error burst of maximum length four. Interleaving can spread such a burst across multiple codewords, although a bit error burst from a single symbol error is unlikely with Gray coding, mild noise and small residual ISI.

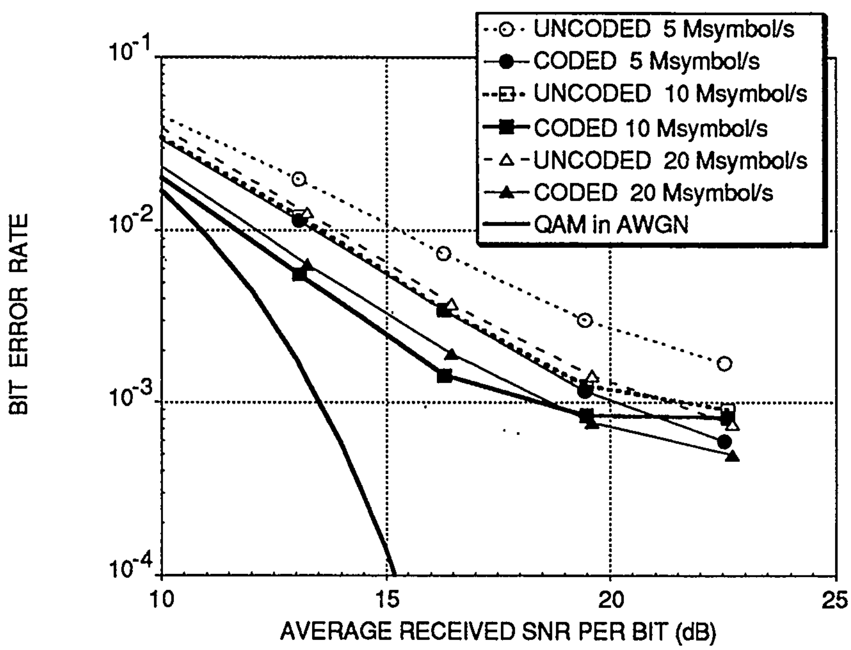

FIGURE 5.13 BER OF GIBBARD PRE-CODER WITH (15,7) BCH CHANNEL CODE

The effect of the (15,7) BCH code on the Gibbard pre-coder's BER performance is shown in Figure 5.13. Coding lowers the BER by approximately one-half at moderate SNR levels. At a 5 Msymbol/s data rate, this gap widens with a higher SNR. For 10 and 20 Msymbol/s, the advantage of coding is diminished when SNR increases. These performance trends are the consequence of error concentration within a few frames. As explained in Sections 3.3.1 and 3.3.2, a general code more easily corrects small numbers of isolated errors. Figure 5.14 shows that a small percentage of frames are rife with errors, thus defying the code's correction capability, while the remainder are error-free, especially at 10 and 20 Msymbol/s data rates. For the indoor wireless channel, the considerable overhead of coding seems unjustified by BER performance unless error events can be deconcentrated, either through a lower initial BER or *inter*-frame interleaving rather than the *intra*-frame method used in this study to more effectively randomize error locations.

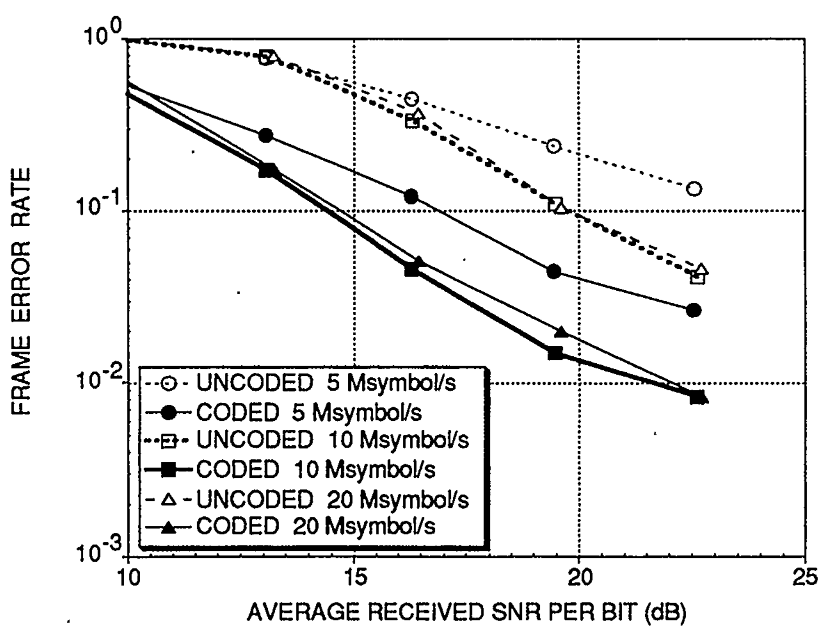

FIGURE 5.14 TRANSMITTED FRAMES CONTAINING ERRORS FOR GIBBARD PRE-CODING WITH (15,7) BCH CHANNEL CODE

When the frame error rates in Figure 5.14 are considered, an advantage of coding becomes apparent. Coding is able to eliminate errors in most data frames that contain a relatively low error concentration, increasing the proportion of error-free frames. For a data rate of 5 Msymbol/s, the number of error-free frames climbs to over 97% of the frame total, while the number exceeds 99% for 10 and 20 Msymbol/s. Once again, the indoor radio channel is found to be an acceptable medium for high-speed data communication with the vast majority of channels.

5.4.2 Error Detection and Ideal ARQ

Automatic repeat request (ARQ) systems are described in Section 3.3.2. Their essential feature is re-transmission of data that cannot be corrected at the receiver. The quasi-static approach used for channel modelling, described in Section 4.3.5, is not suited to accurate assessment of a real ARQ system, due to abrupt changes in channel conditions between data frames rather than small variations likely to be encountered by a re-transmitted data signal. However, the performance of *ideal* ARQ can be estimated, indicating the performance potential of a *real* ARQ system. In the idealized ARQ used in this study, all detected errors are assumed to be corrected accurately. By simply discarding the entire frame in which uncorrectable errors are detected, an ideal Type I ARQ system is modelled. Discarding only codewords in which uncorrectable errors are detected models an ideal Type II ARQ system. For a 10 Msymbol/s data rate, Figure 5.15 shows ideal ARQ performance.

As discussed in Section 3.3.1, only a fraction of all uncorrectable error patterns can be detected by the (15,7) BCH code and performance improvements from discarding faulty *codewords* (Type II) are limited. When the entire *frame* containing a detected but uncorrectable error is retransmitted (Type I), BER improvements are more dramatic. This study has shown that error events are concentrated in a small number of frames, so a decoding failure with one codeword likely indicates the presence of additional, possibly catastrophic, errors elsewhere in the same frame[1]. By rejecting the entire frame, catastrophic errors as well as decoding failures are eliminated and BER improvement is greater than from rejecting only codewords containing detected errors. For a system which retransmits an entire frame containing detected but uncorrectable errors, the concentration of errors in a few frames, which could normally swamp a code's error control capability, is turned into an advantage for error rate reduction. Due to the low initial frame error rate at high SNR, the overhead imposed by retransmitting an entire frame is small. Requests for retransmission reach a minimum value when SNR is high, occurring for less than 1% of frames at the 10 Msymbol/s data rate.

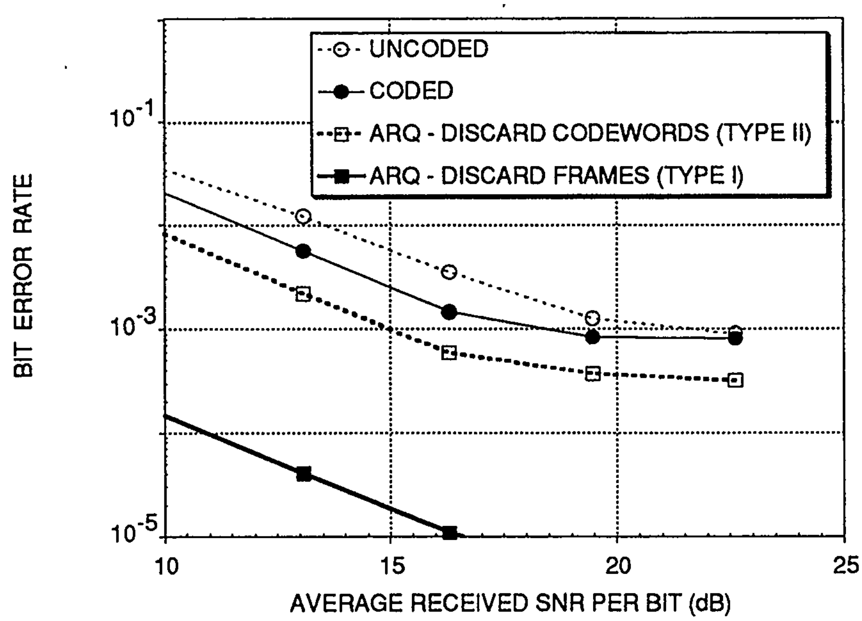

FIGURE 5.15 IDEAL AUTOMATIC REPEAT REQUEST (ARQ) BIT ERROR RATE AT 10 Msymbol/s

[1] The distinction between decoding failure and catastrophic error is described in Section 3.3.3.

5.5 Combined Diversity and Coding

The last investigated system unites dual antenna diversity with the (15,7) BCH code to determine their synergism. As shown in Figure 5.16, diversity and coding together succeed in bringing the BER to the lowest levels yet encountered in this study. At a pre-bit receiver SNR of 20 dB, the BER falls below the estimation capability of the simulation system at 10 and 20 Msymbol/s data rates while the lower 5 Msymbol/s data rate has errors in 0.5% of transmitted data frames. By 23 dB SNR, the BER at the lowest data rate also falls below the estimation capability of the simulation system. The prolonged existence of errors at the 5 Msymbol/s data rate is consistent with the greater vulnerability of narrower-band signals to frequency selective fades. The ability of a combined

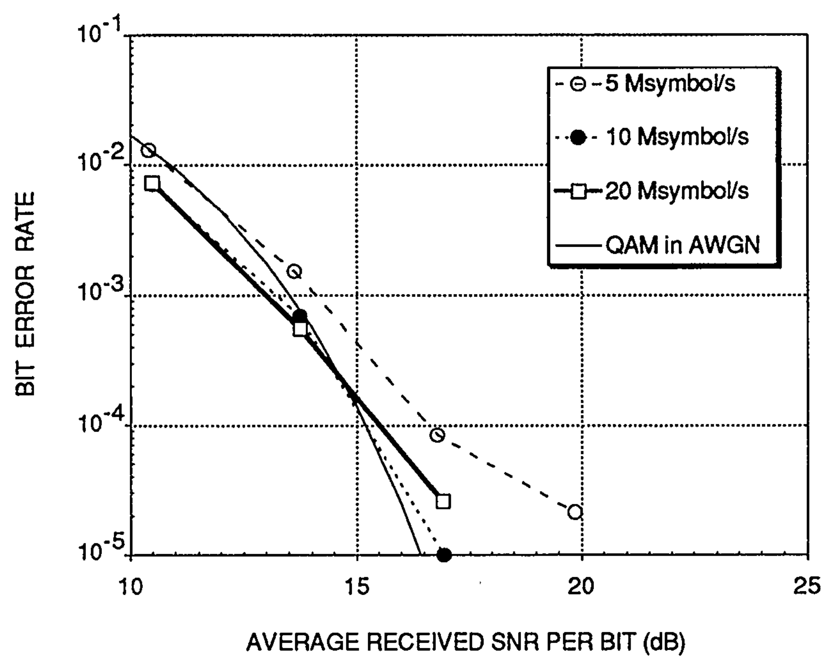

FIGURE 5.16 BER OF GIBBARD PRE-CODER WITH SWITCHED DUAL ANTENNA DIVERSITY AND (15,7) BCH CHANNEL CODE

antenna diversity and coding system to achieve the target BER for wireless LAN applications (10^{-8}) is indicated by the simulated results falling below the smallest detectable BER (4.17×10^{-7}) at all data rates.

A BER comparison of the different error rate reduction techniques used in this study is made in Figure 5.17 for a 10 Msymbol/s data rate. Antenna diversity, in effect, eliminates the severest ISI channels, unleashing the full error correcting capability of the BCH code. A Gibbard pre-coded communication system combining both diversity and coding may achieve a very low error rate, even under worst case conditions encountered in this study. This result strongly supports the case for implementing a wireless LAN with Gibbard pre-coding, if diversity and coding techniques are employed.

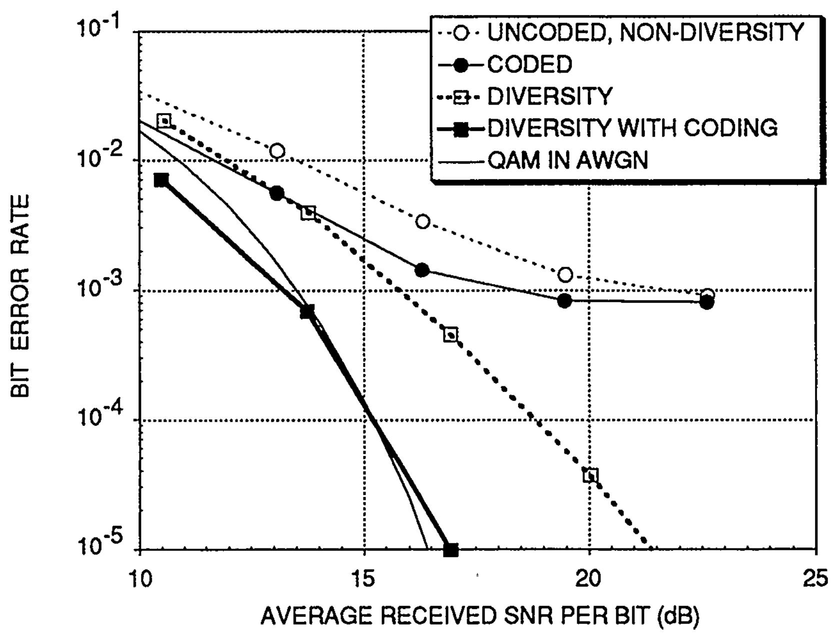

FIGURE 5.17 COMBINED PERFORMANCE OF DUAL SWITCHED ANTENNA DIVERSITY AND (15,7) BCH CHANNEL CODE AT 10 Msymbol/s

5.6 Transmit Power

An assessment of Gibbard pre-coding based on BER performance, a statistic from the receiver, is incomplete unless transmitter behaviour is also considered. Gibbard pre-coding alters the transmit signal in response to the shape of the channel impulse response spectrum. Average transmit power is variable, a function of the pre-coder coefficients derived from the channel impulse response. A key issue for the transmitter is whether the output signal's dynamic range is compatible with efficient power amplifiers.

5.6.1 Effect of TH Pre-Coder Stage

Functionally, the Gibbard pre-coder is divided into two stages, a conventional TH pre-coder which removes postcursive ISI and a feed-forward filter which removes ISI precursors, as represented in Figures 2.9 and 4.2. Mazo

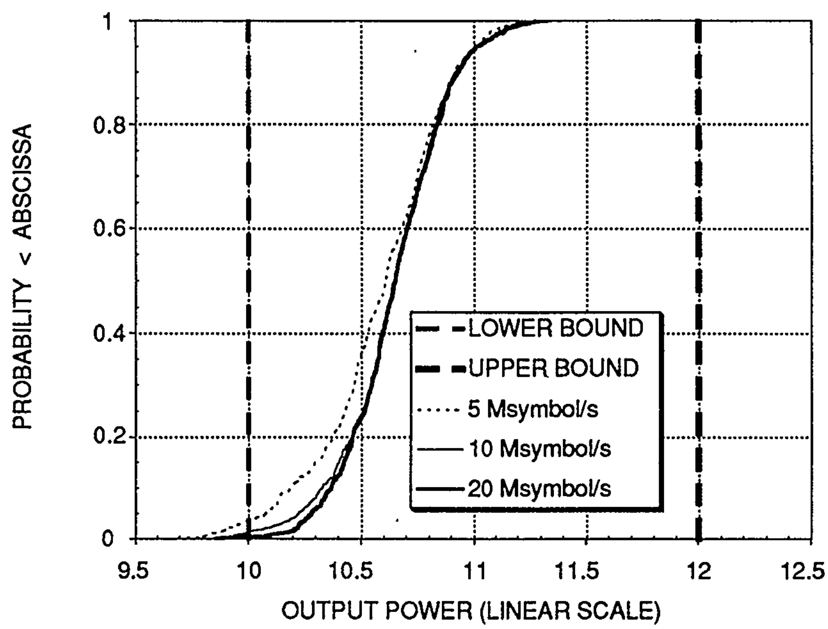

FIGURE 5.18 AVERAGE OUTPUT POWER OF TH PRE-CODER STAGE

and Salz have derived bounds on the TH pre-coder's average output power for random input data, described in Section 2.7.2 [Mazo]. For the 16 QAM constellation used in this study, these bounds are $10 \leq P \leq 12$ on a linear scale, calculated with equation 2.16. Figure 5.18 compares these bounds to the range of average power measurements taken during simulations at the TH pre-coder output.

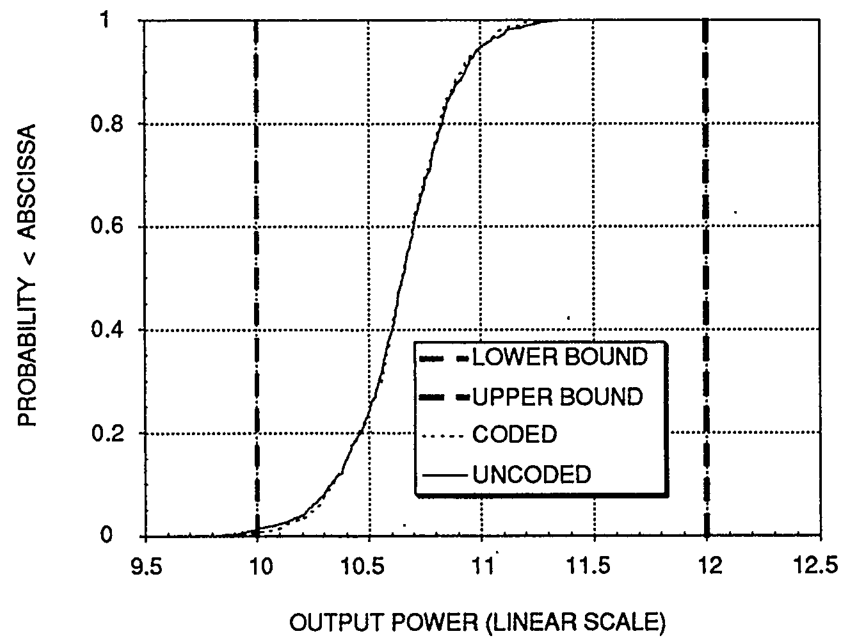

FIGURE 5.19 AVERAGE OUTPUT POWER OF TH PRE-CODER STAGE FOR (15,7) BCH CODED INPUT DATA, 10 Msymbol/s DATA RATE

Data for Figure 5.18 comes from a TH pre-coder using DFE feedback filter coefficients trained at an average received SNR of 21.0 dB per bit. Because the inputs to the DFE feedback filter are noise-free decisions, filter coefficients are largely unaffected by the SNR and the distribution shown in Figure 5.18 is essentially identical to the distribution at other SNR levels. The Mazo-Salz bounds are immutable; uncertainty in the average power estimate causes dips below the theoretical minimum in Figure 5.18. The per channel power estimates are each based on data frames of 1000 symbols. Confidence limits which result from this short frame duration are sufficiently loose to account for estimates below the lower bound. Despite uncertainty, the power estimates do not approach the upper bound. This result is not unexpected as the upper bound is looser than the lower, being derived from an analytically tractable but highly improbable condition. For the upper bound to be reached, the pre-coder feedback filter must provide a constant output, shifting the 16 QAM constellation to the maximum energy constellation of Figure 2.13(B), an unlikely outcome when pre-coder input data is random.

The results in Figure 5.18 show the TH pre-coder causes an average 0.26 dB signal power increase for all data rates and channels. A slightly below average increase for the 5 Msymbol/s data is the result of less severe ISI at this transmission rate. When ISI is milder, the 16 QAM input signal constellation is less affected by TH pre-coding and average power estimates stay closer to the minimum theoretical bound.

The work of Mazo and Salz and the work of Pitstick leaves unresolved the issue of average transmit power when pre-coder input data is non-random [Mazo][Pitstick]. Coding introduces statistical dependence between transmitted symbols and the Mazo-Salz bound, derived on the assumption of random data, may no longer apply. Average TH pre-coder output power for coded data is given in Figure 5.19. For these results the (15,7) BCH code described in Section 3.3.7 is used without interleaving, to preserve the correlation between transmitted symbols. Because the impact of coding on the average power distribution is negligible, even without interleaving, the (15,7) BCH code may be used without concern about its effect on transmit power. Although this analysis is too specific to yield a widely applicable result, it supports one of two possible conclusions. The first possibility is that TH pre-coding sufficiently randomizes transmit data to neutralize the correlation created by channel coding generally. In the alternative, the correlation introduced by the particular (15,7) BCH code is simply too small to affect transmit power.

5.6.2 Effect of Feed-Forward Filter Stage

Following the TH pre-coder, data is convolved with the coefficients of a transmitter feed-forward filter to yield the output of the Gibbard pre-coder. This operation further amplifies the transmit signal, causing a power increase. Average power at the output of the feed-forward filter is shown in Figure 5.20, which reveals very large potential power gain. In comparison to the feed-forward power gain, the gain of the previous TH pre-coding stage is negligible. For coefficients from a DFE trained at 21.0 dB SNR, the feed-forward filter produces

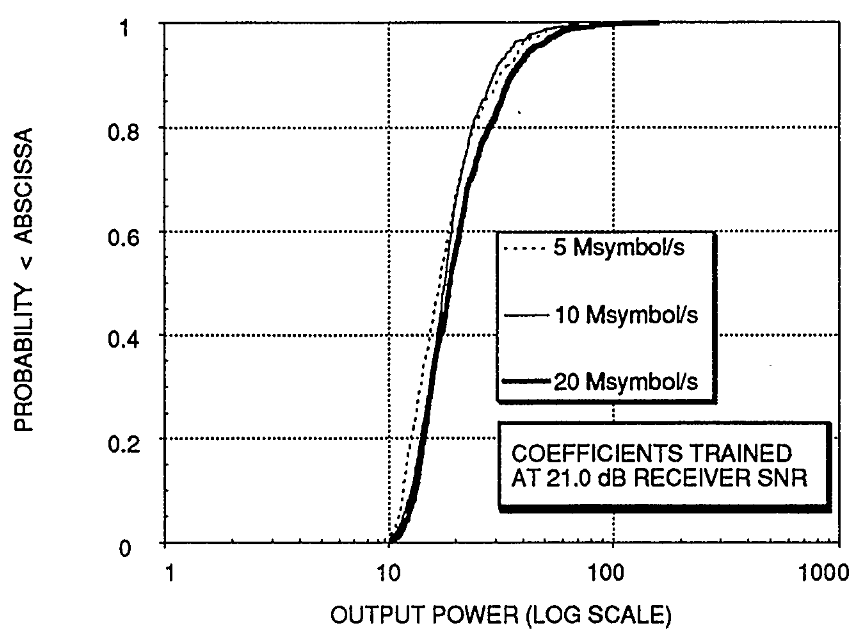

FIGURE 5.20 AVERAGE OUTPUT POWER OF GIBBARD PRE-CODER FEED-FORWARD FILTER

an *average* increase in average power of 2.3 dB, although the *maximum* increase in average power is at a much higher level of 11.7 dB. This range is significant when compared to average transmit power without pre-coding, a constant value regardless of channel conditions.

As with output of the TH pre-coder stage, the feed-forward filter's output power exhibits the effects of ISI. Power gain is greatest for transmission at 20 Msymbol/s, the data rate with the worst multipath effects. At this rate, larger magnitude feed-forward filter coefficients are required to cancel relatively significant precursor ISI, causing greater signal amplification. The difference between 10 and 5 Msymbol/s data rates is not so conclusive, although the gain at 10 Msymbol/s exceeds the 5 Msymbol/s gain throughout most of the transmit power distribution. Greater severity of ISI at the 10 Msymbol/s data rate suggests that power gain should be higher at this data rate.

In Section 2.6, a conjecture was made about the relative advantages of ZF and MMSE feed-forward filter performance criteria. At low SNR levels, the inferiority of the ZF criterion for Gibbard pre-coding was suggested. The criterion would direct transmit signal power to spectral nulls, causing a greater transmit power increase than the MMSE criterion. Because of the duality of noise minimization by a receiver DFE and transmitter signal power minimization by the Gibbard pre-coder, the MMSE criterion was predicted to result in less power amplification by the pre-coder's feed-forward filter, especially at low SNR. This conclusion is supported by results from computer simulations.

In Figure 5.21, the distribution of transmit power is shown at the 10 Msymbol/s data rate, using feed-forward coefficients adaptively derived at five SNR levels. For visual clarity, only the highest probability power levels are shown for each SNR, but the relative power differences are preserved over the entire probability range. Feed-forward filter coefficients derived using the MMSE criterion result in greater signal power amplification when the DFE, the source of the coefficients, is trained at high SNR levels. Coefficients based on the ZF criterion are not derived in this study but their behaviour can be deduced from MMSE coefficients at high SNR. Using the ZF performance criteria, equalizer coefficients would be obtained without reference to noise power and are approached by MMSE coefficients at low noise levels. A comparison of the highest SNR power distribution in Figure 5.21 with lower SNR curves implies that pre-coder transmit power will be less if a MMSE criterion is used instead of a ZF criterion. Although this result is theoretically interesting and may have some significance for more error-tolerant asymmetric communication systems, the power savings obtained with a MMSE criterion may be negligible at higher SNR levels, such as those needed by a wireless LAN to achieve low bit error rates.

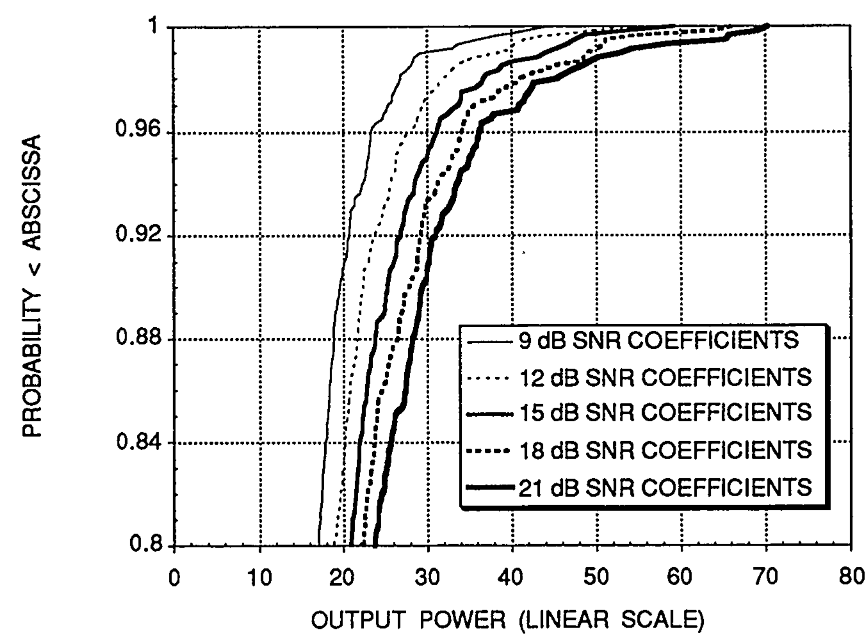

FIGURE 5.21 GIBBARD PRE-CODER FEED-FORWARD FILTER OUTPUT POWER, 10 Msymbol/s

To limit the spread in average Gibbard pre-coder output power levels to a range which can be more efficiently amplified, the output of the Gibbard pre-coder may be scaled down when its average power is excessive. An increased AGC amplification factor would be required at the receiver to restore the signal to levels appropriate for subsequent operations, such as A/D conversion. This scaling feature was not included in this study, but its qualitative effect is not difficult to foresee. By scaling down the transmit signal to accommodate the power amplifier, receiver SNR levels would be reduced and BER performance would suffer.

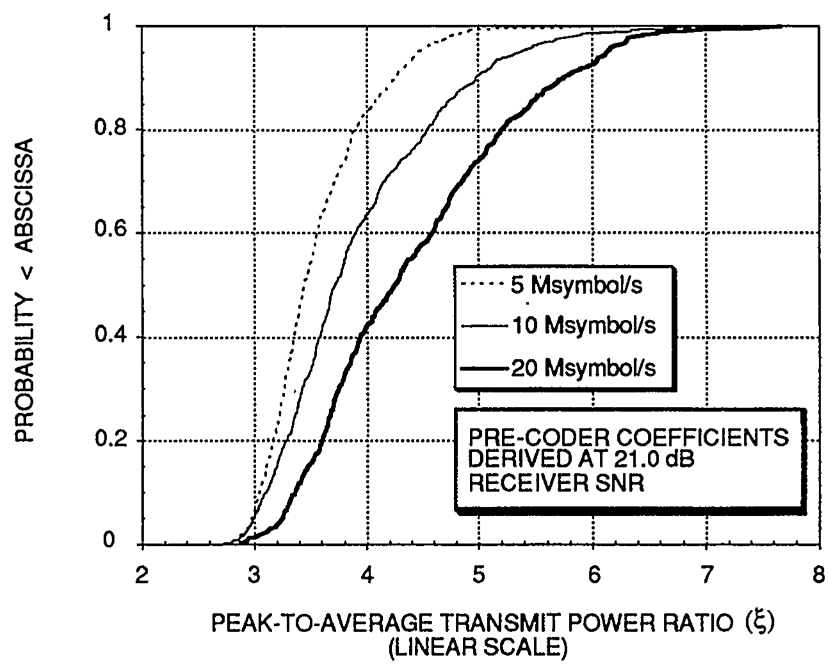

FIGURE 5.22 GIBBARD PRE-CODER PEAK-TO-AVERAGE TRANSMIT POWER RATIO

Although scaling may contain the spread of the Gibbard pre-coder's average transmit power, signal variance about the average may still reduce a power amplifier's efficiency. The dynamic range requirements of Gibbard pre-coding may be assessed with the peak-to-average power ratio. Distribution of this statistic, given in Figure 5.22, reveals a maximum peak-to-average ratio of 8.9 dB. The following expression can be shown to give the peak-to-average ratio for regular QAM without Gibbard pre-coding:

$$\xi = \frac{P_{PEAK}}{P_{AVERAGE}} = \frac{2(M-1)^2}{2(M^2-1)/3} \tag{5.1}$$

Equation 5.1 gives a ratio of 2.6 dB for non pre-coded 16 QAM. When compared to the pre-coder's maximum 8.9 dB peak-to-average ratio, a significant demand imposed on the dynamic range of the transmit amplifier by Gibbard pre-coding is revealed.

5.7 Hardware Requirements

Hardware requirements for pre-coding are discussed generally in Section 2.7.5. Using the approach of Gibbard, a more specific estimate of hardware requirements may be obtained [Gibbard1, 100-101].

The most demanding pre-coder operation during data transmission is the calculation of feed-forward and feedback filter outputs. For each symbol cycle, complex arithmetic imposes a requirement of four multiply and accumulate calculations (MACs) per filter tap. To estimate hardware complexity, the GEC Plessey Semiconductor PDSP16256/A programmable FIR filter may be used as a benchmark. This device can execute 4×10^8 MAC/s with 12 bit filter coefficients and 16 bit data, consuming 3 watts of power [GEC, 57]. Complexity estimates are given in Table 5.1.

TABLE 5.1 ESTIMATED HARDWARE COMPLEXITY FOR GIBBARD PRE-CODING

SYMBOL RATE (Msymbol/s)	FILTER DIMENSION (FF,FB)	REQUIRED CALCULATIONS (MAC/s)	REQUIRED ICs	POWER DISSIPATION (W)
5	(3,3)	1.2×10^8	0.3	0.9
10	(6,6)	4.8×10^8	1.2	3.6
20	(12,12)	19.2×10^8	4.8	14.4

In addition to a Gibbard pre-coder, the base station also requires a DFE to process received signals. The complexity requirements will be slightly less for a DFE than a pre-coder. This difference is a result of discrete QAM symbol decisions which are the input to the DFE feedback filter and may be represented by fewer bits than the continuous values which enter the pre-coder feedback filter. Together, the complexity of a Gibbard pre-coder and DFE may be prohibitive at 20 Msymbol/s, although a DSP implementation at a 10 or 5 Msymbol/s data rate may be viable.

Adaptive training of the DFE to produce DFE and pre-coder filter coefficients imposes an even heavier computational burden. The number of complex multiplication operations for each RLS iteration is approximately 2N(N+1), where N is the total equalizer length [Haykin, 485]. Table 5.2 gives the number of calculations required for DFE RLS training. This very significant computational burden cannot be borne by standard, general DSP devices. An application specific integrated circuit (ASIC) or custom IC will be necessary to execute the RLS algorithm, especially at high data rates.

TABLE 5.2 ESTIMATED HARDWARE COMPLEXITY FOR DFE COEFFICIENT ADAPTATION

SYMBOL RATE (Msymbol/s)	FILTER DIMENSION (FF,FB)	REQUIRED CALCULATIONS (MAC/s)
5	(3,3)	16.8×10^8
10	(6,6)	124.8×10^8
20	(12,12)	960.0×10^8

5.8 Conclusion

Simulation results presented in this chapter show the Gibbard pre-coder to be an effective equalization device. Used without error reduction measures, the Gibbard pre-coder BER levels are on the order of 10^{-3} at average per-bit receiver SNR levels of 23 dB. Over the entire range of receiver SNR levels used in this study, the error rate performance of the pre-coder exceeds that of conventional decision feedback equalization.

A finding, consistent throughout this study, is that a majority of channels can be successfully equalized at high SNR, while a small number of miscreant channels, generally fewer than 5%, cause all error events. In other words, a wireless LAN will *usually* have an acceptable error performance. To shrink the number of error-causing channels, switched antenna diversity may be used, which achieves an order of magnitude improvement in bit and frame error rates. Coding, by itself, proves to be less successful at eliminating errors caused by the severest ISI channels. When such channels are encountered, the number of error events swamps the correction capability of a (15,7) code, even with intra-frame interleaving. An ARQ system might overcome this problem, employing the code's unutilized error detection capability to achieve more substantial BER reductions. Another possibility is to combine diversity and coding, a move which drives the BER below 10^{-5} at SNR levels of 23 dB or less, if data rates are high. In terms of error performance, these results show that Gibbard pre-coding is a viable equalization method for the indoor radio channel.

When hardware requirements are considered, Gibbard pre-coding loses some of its appeal. In part, this is due to the large number of high-speed computations needed for equalization, a computational burden which also applies to conventional DFEs. Significant dynamic range requirements are also imposed upon the transmitter amplifier by Gibbard pre-coding, exceeding those for decision feedback equalization. A larger dynamic range will reduce efficiency and increase complexity of the transmit power amplifier. Amplifier costs are probably justified by Gibbard pre-coding's error performance and suitability for an asymmetric wireless LAN.

Chapter 6

Summary

6.1 Introduction

The purpose of this study is to assess the virtues of TH pre-coding for a high-speed wireless LAN transmitting at 5, 10 and 20 Msymbol/s. At these high data rates, processing of signals transmitted over the indoor wireless channel imposes a significant computational burden, a burden which is better carried at a base station than a portable terminal. A conventional DFE can be used to remove channel-induced frequency selective spectral fades from signals *received* at the base station. To compensate for channel distortion affecting signals *transmitted* from the base station, TH pre-coding may be employed. This study uses a TH pre-coding variant, called Gibbard pre-coding, which includes a feed-forward filter at the transmitter in addition to a conventional TH pre-coder. This structure allows equalization of both pre- and post-cursor ISI at the transmitter.

High-speed data transmission across the indoor channel results in multipath effects, causing frequency selective and flat fading in received signal spectra. Equalization can compensate for frequency selective fades, but alternative techniques are required to transcend flat fading effects. With antenna diversity, flat fading channels can sometimes be bypassed. For additional error rate reductions, channel coding may be used to detect and correct bit errors. This study estimates the effectiveness of switched dual antenna diversity and a compact (15,7) BCH code at reducing the frequency of errors, to achieve wireless LAN performance in excess of that possible with Gibbard pre-coding alone.

For wireless LAN applications, many criteria are necessary to exhaustively evaluate Gibbard pre-coding, alone and in combination with antenna diversity and channel coding. This study concentrates on error performance and demands placed on the transmit amplifier. The latter is important because of significant transmit signal power variations caused by pre-coding.

6.2 Error Performance

For a per-bit received SNR of 23 dB, the BER of Gibbard pre-coding alone is nearly 10^{-3} for data rates of 5, 10 and 20 Msymbol/s. For such high signal power levels, this error rate seems unacceptable, however up to 95% of 4 Kbit data frames are received error free at this SNR. For this frame error rate, even a BER as high as 10^{-3} is acceptable for a wireless LAN if faulty frames can be identified and remedial action taken.

The frame error rate demonstrates the nature of the indoor wireless radio channel: most channels give trouble-free transmission while a few channels cause large numbers of errors. In this study, at SNR levels of 23 dB, errors were usually caused by 5% of the channels, or less with antenna diversity and channel coding.

The addition of switched antenna diversity brings the BER at 23 dB SNR below 10^{-4}. The number of error-free frames climbs to 98% for a data rate of 5 Msymbol/s and to 99.5% for 10 and 20 Msymbol/s. In this study, the implementation of switched antenna diversity requires two DFEs at the base station, one for each antenna, which is an excessive level of complexity for a real wireless LAN system. These results are, nonetheless, important, demonstrating the potential of switched antenna diversity, although a more practical antenna selection method is required.

Channel coding produces more mixed results than antenna diversity. When severe multipath channels are encountered, the number of errors swamps the correction and detection capability of the code and only limited BER reduction is possible. By combining antenna diversity with coding, the worst multipath channels are avoided and the code becomes more effective at reducing errors. At 23 dB SNR, the BER drops below 10^{-5} for all data rates when diversity and coding are both used. Frame error rates show a similar decline. Coding and diversity together achieve a 6 dB SNR gain at the same error performance levels of switched antenna diversity alone.

This study expands the signal constellation used by Gibbard from 4 to 16 QAM [Gibbard1, 59]. The error performance of 16 QAM shows this signal constellation can be successfully equalized at high data rates. With the larger constellation, each symbol represents four bits, doubling the number of bits transmitted with 4 QAM at identical symbol rates.

At the SNR levels used in this study, bit and frame error performance of Gibbard pre-coding is generally superior to that of conventional decision feedback equalization. Noise enhancement and error propagation diminishes DFE performance relative to the pre-coder. Error performance figures support the contention that Gibbard pre-coding at the transmitter is a viable alternative to receiver-based decision feedback equalization.

Bit error and frame error rates show 10 and 20 Msymbol/s data rate signals are generally more immune to spectral fading than signals at a 5 Msymbol/s data rate. This fact creates a conundrum for the designer of a wireless LAN: to take advantage of robustness to fading, high data rates are required, but these impose a prohibitive computational burden. For the system examined in this study, a 5 Msymbol/s wireless LAN may be possible with standard DSP devices while the complexity required for 10 and 20 Msymbol/s data rates is unlikely without ASIC or custom IC processors.

6.3 Transmit Power Performance

Gibbard pre-coding, in altering the transmit signal, also changes the transmit signal's power. The average transmit signal power was calculated for each channel. The maximum-to-minimum ratio of average power levels is nearly 12 dB, a spread almost entirely due to the Gibbard pre-coder's feed-forward filter. This range may be reduced by scaling down the signal at the transmitter, compensating with additional AGC amplification at the receiver. An increase in error probability may be anticipated from such a move.

Even if a constant average transmit power level can be achieved across all channels, the dynamic range of the transmitter amplifier may still be strained. Compared to a peak-to-average power ratio of 2.6 dB for the DFE, Gibbard pre-coding had a peak-to-average power ratio, depending on the channel, of maximum 9.0 dB. Ratios as large as this may significantly impair efficiency of the transmit power amplifier.

6.4 Recommendations for Future Work

A case has been made for employing a Gibbard pre-coder in the base station of a wireless LAN. This case has been bolstered by results from this study but remains unproven. A verdict depends upon the results of additional research, incorporating some of the issues raised below.

- Channel frequency. This study used channel models, taken from a database of measurements, centred at a 1100 MHz frequency. This frequency range, currently allocated to aeronautical radionavigation, is unavailable for wireless LAN usage. Spectrum in the nearby 902-928 MHz ISM band is available but this range is increasingly crowded and bandwidth is insufficient to support high data rates [Freeburg, 61]. Simulations are needed to represent the severity of multipath and shadowing at the intended operating frequency of the wireless LAN. Depending on regulatory considerations, this might be the 2.4 or 5.7 GHz ISM bands, the 5.2 GHz range intended for Europe's HIPERLAN standard or higher frequency bands, such as the 18-19 GHz range used by the *ALTAIR*™ wireless LAN [Bantz, 44][Khayata, 465].

- Amplifier non-linearities. With the large dynamic range of the Gibbard pre-coder's output power, significant non-linearities may be encountered in the response of the transmitter amplifier. Non-linear distortion should be represented to accurately estimate wireless LAN performance. If the response of the amplifier is known, the pre-coder may be used to compensate for amplifier distortion in addition to distortion from the channel.

- Antenna diversity. As implemented in this study, both of the base station's dual antennas use a DFE to determine each channel's MSE. A less complex solution, perhaps based on received signal power, might be used to eliminate one of the equalizers.

- Coding. The selected (15,7) BCH code imposes a large overhead, reducing the effective data rate by 53%. Longer codewords might be used to reduce this overhead without making the decoding operation excessively complex.

- Realistic modelling of components. Ideal components were used in this study to determine the maximum performance potential of the Gibbard pre-coder. Additional simulation is required to represent realistic synchronization, carrier demodulation and AGC operations as well as non-ideal phenomena such as quadrature imbalance.

  While realistic modelling requirements apply to the simulation of any communication system, Gibbard pre-coding, in particular, necessitates modelling of an AGC with a suitable time constant. At the AGC input, Gibbard pre-coded signals often have a standard deviation significantly in excess of the signal standard deviation in the DFE link. If gain control is continuous, large signal variation may impair AGC tracking of envelope variation caused by fading. If gain is locked for the remainder of a frame following an AGC training period, a DFE may scale a signal and correct for fine errors in AGC adjustment. This possibility is lacking for received signals that have been Gibbard pre-coded, necessitating more accurate gain control.

- ARQ simulation. Detection and retransmission of error-bearing frames is a widely used error control method and may be necessary in a LAN to ensure reliable data transmission [Spragins, 7]. Simulation of an ARQ system is inhibited by the channel models used in this study. Models are based on actual indoor measurements but do not incorporate slow variations in channel conditions. Instead, channels remain stationary during a frame, followed by an abrupt transition between frames, to a model derived from measurements taken at a different location. Although indoor channel stationarity may reasonably be assumed for a short data frame, abrupt transitions between channel models hinders accurate simulation of an ARQ system. Such a system would realistically encounter more modest changes in channel conditions when an error-bearing frame is retransmitted. A channel model incorporating slow variations should be implemented to allow accurate ARQ simulation.

6.5 Conclusion

This study has examined the suitability of Gibbard pre-coding for transmitter-based equalization of indoor wireless transmissions originating at a wireless LAN's base station. With switched antenna diversity and coding, error rates below 10^{-5} can be achieved with per-bit receiver SNR levels of 23 dB or less, depending on the data rate. This error performance is adequate to justify the use of a Gibbard pre-coder in a wireless LAN. Asymmetric communication, in which burdensome signal processing tasks are shifted from a portable to a base station, can thus be realized.

The shift of processing tasks does not come without a cost; the Gibbard pre-coder requires a transmit amplifier of higher power than a system transmitting regular 16 QAM. This amplifier must operate at low efficiency to accommodate the peak-to-average power ratio of the pre-coder output. Amplifier cost is probably justified given the error performance of Gibbard pre-coding and the portability and lower manufacturing costs of terminals in an asymmetric wireless LAN.

This is the End.

BIBLIOGRAPHY

[Acampora] Acampora, A.S. and J.H. Winters, "System Applications for Wireless Indoor Communications" in IEEE Communications Magazine, August 1987, vol. 25, no. 8, pp. 11-20.

[Adachi] Adachi, Fumiyuki and J. David Parsons, "Unified Analysis of Postdetection Diversity for Binary Digital FM Mobile Radio" in IEEE Transactions on Vehicular Technology, November 1988, vol. 37, no. 4, pp. 189-198.

[Aman] Aman, Ahmad K., Robert L. Cupo and Nikolaos A. Zervos, "Combined Trellis Coding and DFE through Tomlinson Precoding," in IEEE Journal on Selected Areas in Communications, August 1991, vol. 9, no. 6, pp. 876-883.

[Amitay] Amitay, Noach and Larry J. Greenstein, "Multipath Outage Performance of Digital Radio Receivers Using Finite-Tap Adaptive Equalizers" in IEEE Transactions on Communications, May 1984, vol. COM-32, no. 5, pp. 597-608.

[Arnold] Arnold, H.W., Donald C. Cox and R.R. Murray, "Macroscopic Diversity Performance Measured in the 800-MHz Portable Radio Communications Environment" in IEEE Transactions on Antennas and Propagation, February, 1988, vol. 36, no. 2, pp. 277-281.

[Balaban1] Balaban, Philip and Jack Salz, "Dual Diversity Combining and Equalization in Digital Cellular Mobile Radio" in IEEE Transactions on Vehicular Technology, May 1991, vol. 40, no. 2, pp. 342-354.

[Balaban2] ———— and Jack Salz, "Optimum Diversity Combining and Equalization in Digital Data Transmission with Applications to Cellular Mobile Radio--Part I: Theoretical Considerations" in IEEE Transactions on Communications, May 1992, vol. 40, no. 5, pp. 885-894.

[Balaban3] ———— and Jack Salz, "Optimum Diversity Combining and Equalization in Digital Data Transmission with Applications to Cellular Mobile Radio--Part II: Numerical Results" in IEEE Transactions on Communications, May 1992, vol. 40, no. 5, pp. 895-907.

[Bantz] Bantz, David F. and Frédéric J. Bauchot, "Wireless LAN Design Alternatives" in IEEE Network, March/April 1994, vol. 8, no. 2, pp. 43-53.

[Belfiore] Belfiore, Carlos A. and John H. Park, Jr., "Decision Feedback Equalization" in Proceedings of the IEEE, August 1979, vol. 67, no. 8, pp. 1143-1156.

[Berlekamp1] Berlekamp, Elwyn R., Algebraic Coding Theory, Toronto: McGraw Hill Book Company, 1968.

[Berlekamp2] ———— (ed.), Key Papers in the Development of Coding Theory, New York, New York, USA: IEEE Press, 1974.

[Berlekamp3] ————, "The Technology of Error-Correcting Codes" in Proceedings of the IEEE, May 1980, vol. 68, no. 5, pp. 564-593.

[Berlekamp4] ————, Robert E. Peile and Stephen P. Pope, "The Application of Error Control to Communications" in IEEE Communications Magazine, April 1987, vol. 25, no. 4, pp. 44-57.

[Berrou] Berrou, Claude, Alain Galvieux and Punya Thitimajshima, "Near Shannon Limit Error-Correcting Coding and Decoding: Turbo Codes (1)" in Proceedings, 1993 IEEE International Conference on Communications (ICC '93), Geneva, Switzerland, May 23-26, 1993, vol. 2, pp. 1064-1070.

[Bhargava] Bhargava, Vijay K., "Forward Error Correction Schemes for Digital Communications" in IEEE Communications Magazine, January 1983, vol. 21, no. 1, pp. 11-19.

[Biglieri] Biglieri, Ezio, Dariush Divsalar, Peter J. McLane and Marvin K. Simon, Introduction to Trellis-Coded Modulation with Applications, Toronto: Maxwell Macmillan Canada, Inc., 1991.

[Bingham] Bingham, John A.C., The Theory and Practice of Modem Design, Toronto: Wiley Interscience, 1988.

[Blahut] Blahut, Richard E., "Digital Signal Processing and Error-Control Codes" in in Proceedings, IEEE International Conference on Communications 1983, (ICC '83), Boston, Massachusetts, USA, June 19-22, 1983, vol. 1, pp. 299-302.

[Blais] Blais, J.A.R. and A.A. Vassiliou, Spectral Analysis of One-Dimensional Data Sequences, Report 30010, Calgary: University of Calgary, Department of Surveying Engineering, December 1987.

[Blake] Blake, Ian F. (ed.), Algebraic Coding Theory: History and Development, Stroudsburg, Pennsylvania, USA: Dowden, Hutchinson & Ross, Inc., 1973.

[Brigham] Brigham, E. Oran, The Fast Fourier Transform and Its Applications, Toronto: Prentice Hall, 1988.

[Bucholz] Bucholz, Dale, Paul Odlyzko, Mark Taylor and Richard White, "Wireless In-Building Network Architecture and Protocols" in IEEE Network Magazine, November 1991, vol. 5, no. 6, pp. 31-38.

[Calderbank] Calderbank, A.R. and J.E. Mazo, "Spectral Nulls and Coding with Large Alphabets" in IEEE Communications Magazine, December 1991, vol. 29, no. 12, pp. 58-67.

[Cartledge] Cartledge, John C., "Outage Performance of QAM Digital Radio Using Adaptive Equalization and Switched Space Diversity Reception" in IEEE Transactions on Communications, February 1987, vol. COM-35, no. 2, pp. 166-171.

[Chang] Chang, Li Fung and Justin C.-I. Chuang, "Diversity Selection Using Coding in a Portable Radio Communications Channel with Frequency-Selective Fading" in IEEE Journal on Selected Areas in Communications, January 1989, vol. 7, no. 1, pp. 89-98.

[Chen1] Chen, J. and P. Owsley, "A Burst-Error-Correcting Algorithm for Reed-Solomon Codes" in IEEE Transactions on Information. no. 6, pp. 1807-1812.

[Chen2] Chen, Kwang-Cheng, "Medium Access Control of Wireless LANs for Mobile Computing" in IEEE Network, September/October 1994, vol. 8, no. 5, pp. 50-63.

[Chien1] Chien, R.T., "Cyclic Decoding Procedures for Bose-Chaudhuri-Hocquenghem Codes" in IEEE Transactions on Information Theory, October 1964, vol. IT-10, pp. 357-363; reprinted in Key Papers in the Development of Coding Theory, Elwyn R. Berlekamp (ed.), New York, New York, USA: IEEE Press, 1974, pp. 129-135.

[Chien2] ————, "Block Coding Techniques for Reliable Data Transmission" in IEEE Transactions on Communications Technology, October 1971, vol. COM-19, no. 5, pp. 743-751.

[Chuang] Chuang, Justin C.-I., "The Effects of Time Delay Spread on Portable Radio Communications Channels with Digital Modulation" in IEEE Journal on Selected Areas in Communications, June 1987, vol. SAC-5, no. 5, pp. 879-889.

[Chyi] Chyi, Gwo-Tsuey, John G. Proakis and Catherine M. Keller, "On the Symbol Error Probability of Maximum-Selection Diversity Reception Schemes Over a Rayleigh Fading Channel" in IEEE Transactions on Communications, January 1989, vol. 37, no. 1, pp. 79-83.

[Clairborne] Clairborne, J. David, Mathematical Preliminaries for Computer Networking, Toronto: Wiley-Interscience, 1990.

[Clark] Clark, Martin V., Larry J. Greenstein, William K. Kennedy and Mansoor Shafi, "Optimum Linear Diversity Receivers in Digital Cellular Radio" in Proceedings, Third IEEE International Symposium on Personal, Indoor and Mobile Communications (PIMRC '92), Boston, Massachusetts, USA, October 19-21, 1992, pp. 174-178.

[Comdisco] Comdisco Systems, Inc., DSP & BOSS Communications Library Reference, version 3.0, Foster City, California, USA, September 1992.

["Compaq"] "Compaq to Launch Cellular Modem" in Electronics, July 12, 1993, vol. 66, no. 13, p. 8.

[Conway] Conway, J.H and N.J.A. Sloane, Sphere Packings, Lattices and Groups, second edition, New York, New York, USA: Springer-Verlag, 1993.

[Cowan] Cowan, C.F.N. and P.M.Grant (eds.), Adaptive Filters, Englewood Cliffs, New Jersey, USA: Prentice Hall, Inc., 1985.

[Cox] Cox, Donald C., "Antenna Diversity Performance in Mitigating the Effects of Portable Radiotelephone Orientation and Multipath Propagation" in IEEE Transactions on Communications, May 1983, vol. COM-31, no. 5, pp. 620-628.

[Crow] Crow, E.L. and M.J. Miles, "A Minimum Cost, Accurate Statistical Method to Measure Bit Error Rates" in Proceedings, Third International Conference on Computer Communications, Toronto, August 3-6, 1976, pp. 631-635.

[Dalley] Dalley, Stephanie, Myths From Mesopotamia: Creation, The Flood, Gilgamesh and Others, Oxford: Oxford University Press, 1991.

[Deng] Deng, Robert H. and Daniel J. Costello, Jr., "Reliability Analysis of a Concatenated Coding Scheme" in IEEE Transactions on Communications, July 1987, vol. COM-35, no. 7, pp. 698-705.

[Drukarev] Drukarev, Alexander I. and Kai P. Yiu, "Performance of Error-Correcting Codes on Channels with Memory" in IEEE Transactions on Communications, June 1986, vol. COM-34, no. 6, pp. 513-521.

[Duch] Duch, Krzysztof M., "Baseband Signal Processing" in IEEE Network Magazine, November 1991, vol. 5, no. 6, pp. 39-43.

[Eglowstein] Eglowstein, Howard, "Full Ethernet Networking Without a Wire in Sight" in Byte, July 1991, vol. 16, no. 7, pp. 229-230.

[Eyuboglu1] Eyuboglu, M. Vedat and G. David Forney, Jr., "Trellis Precoding: Combined Coding, Precoding and Shaping for Intersymbol Interference Channels" in IEEE Transactions on Communications, March 1992, vol. 38, no. 2, pp. 301-314.

[Eyuboglu2] ————, "Flexible Precoding for V.FAST", in International Conference on Data Transmission: Advances in Modem and ISDN Technology and Applications, September 23-25, 1992, pp. 13-18.

[Falconer] Falconer, D.D., "Adaptive Equalization of Channel Nonlinearities in QAM Data Transmission Systems" in Bell System Technical Journal, September 1978, vol. 57, no. 7, pp. 2589-2611.

[Fattouche] Fattouche, M., G. Morrison, H. Zaghloul and L. Petherick, "Diversity for Indoor Radio Communications" in Proceedings, Thirty-Third Midwest Symposium on Circuits and Systems, Calgary, August 12-14, 1990, pp. 405-407.

[Feher] Feher, Kamilo (ed.), Advanced Digital Communications Systems and Digital Signal Processing Techniques, Englewood Cliffs, New Jersey, USA: Prentice-Hall, Inc., 1987.

[Ferguson] Ferguson, Thomas J., Bruce L. Johnson and Dean O. Carhoun, "Implementation of a Transform Decoder for Reed-Solomon and Alternant Codes" in Proceedings, IEEE International Conference on Communications 1983, (ICC '83), Boston, Massachusetts, USA, June 19-22, 1983, vol. 1, pp. 303-309.

[Fernandes] Fernandes, José J.G.; Peter A. Watson and José C. Neves, "Wireless LANs: Physical Properties of Infra-Red Systems vs. Mmw Systems" in IEEE Communications Magazine, August 1994, vol. 32, no. 8, pp. 68-73.

[Flanagan] Flanagan, Patrick, "Wireless Data: Closing the Gap Between Promise and Reality" in Telecommunications (Americas Edition), March 1994, vol. 28, no. 3, pp. 25-30.

[Forney1] Forney, G. David, Jr., Concatenated Codes, Cambridge, Massachusetts, USA: M.I.T. Press, 1966, pp. 1-6, 82-90; reprinted as "Performance of Concatenated Codes" in Key Papers in the Development of Coding Theory, Elwyn R. Berlekamp (ed.), New York, New York, USA: IEEE Press, 1974, pp. 90-94.

[Forney2] ——————, "Maximum-Likelihood Sequence Estimation of Digital Sequences in the Presence of Intersymbol Interference" in IEEE Transactions on Information Theory, May 1972, vol IT-18, no.3, pp. 363-378.

[Forney3] ——————, "Efficient Modulation for Band-Limited Channels" in IEEE Journal on Selected Areas in Communications, September 1984, vol. SAC-2, no. 5, pp. 632-647.

[Forney4] —————— and M. Vedat Eyuboglu, "Combined Equalization and Coding Using Precoding" in IEEE Communications Magazine, December 1991, vol. 29, no. 12, pp. 25-34.

[Franks] Franks, L.E., "Carrier and Bit Synchronization in Data Communication--A Tutorial Review" in IEEE Transactions on Communications, August 1980, vol. COM-28, no. 8, pp. 1107-1121.

[Freeburg] Freeburg, Thomas A., "Enabling Technologies for Wireless In-Building Network Communications--Four Technical Challenges, Four Solutions" in IEEE Communications Magazine, April 1991, vol. 29, no. 4, pp. 58-64.

[Friederichs] Friederichs, Karl-Josef and Janos Kovats, "Error Performance of Block Coded Multilevel QAM Systems with Nonlinear Distortions" in IEEE Transactions on Communications, February/March/April 1994, vol. 42, no. 2/3/4, pp. 1571-1579.

[Fujiwara] Fujiwara, Toru, Tadao Kasami and Shu Lin, "Error Detecting Capabilities of the Shortened Hamming Codes Adopted for Error Detection in IEEE Standard 802.3" in IEEE Transactions on Communications, September 1989, vol. 37, no. 9, pp. 987-989.

[Fukawa] Fukawa, Kazuhiko and Hiroshi Suzuki, "Adaptive Equalization with RLS-MLSE for Frequency-Selective Fast Fading Mobile Radio Channels," in Proceedings, IEEE Global Communications Conference, 1991 (Globecom '91), Phoenix, Arizona, USA, December 2-5, 1991, vol. 1, pp. 548-552.

[Gagliardi] Gagliardi, Robert M., Introduction to Communications Engineering, second edition, Toronto: John Wiley & Sons, 1988.

[GEC] GEC Plessey Semiconductors, Digital Signal Processing IC Handbook (Publication PS 2252), Swindon, Wiltshire, United Kingdom, November 1990.

[Gersho] Gersho, Allen, "Adaptive Equalization of Highly Dispersive Channels for Data Transmission" in Bell System Technical Journal, January 1969, vol. 48, no. 1, pp. 55-70.

[Gibbard1] Gibbard, Mark Robert, "Asymmetric Equalization of the Indoor Radio Channel", M.Sc. Thesis, Department of Electrical and Computer Engineering, University of Calgary, 1994.

[Gibbard2] ——————, G. Morrison, A. Sesay and M. Fattouche, "Broadband TDMA Over the Indoor Radio Channel" in Electronics Letters, February 17, 1994, vol. 30, no. 4, pp. 285-287.

[Gitlin1] Gitlin, R.D. and S.B. Weinstein, "Fractionally-Spaced Equalization: An Improved Digital Transversal Equalizer" in Bell System Technical Journal, February 1981, vol. 60, no. 2, pp. 275-296.

[Gitlin2] ——————, Jeremiah F. Hayes and Stephen B. Weinstein, Data Communication Principles, New York, New York, USA: Plenum Press, 1992.

[Godard] Godard, Dominique N., "Passband Timing Recovery in an All-Digital Modem Receiver" in IEEE Transactions on Communications, May 1978, vol. COM-26, no. 5, pp. 517-523.

[Goldie] Goldie, Charles M. and Richard G.E. Pinch, Communication Theory, Cambridge, Great Britain: Cambridge University Press, 1991.

[Gutman] Gutman, Michael, "A Method for Updating a Cyclic Redundancy Code" in IEEE Transactions on Communications, June 1992, vol. 40, no. 6, pp. 989-991.

[Hamming1] Hamming, R.W., "Error Detecting and Error Correcting Codes" in Bell System Technical Journal, April 1950, vol. 29, pp. 147-160; reprinted in Key Papers in the Development of Coding Theory, Elwyn R. Berlekamp (ed.), New York, New York, USA: IEEE Press, 1974, pp. 9-12.

[Hamming2] ————, Digital Filters, third edition, Englewood Cliffs, New Jersey, USA: Prentice-Hall, 1989.

[Hamsher] Hamsher, Donald H., Communication System Engineering Handbook, Toronto: McGraw-Hill Book Company, 1967.

[Harashima] Harashima, Hiroshi and Hiroshi Miyakawa, "Matched-Transmission Technique for Channels with Intersymbol Interference" in IEEE Transactions on Communications, August 1972, vol. COM-20, no. 4, pp. 774-780.

[Harbour] Harbour, T.G., "Binary Cyclic [n,k] Codes Used for Simultaneous tEC and SBD" in IEEE Transactions on Information Theory, May 1989, vol. 35, no. 3, pp. 657-659.

[Hashemi1] Hashemi, Homayoun, "The Indoor Radio Propagation Channel" in Proceedings of the IEEE, July 1993, vol. 81, no. 7, pp. 943-968.

[Hashemi2] ————, "Impulse Response Modeling of Indoor Radio Propagation Channels" in IEEE Journal on Selected Areas in Communications, September 1993, vol. 11, no. 7, pp. 967-978

[Hashemi3] ————, "Statistical Modelling and Simulation of the RMS Delay Spread of Indoor Radio Propagation Channels" in IEEE Transactions on Vehicular Technology, February 1994, vol. 43, no. 1, pp. 110-120.

[Hashemi4] ————, Gang Yun, Mohsen Kavehrad, Farbod Behbahani and Peter A. Galko, "Indoor Propagation Measurements at Infrared Frequencies for Wireless Local Area Networks Applications" in IEEE Transactions on Vehicular Technology, August 1994, vol. 43, no. 3, pp. 562-576.

[Hayes] Hayes, Victor, "Standardization Efforts for Wireless LANs" in IEEE Network Magazine, November 1991, vol. 5, no. 6, pp. 19-20.

[Haykin] Haykin, Simon, Adaptive Filter Theory, second edition, Englewood Cliffs, New Jersey, USA: Prentice Hall, Inc., 1991.

[Hoffman] Hoffman, D.G., D.A. Leonard, C.C. Lindner, K.T.Phelps, C.A. Rodger and J.R. Wall, Coding Theory: The Essentials, New York, New York, USA: Marcel Dekker, Inc., 1991.

[Jakes] Jakes, William C. (ed.), Microwave Mobile Communications, Toronto: Wiley-Interscience, 1974.

[Jeruchim] Jeruchim, Michel C., Philip Balaban and K. Sam Shanmugan, Simulation of Communication Systems, New York, New York, USA: Plenum Press, 1992.

[Kahn] Kahn, Joseph M., John R. Barry, Malik D. Audeh, Jeffrey B. Carruthers, William J. Krause and Gene W. March, "Non-Directed Infrared Links for High-Capacity Wireless LANs" in IEEE Personal Communications, second quarter 1994, vol. 1, no. 2, pp.12-25.

[Kallel] Kallel, Samir, "Analysis of Memory and Incremental Redundancy ARQ Schemes Over a Nonstationary Channel" in IEEE Transactions on Communications, September 1992, vol. 40, no. 9, pp. 1474-1480.

[Kammeyer] Kammeyer, K.D., "Equalization Problems in a Digital FM Receiver" in Signal Processing, December 1985, vol. 9, no. 4, pp. 263-276.

[Kanal] Kanal, Laveen N. and A.R.K. Sastry, "Models for Channels with Memory and Their Applications to Error Control" in Proceedings of the IEEE, July 1978, vol. 66, no. 7, pp. 724-744.

[Karam] Karam, Georges and Hikmet Sari, "Improved Data Predistortion Using Intersymbol Interpolation" in Proceedings, IEEE International Conference on Communications 1989 (ICC '89), Boston, Massachusetts, USA, June 11-14, 1989, vol. 1, pp. 286-291.

[Kasturia] Kasturia, S. and J.M. Cioffi, "Precoding for Block Signalling and Shaped Signal Sets" in Proceedings, IEEE International Conference on Communications 1989 (ICC '89), Boston, Massachusetts, USA, June 11-14, 1989, vol 2., pp. 1086-1090.

[Keiser] Keiser, Gerd E., Local Area Networks, Montreal: McGraw-Hill Book Company, 1989.

[Kennedy] Kennedy, Robert S., Fading Dispersive Communication Channels, Toronto: Wiley-Interscience, 1969.

[Khayata] Khayata, R. Ellen, "HIPERLAN, The European Standard for High Data Rate Wireless LANs" in Proceedings, Sixth International Conference on Wireless Communications (Wireless '94), Calgary, July 11-13, 1994, vol. 2, pp. 460-466.

[Korn1] Korn, Israel, "A Partial Response Binary Communication System with Erasure" in IEEE Transactions on Communications, February, 1979, vol. COM-27, no. 2, pp. 493-498.

[Korn2] ————, Digital Communications, New York, New York, USA: Van Nostrand Reinhold Company, 1985.

[Kraft] Kraft, Clifford, "Closed Solution of Berlekamp's Algorithm for Fast Decoding of BCH Codes" in IEEE Transactions on Communications, December 1991, vol. 39, no. 12, pp. 1721-1725.

[Krauss] Krauss, Herbert L., Charles W. Bostian and Frederick H. Raab, Solid State Radio Engineering, New York, New York, USA: John Wiley & Sons, 1980.

[Kruys] Kruys, Jan, "HIPERLAN, Applications and Requirements" in Proceedings, Third IEEE International Symposium on Personal, Indoor and Mobile Communications (PIMRC '92), Boston, Massachusetts, USA, October 19-21, 1992, pp. 133-138.

[Krzymien] Krzymien, Witold A. and Thomas D. Bilodeau, "Performance Evaluation Study of Signal Design and Equalization Options for High-Bit-Rate Digital Subscriber Line Transceivers" in International Journal of Digital and Analog Communication Systems, January-March 1992, vol. 5, no. 1, pp. 15-28.

[Laroia] Laroia, Rajiv, Steven A. Tretter and Nariman Farvardin, "A Simple and Effective Precoding Scheme for Noise Whitening on Intersymbol Interference Channels," in IEEE Transactions on Communications, October 1993, vol. 41, no. 10, pp. 1460-1463.

[Leclert1] Leclert, A. and P. Vandamme, "Timing Synchronization in Digital Radio Systems with Multipath Propagation" in Proceedings, IEEE International Conference on Communications 1983, (ICC '83), Boston, Massachusetts, USA, June 19-22, 1983, vol. 1, pp. 530-534.

[Leclert2] ———— and Patrick Vandamme, "Decision Feedback Equalization of Dispersive Radio Channels" in IEEE Transactions on Communications, July 1985, vol. COM-33, no. 7, pp. 676-684.

[Lee] Lee, Edward A. and David G. Messerschmitt Digital Communication, second edition, Boston, Massachusetts, USA: Kluwer Academic Publishers, 1994.

[Links] Links, Cees, Wim Diepstraten and Vic Hayes, "Universal Wireless LANs" in Byte, May 1994, vol. 19, no. 5, pp. 99-108.

[Liu] Liu, Q. and Y. Wan, "An Adaptive Maximum-likelihood Sequence Estimation Receiver with Dual Diversity Combining/Selection" in Proceedings, Third IEEE International Symposium on Personal, Indoor and Mobile Communications (PIMRC '92), Boston, Massachusetts, USA, October 19-21, 1992, pp. 245-249.

[Longo] Longo, G. (ed.), Algebraic Coding Theory and Applications, New York, New York, USA: Springer-Verlag, 1979.

[Lo] Lo, Norm W.K., David D. Falconer and Asrar U.H. Sheikh, "Adaptive Equalization and Diversity Combining for Mobile Radio Using Interpolated Channel Estimates" in IEEE Transactions on Vehicular Technology, August 1991, vol. 40, no. 3, pp. 636-645.

[Lucky1] Lucky, R.W., "Automatic Equalization for Digital Communication" in Bell System Technical Journal, April 1965, vol. 49, no. 4, pp. 547-588.

[Lucky2] ————, "Techniques for Adaptive Equalization of Digital Communications Systems" in Bell System Technical Journal, February 1966, vol. 45, no. 2, pp. 255-286.

[Mazo] Mazo, James E., and Jack Salz, "On the Transmitted Power in Generalized Partial Response" in IEEE Transactions on Communications, March 1976, vol. COM-24, no. 3, pp. 348-352.

[Messerschmitt] Messerschmitt, David G., "Generalized Partial Response for Equalized Channels with Rational Spectra" in IEEE Transactions on Communications, November 1975, vol. COM-23, no. 11, pp. 1251-1258.

[Mitzlaff] Mitzlaff, James E., "Radio Propagation and Anti-Multipath Techniques in the WIN Environment" in IEEE Network Magazine, November 1991, vol. 5, no. 6, pp. 21-26.

[Monsen] Monsen, Peter, "Feedback Equalization for Fading Dispersive Channels" in IEEE Transactions on Information Theory, January 1971, vol. IT-17, no. 1, pp. 56-64.

[Morii] Morii, Masakatu, Masao Kasahara, "Generalized Key-Equation of Remainder Decoding Algorithm for Reed-Solomon Codes" in IEEE Transactions on Information Theory, November 1992, vol. 38, no. 6, pp. 1801-1807.

[Morris] Morris, Bradley J., "Optimization of a Broadband Modulation Scheme for the Indoor Radio Channel", M.Sc. Thesis, Department of Electrical and Computer Engineering, University of Calgary, 1993.

[Morrison1] Morrison, Gerald D., "A Frequency Domain Measurement System For Indoor Ultrahigh Frequency Radio Propagation Studies", M.Sc. Thesis, Department of Electrical and Computer Engineering, University of Calgary, 1991.

[Morrison2] ——————, M. Fattouche, H. Zaghloul, D. Tholl, "Frequency Measurements of the Indoor Channel" in Proceedings, Third National Seminar & Workshop on Wireless Personal Communications (Wireless '91), Calgary, July 8-10, 1991.

[Muller] Muller, Nathan J., Wireless Data Networking, Boston, Massachusetts, USA: Artech House, 1995.

[Nix] Nix, A.R. and J.P. McGeehan, "Modelling and Simulation of Frequency Selective Fading Using Switched Antenna Diversity" in Electronics Letters, October 25, 1990, vol. 267, no. 22, pp. 1868-1869.

[Oppenheim] Oppenheim, Alan V. and Ronald W. Schafer Discrete-Time Signal Processing, Englewood Cliffs, New Jersey, USA: Prentice Hall, 1989.

[Pahlavan] Pahlavan, Kaveh, Steven J. Howard and Thomas A. Sexton, "Decision Feedback Equalization of the Indoor Radio Channel" in IEEE Transactions on Communications, January 1993, vol. 41, no. 1, pp. 164-170.

[Pitstick] Pitstick, Gerald M. and J.R. Cruz, "An Efficient Algorithm for Computing Bounds on the Average Transmitted Power in Generalized Partial Response" in Proceedings, IEEE Global Telecommunications Conference 1993 (Globecom '93), Houston, Texas, USA, November 29-December 2, 1993, vol. 3, pp. 2006-2010.

[Pottie] Pottie, Gregory J. and M. Vedat Eyuboglu, "Combined Coding and Precoding for PAM and QAM HDSL Systems" in IEEE Journal on Selected Areas in Communications, August 1991, vol. 9, no. 6, pp. 861-870.

[Proakis1] Proakis, John G., Digital Communications, second edition, Toronto: McGraw-Hill Book Company, 1989.

[Proakis2] ———————, "Adaptive Equalization for TDMA Digital Mobile Radio" in IEEE Transactions on Vehicular Technology, May 1991, vol. 40, no. 2, pp. 333-341.

[Proakis3] ——————— and Masoud Salehi, Communication Systems Engineering, Englewood Cliffs, New Jersey, USA: Prentice Hall, 1994.

[Qureshi] Qureshi, Shahid U.H., "Adaptive Equalization" in Proceedings of the IEEE, September 1985, vol. 73, no. 9, pp. 1349-1387.

[Ramabadran] Ramabadran, Tenkasi V. and Sunil S. Gaitonde, "A Tutorial on CRC Computations" in IEEE Micro, August 1988, vol. 8, no. 4, pp. 62-75.

[Rash] Rash, Wayne, Jr., "WaveLAN: A Network with No Strings Attached" in Byte, June 1991, vol. 16, no. 6, pp. 294-296.

[Read] Read, R.J., P.G. Bishop and E.V. Jones, "Modems for the General Switched Telephone Network: Development, Design and the Future" in Electronics and Communications Engineering Journal, February 1994, vol. 6, no. 1, pp. 40-48.

[Rice] Rice, Michael D. and Stephen B . Wicker, "Modified Majority Logic Decoding of Cyclic Codes in Hybrid-ARQ Systems" in IEEE Transactions on Communications, September 1992, vol. 40, no. 9, pp. 1413-1417.

[Rypinski] Rypinski, Chandos A., "Motivation for Centralized Wireless LAN Functions" in Proceedings, Third IEEE International Symposium on Personal, Indoor and Mobile Communications (PIMRC '92), Boston, Massachusetts, USA, October 19-21, 1992, pp. 153-158.

[Sacks] Sacks, Tony, "Wire-less networks: the cable slayers?" in Electrical Review, September 6-19, 1991, vol. 224, no. 17, pp. 24-25.

[Salz] Salz, Jack, "On Mean-Square Decision Feedback Equalization and Timing Phase" in IEEE Transactions on Communications, December 1977, vol. COM-25, no. 12, pp. 1471-1476.

[Scott] Scott, Kenneth Edward, "Adaptive Equalization and Antenna Diversity in Digital Radio", Ph.D. Thesis, Department of Electrical and Computer Engineering, University of Calgary, 1991.

[Seshadri] Seshadri, Nambi, Carl-Erik W. Sundberg and Vijitha Weerackody, "Advanced Techniques for Modulation, Error Correction, Channel Equalization and Diversity" in AT & T Technical Journal, July/August 1988, vol. 72, no. 4, pp. 48-63.

[Sexton] Sexton, Thomas A. and Kaveh Pahlavan, "Channel Modelling and Adaptive Equalization of Indoor Radio Channels" in IEEE Journal on Selected Areas in Communications, January 1989, vol. 7, no. 3, pp.114-121.

[Shayan] Shayan, Yousef R., Tho Le-Ngoc and Vijay K. Bhargava, "A Versatile Time-Domain Reed-Solomon Decoder" in IEEE Journal on Selected Areas in Communications, October 1990, vol. 8, no. 8, pp. 1535-1542.

[Simmons] Simmons, S.J., "Alternative Trellis Decoding for Coded QAM in the Presence of ISI" in IEEE Transactions on Communications, February/March/April 1994, vol. 42, no. 2/3/4, pp. 1455-1459.

[Sklar] Sklar, Bernard, Digital Communications: Fundamentals and Applications, Englewood Cliffs, New Jersey, USA: PTR Prentice Hall, Inc., 1988.

[Smulders] Smulders, P.F.M. and H.T. Muskens, "Bit Rate Performance of Millimetre-Wave Indoor Radio Systems" in Electronics Letters, November 5, 1992, vol. 28, no. 23, pp. 2152-2154.

[Spragins] Spragins, John D., Joseph L. Hammond, Krzysztof Pawlikowski, Telecommunications Protocols & Designs, Don Mills: Addison-Wesley Publishing Co., 1991.

[Steele] Steele, Raymond, "The Evolution of Personal Communications" in IEEE Personal Communications, second quarter, 1994, vol. 1, no. 2, pp. 6-11

[Stremler] Stremler, Ferrel G., Introduction to Communication Systems, second edition, Don Mills: Addison-Wesley Publishing Company, 1982.

[Tolly] Tolly, Kevin and David Newman, "Wireless Internetworking" in Data Communications International, November 21, 1993, vol. 22, no. 17, pp. 60-72.

[Tomlinson] Tomlinson, M., "New Automatic Equalizer Employing Modulo Arithmetic" in Electronics Letters, March 25, 1971, vol. 7, nos. 5/6, pp. 138-139.

[Trachtman] Trachtman, Ayal, Irving Kalet and Shlomo Shamai (Shitz), "Limiter-Discriminator Detection of Continuous Phase Modulation (CPM) Tomlinson Filtering" in IEEE Transactions on Communications, February/March/April 1994, vol. 42, no. 2/3/4, pp. 819-825.

[Tranter] Tranter, William H. and Kurt L. Kosbar, "Simulation of Communication Systems" in IEEE Communications Magazine, July 1994, vol. 32, no. 7, pp. 26-35.

[Tuch] Tuch, Bruce, "Development of WaveLAN®, an ISM Band Wireless LAN" in AT & T Technical Journal, July/August 1993, vol. 72, no. 4, pp. 27-37.

[Ungerboeck1] Ungerboeck, Gottfried, "Fractional Tap-Spacing Equalizer and Consequences for Clock Recovery in Data Modems" in IEEE Transactions on Communications, August 1976, vol. COM-24, no. 8, pp. 856-864.

[Ungerboeck2] ——————, "Trellis-Coded Modulation with Redundant Signal Sets Part I: Introduction" in IEEE Communications Magazine, February 1987, vol. 25, no. 2, pp. 5-11.

[Vannucci] Vannucci, Giovanni and Robert S. Roman, "Measurement Results on Indoor Radio Frequency Re-use at 900 MHz and 18 GHz" in Proceedings, Third IEEE International Symposium on Personal, Indoor and Mobile Communications (PIMRC '92), Boston, Massachusetts, USA, October 19-21, 1992, pp. 308-314.

[Vaughan] Vaughan, Rodney G., "On Optimum Combining at the Mobile" in IEEE Transactions on Vehicular Technology, November 1988, vol. 37, no. 4, pp. 181-188.

[Vucetic] Vucetic, Branka, "An Adaptive Coding Scheme for Time-Varying Channels" in IEEE Transactions on Communications, May 1991, vol. 39, no. 5, pp. 653-663.

[Whiting] Whiting, Joseph S., "An Efficient Software Method for Implementing Polynomial Error Detection Codes" in IEEE Micro, March 1975, vol. 14, no. 3, pp. 73-77.

[Williard] Williard, Merwin W., "Introduction to Redundancy Coding" in IEEE Transactions on Vehicular Technology, August 1978, vol. vt-27, no. 3, pp. 86-98.

[Wilson] Wilson, Keith, "Spaghetti Injunction?" in What's New in Computing, May 1994, pp. 26-28.

[Winters1] Winters, Jack H., "On the Capacity of Radio Communication Systems with Diversity in a Rayleigh Feding Environment" in IEEE Journal on Selected Areas in Communications, June 1987, vol. SAC-5, no. 5, pp. 871-878.

[Winters2] ——————, Jack Salz and Richard D. Gitlin, "The Impact of Antenna Diversity on the Capacity of Wireless Communication Systems" in IEEE Transactions on Communications, February/March/April 1994, vol. 42, no. 2/3/4, pp. 1740-1751.

["Wireless"] "Wireless LANs: More Than Just a Niche Technology" in Telecommunications (Americas Edition), February 1993, vol. 27, no. 2, p. 12.

[Woerner] Woerner, Brian D., Jeffrey H. Reed and Theodore S. Rappaport "Simulation Issues for Future Wireless Modems" in IEEE Communications Magazine, July 1994, vol. 32, no. 7, pp. 42-53.

[Wu] Wu, Kou-Tan and Shuenn-An Tsaur, "Selection Diversity for DS-SSMA Communications on Nakagami Fading Channels" in IEEE Transactions on Vehicular Technology, August 1994, vol. 43, no. 3, pp. 428-438.

[Yasuda] Yasuda, Yutaka, Kanshrio Kashiki and Yasuo Hirata, "High-Rate Punctured Convolutional Codes for Soft Decision Viterbi Decoding" in IEEE Transactions on Communications, March 1984, vol. COM-32, no. 3, pp. 315-318.